IVANE JAVAKHISHVILI TBILISI STATE UNIVERSITY
ILIA VEKUA INSTITUTE OF APPLIED MATHEMATICS
GEORGIAN ACADEMY OF NATURAL SCIENCES

TBILISI INTERNATIONAL CENTRE OF
MATHEMATICS AND INFORMATICS

L E C T U R E N O T E S

of

TICMI

Volume 20, 2019

Teimuraz Davitashvili

MODELING EXTREME EVENTS AND STUDYING SOME FEATURES OF CLIMATE CHANGE IN GEORGIA

Tbilisi

Table of Contents

Abstract. The main goal of the book is to obtain more complete information about extreme events in Georgia and provide more detailed climate forecasts on a regional scale. The innovative methodology used in the book (a multi-model regional ensemble system (WRF, WRFchem/climate;RegCM, PRESIS, HYSPLIT) and modern computing and satellite information technologies (RCMES, meteorological data GDAS, MODIS, CALIPSO) is applied for a better understanding of the causes and problems associated with current climate change in regions with a complex orography. The book discusses and simulates the acceleration of extreme events in Georgia, some features of climate cooling in Western Georgia, as well as droughts (desertification) in Eastern Georgia, dust transfer from deserts to the South Caucasus and the dust effect in the formation of a regional climate Georgia. As well as future scenarios of extreme air temperatures prediction based on the statistical downscaling method are modelled and studied.

2000 Mathematical Subject Classification: 37M05, 65D30, 86A10

Key words and phrases

Modeling, extreme events, regional climate, Georgia

Acknowledgment: This research was supported by the Shota Rustaveli National Scientific Foundation grant N FR17_548 on "Study of some climate characteristic parameters variability over the territory of Georgia based on regional climate prediction modeling ensemble system".

T. Davitashvili
Ivane Javakhishvili Tbilisi State University
I.Vekua Institute of Applied Mathematics
2, Universitety Str., 0186 Tbilisi, Georgia
Email: tedavitashvili@gmail.com

Received 12/01/2019; Revised 20/11/2019; Accepted 22/12/2019

Preface

At present, Georgia, as the whole Caucasus, is exposed to the negative consequences, associated with regional climate change. Namely, retreat and melting processes prevail in modern Georgian glaciers; the size of large glaciers breaks up into smaller ones, the volume and length of glaciers decrease. A new inventory of glaciers shows that the number of glaciers from 2349 in 1960 decreased to 2209 glaciers in 1986 and further to 2020 glaciers in 2014. Also over the past four decades, the number of extreme weather events and natural disasters (floods, landslides, storms, showers, hails) has tripled compared to the 60-year period (1920-1980) of the last century in Georgia. In order to timely inform the population and mitigate the consequences of accidents, it is necessary to take more effective scientific steps against the freaks of nature. Thus, the question of studying the causes and consequences of growth trends in hazardous phenomena (showers, droughts, landslides, floods, hails, dust storms, dangerous fogs etc.) against the backdrop of global climate change based on modern scientific methods is relevant for Georgia.

The main goal of the book is to provide more detailed climate forecasts at the regional level and to get better information about extreme events over the territory of Georgia. To achieve this goal, the book is divided into a number of scientific and technical tasks with their own operational goals, which are compiled by closely connected with each other research objectives. This manuscript combines information and research from statistical to model studies on various aspects of the climate and climate change in Georgia. Some mitigation measures in the region are also scattered in some chapters of the book. Though it does not provides policy-relevant information on the relation between the climate stabilization targets and the timing and amount of measures, necessary to mitigate. The book discusses several aspects and features, inherent in climate change that represent the main early indicators of climate change on the territory of the Caucasus (Georgia). To reproduce the hydrological state, the book contains some data describing Georgian water resources. To show expected changes in climate parameters until 2050, some results of PRECIS calculations (with a resolution of 25 km x 25 km) are presented. A considerable part of the book is devoted to the study of some features of climate cooling in Western Georgia and climate warming in Eastern Georgia. To study the trend of climate cooling in the western part of Georgia, the influence of thermal and advective-dynamic factors on climate change is studied. To study the influence of the orography of the Georgian ranges (Surami) on the zonal air flow over the West Georgian region, a three-dimensional hydrostatic non-stationary model is used that describes the mesoscale transfer of atmospheric flows over complex terrain. To study the specific properties of the regional process in eastern Georgia (climate warming), statistical methods with mathematical modeling are used. To this end, to describe the processes contributing to desertification against the backdrop of climate change in eastern Georgia, the correlation between the temperature of the Earth's surface and precipitation data is studied. Aerosol is one of the main sources of uncertainty in modern climate variability. Dust aerosol is one of the main pollutants in Georgia and the penetration of dust aerosol into Georgia from neighboring deserts has not yet been studied. That is why in this monograph the possible ways of aeolian dust masses transfer from neighbor deserts to the South Caucasus (Georgia) territory are studied, using the WRF-Chem online coupled with dust module. Namely, the numerical modeling (using the WRF-Chem and HYSPLIT models) along with remote sensing products (CALIPSO and MODIS) are used for studying the transfer, dispersion and accumulation of dust from neighbouring deserts to the territory of the South Caucasus

(Georgia). Besides, the strengths and weaknesses of the direct effects of dust and its impact on the climate of Georgia are investigated, based on the calculation results of the Regional Climate Model RegCM interactively coupled with a dust model. And finally, using Regional Climate models Evaluation System (RCMES) package, with four different methods for 27 selected meteorological stations located in Georgia some future scenarios of 2-meter air temperature maximums and minimums are studied from three GCMs of CMIP5 database, based on statistical downscaling method.

The author has been working on the problem of regional climate change and modeling extreme events for several decades and has published numerous publications in this field, most of which have been prepared in accordance with international, scientific and technical programs and published in authoritative publications abroad. It were these studies together with the new researches that formed the basis of this monograph, but for a thorough study of the problem, the monograph also summarizes ideas from existing literature that have stood the test of time and received appropriate justification and development. This research was supported by the Shota Rustaveli National Scientific Foundation grant on "Study of some climate characteristic parameters variability over the territory of Georgia based on regional climate prediction modeling ensemble system" № FR17_548 2017-2020.

The fulfillment of this research is fully based on the assistance, advice and backing of the following author team for which I am grateful: Prof. A. Khantadze, Prof. Z. Khvedelidze, Prof. D. Gordeziani, Prof. K. Tavartkiladze, Dr. D. Demetrashvili, Dr. N. Kutaladze, Dr. L. Megreladze, Dr. R. Kvatadze Mr. G. Mikuchadze, Mrs. I. Samkharadze. The implementation of this research and assessment process was supported by the I. Vekua Institute of Applied Mathematics of I. Javakhishvili Tbilisi State University. Technical Support Unit (providing computer time for some of these studies) was provided by the Georgian Research and Education National Association GE-01-GRENA under the leadership of Dr. R. Kvatadze.

Author

Introduction

Currently, global warming is one of the main threats, facing the planet Earth. The current climate change is mainly associated with an increase in the concentration of greenhouse gases (water vapor, carbon monoxide, methane), which, in accordance with various climate projections, leads to a temperature increase of 2.1-5.2^{0}C at the end of the 21st century and, as a result, it has many destructive effects (an increase in the frequency of showers, floods and landslides, melting glaciers and their partial disappearance, sea level rise, desertification of vast territories, etc.) on the flora and inhabitants of the Earth. At present, the Earth's climate is changing faster than expected several decades ago. Some of these changes are associated with natural changes that have occurred over millions of years, but increased human activity has contributed to the release of more and more greenhouse gases into the atmosphere, which promoted to the "greenhouse effect". According to the Intergovernmental Panel on Climate Change (IPCC 2007 [12]), the best estimate of global warms for average surface temperature over the current century ranges from 1.8°C to 4.0°C, which has not been the case for at least the past 10,000 years (IPCC 2007 [12]). Climate change problem is also associated with a growing crisis in environment pollution, food production and health safety (IPCC, 2007 [12]). Indeed it became obvious that there is threat on food production through increased heavy precipitation, catastrophic flooding, growing desertification processes. Global climate change has impacted on durability of seasons too. Namely in middle latitudes the summers became hotter, the winters colder, length of the spring has shortened with lower temperatures and only durations of the autumns have elongated with warm weather (SNCU NFCCE 2009 [23]; Westphal, et al. 2011 [31]). These changes have affected flora and fauna and especially the plants of particular regions of the earth having non homogenous topography and habitat (SNCU NFCCE 2009 [23]). The stable equilibrium of the Sun-atmosphere-Earth's surface energy system has been in decline for more than a century (IPCC, 2007 [12], Westphal et al. 2011 [31], B. Beritashvili 2011 [1]). The energy obtained due to changes in the gas composition of the atmosphere and the physical properties of the substrate surface is still insignificant, but tends to exceed the amount of energy released. This is the result of a gradual increase in the surface temperature and the surrounding ambient air, resulting in a gradual warming of the climate (IPCC, 2007 [12]). This process takes place at different intensities in different parts of the oceans and continents. As a result, in parallel to the thawing, even in some regions, there is a decrease in temperature. The classic example of such regions is the territory of Georgia. From the literary sources it is known that while the warming process was over in Valley and Meskhet-Javakheti in eastern Georgia, the climate in the high slopes of the southern slope of the Caucasus was almost unchanged, and in the foothills of western Georgia there was a process of small cooling (E. Elizbarashvili, 2007 [5]).

The study of the climate of Georgia has a long history, as evidenced by the work of ancient philosophers, historians and geographers such as Herodotus, Hippocrates (V c. BC), Strabo (I c. BC), etc. (Elizbarashvili, 2007 [5]). Later, based on visual observations, the climatic features of some regions of Georgia are found in the works of medieval historians and travelers. Among the first studies on the basis of instrumental observations, can be mentioned the works which presented the first maps of isotherms. At the beginning of the 20th century, a number of climatologists dedicated their work to the study of the climatic features (among others distribution of air temperature and precipitation) in Georgia. In the following years, a number of monographs were published that generalize the nature and method of distribution of certain climate

elements (radiation and thermal conditions of the atmosphere, precipitation and the conditions of their territorial distribution) on the territory of Georgia (Kordzakhia 1961 [17], Mumladze 1991 [20], Khvedelidze and Elizbarashvili 1982 [16], Javakhishvili 1977 [13], 1981 [14], Gvasalia 1986 [11], Gigineishvili 1960 [9], Papinashvili 1963 [21], Kvaratskhelia 1971 [19] Ushveridze 1977 [30], Gogishvili 1974 [10]; Zanina 1961 [32], Svanidze et al. 1987 [26], 1988 [25], Turmanidze 1981 [29], Sulakvelidze 1988 [24], Elizbarashvili et al. 1992 [6], Tavartkiladze et al. 1999 [27], Elizbarashvili M.1999 [8]; Elizbarashvili E. and Elizbarashvili M. 2006 [7]; Elizbarashvili E. 2007 [5]; Beritashvili 2011 [1]). The state of studies of climatic resources of Georgia until 2006 is summarized in the monograph by E. Elizbarashvili (2007 [5]) and prospects for their effective use are outlined.

Currently climate change is in progress on the territory of the Caucasus (Georgia). Namely, Georgia as a whole in the Caucasus is subject to these negative consequences associated with regional climate change: the frequency of showers is increasing, the glaciers of the Caucasus are melting and disappearing, the level of the Black Sea is rising, the frequency of drought is increasing, etc (Third National Report of Georgia 2006 [28]; Davitashvili 2018 [3]). Studies of the ice cores of the Caucasus glaciers and regional climate change using statistical and dynamic downscaling modeling have shown that large climatic changes have occurred, and very large ones can occur over several decades or even years for regional changes in temperature and precipitation (Shahgedanova et al. 2013 [12], Second National Communication to the UNFCCCC 2009 [23], Third National Report of Georgia 2006 [28], Krapivin and Kondratyev 2002 [18], Davitashvili et al. 2018[4], Davitashvili 2018 [3]). Besides, studies of extreme changes in climatic parameters over the past few decades have shown that some initial concerns now seem less sinister, but new ones could occur in the climate system (Third National Report of Georgia, 2006 [28]). So it is obvious that the climate of the Caucasus (Georgia) has changed dramatically over several decades (Third National Report of Georgia, 2006[28]; Westphal et al. 2011 [31], Davitashvili et al. 2018 [4], Davitashvili 2018 [3]). Currently, great progress has been made in expanding our understanding of climate change in Georgia and its causes, but in any case there is no clearer picture of current and future climate changes, since the processes in the Caucasus (Georgia) are strictly non-linear (Khantadze et al. 1997 [15], Davitashvili and Khantadze, 2008 [2], Westphal et al. 2011 [31]).

The emergence of unstable climatic equilibrium of the global climate and its monotonous change can have many undesirable consequences for humanity. For example, if the average surface temperature of the Earth's surface rises by 4-5°C, many species of living organisms on Earth will gradually disappear (IPCC, 2007 [12]). In Georgia (with complex topography and trending change in climate parameters) it is extremely important to conduct a comprehensive fundamental study of changes in atmospheric processes and climate parameters that contribute to the intensification of extreme processes. A lot of work has been done in this area, but we do not believe that for the Caucasus region (Georgia), comprehensive methods have been developed for quantifying the intensification of extreme processes. In order to get closer to current and future climate change processes taking place in Georgia, this study mainly uses both statistical methods and non-linear mathematical models that more or less describe these processes. The subjects of this book include both changes in the physical climate system and the consequences in natural systems, caused by the gradually changing climate in the Caucasus (Georgia). The time scale of our study of climate change is years or decades, and it has been established that the main characteristics of regional climate change are those that are unfolding faster than planned (Third National Report of

Georgia, 2006 [28]; Westphal et al. 2011 [31]; Davitashvili et al. 2018 [4]). The material in the book is designed to better understand the cause of climate change in Georgia, based on statistics and mathematical modeling. Studies show that human activities (especially the burning of fossil fuels) with some natural phenomena (aerosol emissions into the atmosphere) are the main causes of warming and related changes in Georgia. It also summarizes forecasts of future climate change in Georgia and the expected consequences for this century. This book is based on a series of scientific reports and studies on climate change in the Caucasus (Georgia), based on many years of data, and superficially shed light on the actions that can be taken to mitigate climate change in Georgia.

Chapter 1 discusses some of the features of climate change that have affected flora, fauna and habitat in selected regions of Georgia with heterogeneous topography. In particular, it discusses an increase in the amount of heavy precipitation (rainfall, hail), catastrophic floods, droughts, growing desertification and the melting of glaciers, which represent the main early indicators of climate change in Georgia. The results of some studies on the melting of Georgian glaciers and an increase in extreme rainfall are also presented. Namely, against the background of the melting of modern Georgian glaciers, a natural disaster in the Dariali Gorge (with its consequences), caused by the melting and collapse of the Dariali Glacier is discussed. The reliability of the expression, which correlating changes between the average temperature of the atmosphere (at an altitude of 2 m) and the corresponding height of the glaciers is studied on the example of the Devdodaraki glacier. In order to discuss the expected changes in climate parameters in Georgia until 2050, the results of Regional Model for Climate Prediction for Impact Research (PRECIS) calculations (with a resolution of 25 km x 25 km) is used. The calculation results have shown that by 2050 throughout the whole territory of Georgia the amount of precipitation decreases and the temperature rises, which will lead to a decrease in glaciers and cause problems with water supply. Chapter 2 is devoted to the study of some features of climate change (cooling) processes in Western Georgia. To study the climate cooling trend in the western part of Georgia, the influence of thermal and advective-dynamic factors on climate change is studied. A formula is obtained that proves the existence of a monsoon type circulation in Western Georgia. This formula describes the action of constantly acting factors in the territory of this region and practically proves its stability. It is shown that the disproportionate warming of the Black Sea and Kolkhi lowlands causes an intensive increase in circulation, and this factor can play an important role in the process of cooling the climate in Western Georgia. Since western and eastern atmospheric processes with zonal transfer of atmospheric masses from the Black Sea to the Caspian Sea and vice versa account for about 55% of all common processes prevailing in Georgia, for a better understanding of climate cooling in western Georgia, the structural variability of meteorological fields in the lower layers atmospheres (when atmospheric flows are transferred from the Black Sea to land and vice versa) are studied using a three-dimensional hydrostatic non-stationary model. An analysis of the results in a vertical plane showed that over the topography, the amplitudes of the wave current and the formation of vortex structures in the entire troposphere significantly contribute to the generation of circulation flows. Chapter 3 discusses the specific properties of the regional process of climate warming in eastern Georgia using statistical methods and mathematical modeling. The impact of climate change in eastern Georgia on the risk of desertification has been studied. To describe the processes contributing to desertification in Georgia, data on temperature and precipitation of the earth's surface are studied. It follows from the theoretical model of desertification discussed in this chapter that in order to stop the desertification

process, it is necessary to stop the non-linear thermal process occurring in the soil, causing its structural changes as a result of the "greenhouse effect". To achieve this goal, it is necessary to take measures that reduce the load of solar radiation on the soil and, naturally, lead to the disappearance of the "greenhouse effect" in its active layer. The desertification process is estimated in the Shiraki Valley (which in recent years is characterized by an increase in the frequency of droughts) using one statistical method. Then we studied the temperature of the soil surface at the selected station and changes in precipitation and established climatic parameters that can be considered as the beginning of desertification. For this, a normalized autocorrelation matrix was compiled for the Shiraki Valley, which is determined by the temperature of the soil surface and average annual and seasonal precipitation anomalies. In chapter 4, numerical simulation along with remote sensing products is used for the first time to study the transfer, dispersion and accumulation of dust from deserts to the territory of the South Caucasus (Georgia). Namely, WRF-Chem v.3.6.1 (with its dust research module) and the HYSPLIT models together with the satellite products CALIPSO and MODIS are used to study the transport of intense dust storms (occurring in the largest deserts adjacent to the Caucasus): Sahara and Sahel in Africa, Arab deserts and deserts of Ar-Rub-al-Khali in the Middle East, Kyzyl-Kum and Kara-Kum in Central Asia) to the territory of the South Caucasus (Georgia). The calculation results of the WRF-Chem model, performed from December 2017 to November 2018, showed that nine cases of dust transfer to the territory of the South Caucasus (Georgia) were noted. Two of them, held on March 22-24 and July 25-26, 2018, are modelled and discussed in this chapter. Chapter 5 analyzes the strengths and weaknesses of the direct effects of dust and its impact on the climate of Georgia using a Regional Climate Model RegCM interactively coupled with a dust model.

This book is needed for a better understanding of the causes, problems associated with climate change in regions with a comprehensive orography, for the better transformation of environmental management in relation to health and well-being, industry, agriculture, tourism, etc. on the background of current climate change. The innovative methodology used in the book is a multi-model regional ensemble (WRF, WRFchem / climate; RegCM, PRESIS) and modern computing and satellite information technologies (RCMES, meteorological data GDAS, MODIS, CALIPSO). In the book the main advective-dynamic sources and factors that caused the cooling of western Georgia and the warming of eastern Georgia are identified. It was also found that aeolian mineral dust is carried not only from the Sahara and the Middle East, but also from the Karakum and Kyzylkum deserts and dust is one of the main sources influencing climate change in Georgia. Scenarios of climate change (extreme events), are important for planning development projects, including water supply, agriculture, irrigation, groundwater throughput (during heavy rains), roads, railways, buildings, and tourism development. Therefore, the results of our research in the field of forecasting extreme events and their impact on socio-economic sectors at different time periods are of great scientific importance not only for the scientific, environmental, economic, agricultural, industrial and tourist communities in Georgia, but also for agencies and companies from neighboring countries of the Caucasus region.

The author of the monograph tried to develop classical and integrated methods for studying climate, taking into account the specifics of a mountainous country. The interim and final results of the assessment of climate parameters in Georgia are presented in the form of maps, tables and figures, which makes it easier for the reader to perceive these results and their use in solving essential ecological, economic and so on problems connected with regional climate change. The book is intended for specialists

in climate modeling, climatologists, meteorologists, geographers, agro-meteorologists, power engineers, medical professionals and for anyone interested in regional climate change problems and with perspectives of use. The book can be used as supporting guide in regional climate modeling, ecology and environment pollution for students, masters and graduate students.

References to introduction

1. Beritashvili B, Climate and its change, Technical University, 2011, P. 175.
2. Davitashvili T and A. Khantadze, 2008. On climate, desertification and water pollution problems for the territory of Georgia" Netherlands: Springer-Verlag, 2008,pp. 453-469.
3. Davitashvili T, (2018). On Some Aspects of Climate Change in Georgia, *International Journal of Energy and Environment,* Vol.12, 2018, pp. 80-86.
4. Davitashvili T,, Kutaladze N., Kvatadze R., Mikuchadze G. (2018). Effect of dust aerosols in forming the regional climate of Georgia. Scalable Computing: Practice and Experience, 2018, Volume 19, Number 2, pp. 199–208. http://www.scpe.org
5. ElizbaraShvili E, Climatic resources of Georgia, 2007, Hydrometeoroligical Institute of Georgia, p. 425 (Georgian).
6. Elizbarashvili E., Chavchanidze Z. Droughts, rainless and Rainy periods in Georgia. Tb., 1992 (Georgian).
7. Elizbarashvili E.Sh. and M.E. Elizbarashvili. The main problems of landscape climatology. Tbilisi, Zeon, 2006, 118 pp. (Russian).
8. Elizbarashvili M. Temperature field of Georgia. Tb 1999 (Georgian).
9. Gigineishvili V.M. hail in eastern Georgia.L., 1960 (Russian).
10. Gogishvili K.S. The study of circulating factors genesis of the climate of Georgia. Tb., 1974 (Russian).
11. Gvasalia N.S. The heat balance of Georgia. Tb., 1986 (Russian).
12. IPCC, 2007. Climate Change 2007: Synthesis Report. Pachauri, R.K. and A. Reisinger (eds.), Contribution of Working Groups I, II and III to the Fourth Assessment. Report of the Intergovernmental Panel on Climate Change. IPCC, Geneva, Switzerland. 104 pp.
13. Javakhishvili Sh. Atmospheric precipitation on the territory of Georgia. Tb., 1981(Georgian).
14. Javakhishvili Sh. Climatography of the Georgian SSR. Tb., 1977(Georgian).
15. Khantadze A., Gzirishvili T. and G.Lazriev 1997, On the Non-linear Theory of Climatic Global Warmining,. *Bulletin of CRNC.* No 6, p.3-33.
16. Khvedelidze Z., Elizbarashvili E. Influence of terrain on atmospheric processes. Tb., 1982 (Georgian).
17. Kordzakhia M. Georgian weather. Tb., 1961 (Georgian).
18. Krapivin V., K.Kondratyev,2002,Environmental Global Change: Ecoinformatics, 476*, Gidrometeoizdat Press.*
19. Kvaratskhelia I.F. Aerological research in Transcaucasia., 1971

20. Mumladze d. Modern climate change in Georgia. Tb., 1991 (Georgian).
21. Papinashvili K.I. Atmospheric processes in the Caucasus and their connection with macrocirculation processes over Eurasia. L., 1963.
22. Shahgedanova M, Kutuzov S, White K H. et al. 2013. Using the significant dust deposition event on the glaciers of Mt. Elbrus, Caucasus Mountains, Russia on 5 May 2009 to develop a method for dating and "provenancing" of desert dust events recorded in snow pack. Atmospheric Chemistry Physics., 13: 1797–1808.
23. SNCUNFCCC-*Second National Communication to the United Nations Framework Convention on Climate Change*; Ministry of Environment Protection and Natural Resources, Republic of Georgia. 2009, www.unfccc.int, p. 240.
24. Sulakvelidze Ya.G. Heavy rainfall in mountainous countries on example of the Caucasus. Tb., TSU, 1988 (Russian).
25. Svanidze G.G., Gagua V.P., Sukhishvili E.V. Renewable energy resources of Georgia. L., 1987 (Russian).
26. Svanidze G., Tsomaia V. et.al, 1988: Water Resources of Trancaucasia. Leningrad: Gidrometizdat Press.
27. Tavartkiladze K., Elizbarashvili E., Mumladze D., Vachnadze J. Terrestrial temperature an empirical model of field change. Tb., 1999 (Georgian).
28. Third National Report of Georgia on the Implementation of the UN Convention to Combat Desertification, May, 2006, Tbilisi, Georgia, p.24
29. Turmanidze T.I. Climate and grape harvest. L., 1981.
30. Ushveridze G.A. Guidelines for climatotherapy. Tb., 1977.
31. Westphal M. I., Mehtiyev M., Shvangiradze M. and V. Tonoyan, 2011, Regional Climate Change Impacts Study for the South Caucasus Region, p.63.
32. Zanina A.A. Climate of the USSR. Issue 2, Caucasus. L., 1961(Russian).

Chapter 1. SOME FEATURES OF CLIMATE IN GEORGIA

Formation of climate on the territory of Georgia is a result of joint action of large-scale synoptic and especially local processes which are basically stipulated by the complex orography of the Caucasus (Georgia). Geographic location of Georgia plays an impotent role for spatial-temporal distribution of meteorological fields and local climate formation. Namely, Georgia lies between the Black and Caspian Seas (along the Black Sea eastern coast), to the south of the Main Caucasus Ridge and to the north of the Lesser Caucasus Mountains (the Lesser Caucasus Mountains occupy the southern part of Georgia). These two mountain systems are linked by the Likhi (Surami) mountain range, which is located almost along the meridian and bisects the country into western and eastern parts (see Fig.1).

Fig. 1. A map of the Caucasus

To the west of the Surami Range the relief becomes much lower, and elevations are generally less than 100 m along the river valleys and the coast of the Black Sea. On the eastern side of the Surami Range, a high plateau known as the Kartli Plain extends along the river Kura. The two largest rivers in Georgia, the Kura and the Rioni, flow in opposite directions: the Kura, which originates in Turkey, runs generally eastward through Georgia and Azerbaijan into the Caspian Sea, while the Rioni runs generally westward through the lower Rioni valley and drains into the Black Sea. Besides to these largest rivers Georgia rich of river network. An average density of the river network in Georgia is 0.6 km/km^2. The density of the river network is conditioned by the impact of physical-geographical, climatic factors. The quantity of atmospheric precipitation plays a special critical role. Generally the density of the river network in Georgia decreases in parallel with the reduction of atmospheric precipitation from the west to the east. In particular, the density of the river network in Western Georgia is about 1.07 km/km^2, while in Eastern Georgia this figure equals to 0.68 km/km^2 and density of the river network in Eastern driest regions of Georgia is very low and it equals to 0.1 km/km^2 (Svanidze at al. 1988, [40]). There is almost no river network in the eastern driest regions of Georgia, where the annual quantity of atmospheric precipitation is very low and equals to 100-250 mm, and the level of evaporation is extremely high. it should be noted that about 99% of the Georgian rivers are less than 25 km and only one river, the river Kura, is longer than 500 km. Georgia is also rich with surface water and

groundwater resources. There are 43 natural and artificial lakes in Georgia, of which 35 in East Georgia, for irrigation or hydropower generation. Surface water and groundwater resources include numerous thermal and mineral springs. Many snow- and glacier-fed rivers are present in the Greater Caucasus. Groundwater resources are abundant, especially in the lower slopes of the Greater Caucasus and in the lava 0plateaus of Javakheti mountains (Svanidze at al. 1988 [40]). In Georgia, about 1600 water-suppliers provide a total of 620 million m^3 of drinking water per year. From this quantity 90% is consumed by urban population and 10% by rural (Mindorashvili 2002 [28]). Main source of drinking water is groundwater, accounting for about 90% of the total amount of water feeding the centralized water-supply networks. No special treatment of groundwater takes place before it is supplied to the users, the water is chlorinated only. When surface water is used as raw material, this water is specially treated – precipitated and chlorinated. So the water resources of Georgia is conditioned by the physical-geographical (decreases in parallel with the reduction of atmospheric precipitation from the west to the east) and impact of climatic factors. Namely the change of mean annual precipitation sums in the period of 1955-2005 (the change is assessed by comparing average values for two sub-periods: 1955-1970 and 1990-2005) at 8 meteorological stations in Georgia's most populated areas was studied by Beritashvili and Kapanadze (2008 [3]). The results of investigations showed that the change in the annual sums of precipitation between these time periods have increased on the average by 9% in West Georgia, remained on the average the same in East Georgia, while in South Georgia they have slightly decreased by 3%. It should be noted that almost all types of climate (11 types) are found in Georgia, with the exception of tropical, savannah and deserts (Javakhishvili, 1981 [20]). Formation of these peculiar climate zones on the territory of Georgia is a result of jointly action as large-scale synoptic processes as well local atmospheric processes stipulated by distinctive features of the Caucasus (Georgian) complex topography and geographic location of the Georgian territory. Indeed, among the local factors deforming large-scale air flows the complex relief of Georgia has decisive importance as about 75% of the total land area (about 69 700 sq. km) represents mountains and mountain ranges with compound topographic sections (Javakhishvili, 1981 [20]). Climate change is well expressed in the South Caucasus region where is a strong evidence of increasing trends in mean annual temperature with mean daily minimum temperature and mean daily maximum temperature (Second National Communication to the UNFCCC, 2009 [37]; Westphal et al. 2011 [46]). The single longest dataset available (IPCC, 2013 [19]) shows that the total increase between the average of the1850–1900 period and the 2003–2012 period accounts for 0.78^0 C ($0.72–0.85^0$C). As to Georgia temperature increased between 0.1–0.5^0 C in Eastern Georgia and decreased by 0.1–0.5^0C in Western Georgia during 1906–1995 (World Bank, 2006 [47], SNCUNFCCC 2009 [37]). Studies show that extreme climatic events (e.g., extreme temperatures) have large variations and trends and, therefore, respond to climate change more sensitively than mean climate values (IPCC, 2007 [18]; Aguilar et al., 2009 [1]; Zhang et al., 2005 [48]; Elizbarashvili et al., 2011 [10]; Levitus 2001 [25]). Studies of past observed changes in extreme temperatures and related weather and climate phenomena such as drought, hurricanes and frosts over Georgia were carried out mainly on the basis of monthly data, and it was found that the frequency of extremely hot months during the 20^{th} century increased and extremely cold months decreased faster in Eastern Georgia than in its Western counterpart (Keggenhoff et al. 2010 [21]; Elizbarashvili et al. 2009a [12], 2011 [10], 2013 [11]). Also, the highest rates of warming trends in average annual air temperature are observed in the mountains of the Caucasus, and the lowest - in arid regions of Eastern Georgia. Nowadays climate

change on the territory of Georgia is evident at least on the background of the Caucasus (Georgian) glaciers melting (Second National Communication to the UNFCCC, 2009 [37]; Huggel et al. 2003 [16]). Increased heavy precipitation (shower, hail), catastrophic flooding, drought, growing desertification with glaciers melting processes represent main early climate change indicators in Georgia.

1.1. Early climate change indicators in Georgia

Hydrothermal processes which link the lithosphere, hydrosphere, atmosphere and biosphere have played an important role in the evolution of climate in the Caucasus (Davitashvili and Khantadze 2008 [6]; Gogishvili 1974 [14]). The Caucasus is characterized by a diverse climate and, as a result, is rich in biological diversity (this is one of the most biologically rich areas on Earth and is one of the 25 most diverse and endangered ecosystems on the planet). Despite the small size of the territory, the precipitation rates on the territory of Georgia are very diverse from west to east and from north to south (Gigineishvili 1960 [13], Gogishvili 1974 [14]). For example the annual rainfall on the Black Sea coast ranges from 1,500– 2,500 mm, while on the plains in Eastern Georgia, precipitation is only 400–600 mm / year (Third National Report of Georgia on IUNCCD, 2006 [42]). Heavy rains, hail, floods and drought are the main climatological hazards in the country (Davitashvili et al. 2002 [7]). It is reported that floods kill more people, but droughts affects far more people and causes more economic damage in Georgia. For example, a severe drought in 2000 affected 700,000 people and caused damage of 5.6% of GDP due to its impact on agriculture and hydropower production (Third National Report of Georgia on IUNCCD, 2006 [42]). Glaciers are one of the main early indicators of ongoing climate change and change in glacier extent is an easily measured parameter, which provides an indirect, filtered signal of climate change (SNCU NFCCE, 2009 [37]; Huggel et al. 2003[16]). Studies on the growing melting of glaciers against the backdrop of modern climate change are conducted in many mountainous countries. For example, according to Shea et al. (2015 [35]) yet the sensitivity of glaciers in the Everest region of Nepal to climate change is very high. On the other hand glaciers themselves play major roles in influencing regional and global climates. Also glaciers are fresh water storage resources too and in many countries (in Georgia too) millions of people depend on glaciers for drinking water, agriculture, and industry and power generation during key parts of the year (SNCU NFCCE 2009 [37]; Andreas et al. 2006 [2]). Fluctuations of glaciers and ice caps in cold mountain areas have been systematically observed for more than a century in various parts of the world (Oerlemans et al. 1998 [30]). During the last century, glaciers in the European Alps and the Caucasus Mountains have decreased to half their size, while in Africa only 8% of Mount Kenya's largest glacier remains (Braithwaite and Olesen, 1989 [4]). If current trends continue, by the end of this century many of the world's mountain glaciers, will have vanished entirely (Shea et al. 2015 [35]; Westphal et al. 2011 [46]).

1.1.1. Extreme events acceleration on the territory of Georgia

Unfortunately for the last four decades a number of the extreme weather events on the territory of Georgia has increased. For this period about three times has increased a number of natural hazards in comparison with the 60 years of the last century and as a consequence economic expenses have increased eight times (the economic expenses only for 2004 reached 150 billion USD $) (SNCU NFCCE 2009 [37]; Westphal et al.

2011 [46]). For the last four decades among the main natural disasters can be separated out an increased number of droughts, floods, landslides, storms, heavy showers on the territory of Georgia. There is also evidence of extension of desertification processes in some south and eastern regions of the territory of Georgia, reduction of numbers of glaciers in the Caucasus Mountains and volumes of drinking waters in the eastern reservoirs (SNCU NFCCE 2009 [37]; Westphal, et al. 2011 [46]). Investigation dedicated to the question of intensity in formation of hazardous floods on the background of modern climate change on the territory of Eastern Georgia has been carried out for the period of 1921-2000. Analysis of data of intensity hazardous floods has shown that in the East Georgia frequency of recurrence of hazardous floods for the period of 1961-2000 in comparison with the period of 1921-1960 has increased on 150% while extreme abundant precipitations have increased only on 12% and there are no reliable methods for prediction of these natural hazard events for short and long time periods. Especially for the last two decades there was increased number of floods, landslides, heavy showers on the territory of Georgia. For instance an accident takes place on 13 06 2015 in the capital city of Georgia Tbilisi. For about 2.5 hours there was heavy shower in Tbilisi and suburbs and as a consequence near Tbilisi there occurred a heavy landslide (with a big amount of soil, rocks and trees) which blocked the Vere River's canyon, formed a water-storage basin (the Vere River flows from the Didgori mountain to Tbilisi through the territory of the zoo in Tbilisi and further under the square of Heroes by pipe into the Kura River) and the strong wave (mass of water-slush, rocks and trees) run across the Vere River canyon and washed everything away until the square of Heroes in Tbilisi (see Fig.1.1).

Fig. 1.1. View of the Vere River after a flood on June 14, 2015 in the capital of Georgia, Tbilisi

Unfortunately it was accompanied by sacrifices (officials had announced that 20 persons passed away, about 4 were vanishing out of sight). Also owing to downpour a lot of animals were suffocated in the zoo, some tigers, lions, punters and wolves were killed in the streets of Tbilisi. Heavy rains of such size (accompanied by floods, but without casualties) became a frequent natural occurrence in Georgia in the warm season to the present day. An increase in the frequency of such incidents is one of the obvious indicators of regional climate change in Georgia.

1.1.2. Natural disasters in the Dariali Gorge

Currently, the mountains of Georgia are dominated by the processes of retreat and melting of glaciers - the size of large glaciers breaks up into smaller ones, the volume and length of glaciers decrease (Second National Communication to the UN FC CC 2009 [33]). A new glacier inventory (based on multi-time data sets) shows that the number of glaciers from 2349 (with a total glacier surface area of 1674.9 ± 70.4 km^2) decreased to 2209 glaciers (with a total glacier surface area of 1482.1 ± 64.4 km^2) from 1960 to 1986 and further reduced to 2020 (with a total glacier surface area of 1193.2 ± 54.0 km^2) until 2014. Temporary changes in the number and area of glaciers indicate that the Lesser Caucasus glaciers (0.61% yr^{-1}) retreated much faster than the Greater Caucasus glaciers (0.50% yr^{-1}) between 1960 and 2014 and glaciers in the eastern areas of the Greater Caucasus (0.98% yr^{-1}) decreased significantly more than in the central (0.46% yr^{-1}) and western (0.52% yr^{-1}) parts of the Greater Caucasus (Tielidze and Wheate 2018 [43]). It is noted that if the decrease in the surface area of glaciers in the Greater Caucasus continues in the same way then many of them will disappear at the end of 2100 (Tielidze and Wheate, 2018 [43]). Currently, as a result of melting glaciers, many negative landforms have appeared, such as circuses, frugally of the valley, exterminated relief, and others. These landforms formed lake dams, which in most cases are located inside glaciers. In total, there are about 16 such types of glaciers in Georgia. (Gorgijanidze and Tsintsadze 2007 [15]; Huggel et al. 2004 [17]). In Georgia, glaciers play an important positive role in the formation of surface and underground reservoirs and the regulation of their balance, but sometimes they cause accidents. Sometimes, due to rapid melting, glaciers moisten the base and degraded soil along with water, stones and shrubs fall into river gorges, create natural dams, and then overflowing natural dams are destroyed and lead to accidents. A recent example of this phenomenon was the large-scale disaster that occurred on May 17, 2014 in the Dariali gorge of the Kazbegi region. The fragments of the Devdoraki glacier (see Fig. 2) with an accumulated mass of stones and bushes fell into the Tergi River, blocked the passage through the Tergi River, and overflowing natural dam and the resulting flood destroyed the road formerly known as the Georgian Military Road connecting Georgia with Russia.

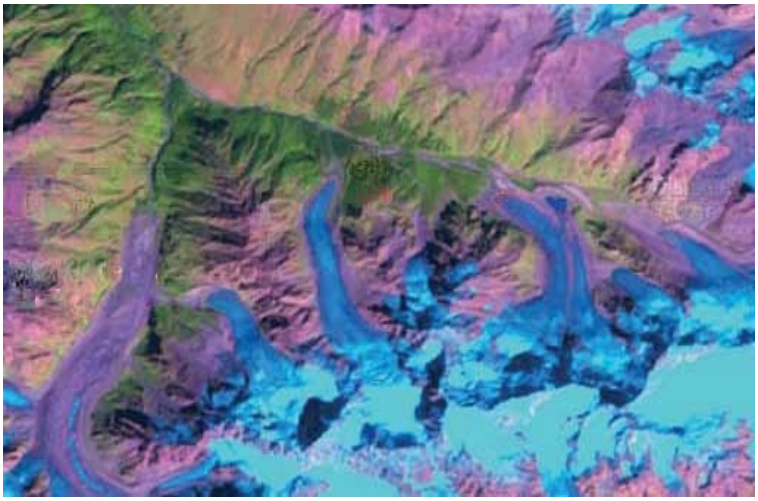

Fig. 1.2. Devdoraki glacier

Unfortunately, during the accident in the Darial Gorge, several people died and others went missing (according to the State Security and Crisis Management Council in Georgia, several people were trapped in the derivation tunnel of the Darial Hydroelectric Power Station (where construction work was carried out) when the landslide hit). Another accident occurred very soon on August 20, 2014. Due to heavy rains in the second decade of August 2020 and especially heavy rain that took place on August 20, 2014, large fragments of the Devdoraki glacier fell and a large amount of clastic material, accumulated on the slopes of the mountain, dropped into the Tergi River and once again partially blocked the riverbed. As a result, water from the destroyed dam devastated the existing infrastructure: road, conventional, and almost complete hydroelectric power (Kordzakhia et al. 2015 [23]). Such events, reflecting the quirks of the current climate change, have become a frequent occurrence in Georgia in recent years.

1.1.3. Glaciers' melting on the territory of Georgia

According to the first catalog of Caucasus glaciers, the modern process of glacier retreat began with the "Fernau" stage in 1850, when the total area of the Caucasus glaciers decreased by 333km^2, and made 1997km^2 (Podozersky 1911 [31]). According to a newer catalog of glaciers, the total area of the Caucasus glaciers decreased by 511 km^2, while in the northern regions of the Caucasus, the area of glaciers decreased more significantly. Over this period, the total area of the Caucasian glaciers on the territory of Georgia decreased by 231 km^2 (Svanidze and Tsomaya 1999 [39], Tielidze and Wheat 2018 [43]). At present, modern Georgian glaciers are dominated by processes of retreat and melting (the size of large glaciers breaks into smaller ones, the volume and length of glaciers decrease) due to accelerated climate change. Studies conducted for Western Georgia showed that during the extremely hot and cold months of 1961-1999, glacier runoff decreased by 2-15%, which was due to an increase in heavy snowfall in winter and an increase in cloud cover in the north of Western Georgia (Tsomaia and Meskhia 2007 [44]). Over the same period, glacial flow in eastern Georgia increased by 14-23% compared with 1931-1960, due to a decrease in rainfall and snowfall during very hot and cold months and an increase in the frequency of extremely hot months (which was accompanied by accelerated melting of glaciers). As a result of the melting of the glaciers, many negative landforms appeared, such as circuses, frugally of the valley, exterminated landforms, etc. (Huggel et al. 2003 [16]; Andreas et al. 2006 [2]; Gorgijanidze and Tsintsadze, 2007 [15]). These landforms gave rise to dam lakes, which in most cases are located inside glaciers. In total, there are about 16 such types of glaciers in Georgia (Gorgidzhanidze and Tsintsadze 2007 [15]). The influence of glacier fluctuations (melting) on water resources has been recognized since the end of the 19th century (Oerlemans 1997 [29]). As a rule, glacier vibrations affect human activities, such as the construction and operation of hydropower plants, and runoff for irrigation purposes (Van de Wal and Wild 2001 [45]). In addition, glacier melting contributes significantly to secular sea level fluctuations (Oerlemans et al. 1997 [29], Dyurgerow and Meier 1997 [9], Zuo and Oerlemans 1997 [29]).

Numerical modeling is a good tool for understanding the behavior of individual glacier flows, since each glacier has its own geometry and dynamic behavior (Shakhgedanova et al., 2009 [34]). So a study glacier fluctuation is of paramount importance in knowledge and in predicting the distribution of water resources in Georgia. Modeling and estimation of rapid changes in the parameters of glacier melting in high mountains (usually, in the absence of observational data on the spot) leads to the

use of high-tech remote sensing and GIS systems (Huggel et al. 2003 [16], 2004 [17], Shengelia et al. . 2012 [36]). Based on these observational data, a number of formulas were developed that expressed the correlation between the change in the average temperature of the atmosphere and the corresponding height of mountain glaciers (Svanidze and Tsomaya 1999 [39], Tsomaya and Meskhiya 2007 [44], Davitashvili et al. 2008 [8]). A similar simple formula (1.1) was developed for the Caucasus glaciers based on observational data (Davitashvili et al., 2008 [8]).

$$T_i = T_o + K \cdot (H_i - H_o) \tag{1.1}$$

where H_0, H_i, and T_0, T_i are the values of the corresponding glacier heights and temperatures at the initial and studied time instants, respectively. K is a constant parameter, value of which is determined individually for each glacier.

In the framework of this study, formula (1.1) was considered on the example of the Devdodaraki and Gergeti glaciers. The results were estimated by ERA-Interim and in situ data (over the past 20 years, obtained from the Kazbegi high-altitude weather station), located on the snowline of 3650 m). The calculation results showed that K = 0.00620 ° C m^{-1} for the Gergeti and Devdoraki glaciers, since the difference between the calculated and real (observed) values did not exceed 1.4-2%. Thus, within the framework of such an error, Formula (1.1) can be used to assess the vulnerability of glaciers to expected climate changes. According to studies in modern climate warming, the risk of a temperature increase of 2 ° C in Eastern Georgia is high by 2050 (IPCC 2007 [18], Sylven et al. 2008 [41], Tielidze and Pshenitsa (2018 [43])., Shakhgedanova et al. 2009 [34]). Based on this assumption and considering that H0 = 3670, Ti-T0 = 2 ° C, from (1.1) we get that Hi = 3992. This means that with an increase in temperature by 2 ° C, the Gergeti glacier will completely disappear. Almost the same conclusions were obtained for Devdoraki and other glaciers of the eastern Caucasus, located almost at the same heights or below. The disappearance of glaciers against the background of prolonged warming of the weather will undoubtedly have a significant negative impact on agriculture and the availability of water in reservoirs (Summary of the IPCC Analytical Report 1991 [38]). Long-term fluctuations of glaciers are mainly determined by the influence of air temperature, solid precipitation and the total volume of the glacier (Schneeberger 2006 [32]). When modeling changes in the mass balance of the glacier, it is necessary to know the current volume of the glacier, which is not a trivial task. Indeed, it is not easy to determine the volume (thickness and topography of the bed) of glaciers, even having some data on glaciers obtained using remote sensing, aerial surveys and radio-sounders (Shengelia et al. 2012 [36]).

To overcome this problem (lack of data), several methods have been proposed for simple estimation of ice volume based on glacier surface area and empirical ratios of area and volume (Chen and Ohmura 1990 [5]). For a glacier in steady state, Chen and Omura (2009 [5]) proposed scale dependences between the volume V of the glacier and the surface area S, using the formula $V = 28.5 \cdot S^{1.357}$. Such relationships allow the use of remote sensing, radio sounding and other methods to determine the volume of the glacier, if the surface area of the glacier is known. If we assume that the volume-to-area ratio is always satisfied, then we can use it to obtain an aria with decreasing volume (Meier and Bahr, 1996 [27]; Braithwaite and Olesen, 1989 [4]). Based on similar methods, Van de Val and Wild (2001 [45]) found that the mass of all glaciers would decrease by 15–20% over the next 70 years. But these conclusions were drawn on the assumption that the scale relations between the volume V of the glacier and the surface

area S, will be preserved in the future, which is a controversial issue both in this case and for K = 0.00620 ° C m-1 in (1.1) too. We used the Van de Val and Wild method (2001 [45]) to determine the melting rate of some Caucasus glaciers. For example, it was found that the mass of the Devdoraki glacier will decrease by about 40-45% over the next 70 years, which is not consistent with the results obtained from (1.1). Thus, for a better understanding of the main features of regional processes of climate change in mountainous areas, it becomes necessary to use more reliable methods of mathematical modeling based on the integration of complete systems of equations of hydrothermodynamics.

1.2. Forecast of changes in some climatic parameters using the PRECIS model

Due to the civil war and the difficult economic situation, the number of weather stations in Georgia over the past four decades has decreased from 86 to 11, and therefore there is a need to more intensively use modern satellite technologies with reliable mathematical modeling methods to better understand regional processes of climate change (degradation of the surface soil layer, melting of glaciers, acceleration of extreme events, desertification, etc.) (Kondratiev and Galindo 2002 [22]). To predict the expected changes in some climatic parameters until 2050 in Georgia, it became necessary to use Providing Regional Climate Research for Impact Studies (PRECIS) model (with a resolution of 25 km x 25 km) with the MAGICC / SCENGEN statistical software (Kutaladze et al. 2005 [24]). The PRECIS system was designed for researchers (with a focus on developing countries) to study the impact, vulnerability and adaptation of climate change to their region of interest. The PRECIS system contains two regional climate models- HadRM3P and HadRM3Q0. The HadRM3P is based on the UK Met Office's HadCM3 General Circulation Model (GCM), which use the Navier–Stokes equations on a rotating sphere with thermodynamic terms for various energy sources (radiation, latent heat etc).

The results of calculations performed according to the PRECIS model showed that by 2050 the amount of precipitation decreases and the temperature rises throughout Georgia, which will lead to a decrease in the flow of Georgian rivers and cause problems with water supply (a 5% decrease in the total amount of precipitation in Georgia is expected to be strong interseasonal variability). These problems will be more vulnerable in high-consumption rivers in eastern Georgia (such as Iori). It is also expected that the climate change process will affect different regions of Georgia in different ways. It is expected that in Eastern Georgia (especially in the Dedoplistskaro region) the amount of precipitation will decrease on average by 7%, and in the summer - by 30%. This will increase the frequency of droughts and reduce annual runoff by 5-6% in the Iori River (which is the most vulnerable). On the territory of Western Georgia and especially in the coastal zone, the frequency of storms, floods, runoff and sedimentation in rivers will increase due to an increase in temperature gradients, precipitation and melting glaciers (Kutaladze et al. 2005, [24]). Currently, a decrease in annual precipitation of 4% is observed in the coastal zone of Georgia, but PRECIS calculations have shown that only seasonal winter precipitation will increase by 14%. The calculation results also showed that this will lead to an increase in river flow by 5-10% in the Rioni and Tskhenistskali rivers in the spring seasons and, thus, a strong negative impact on the frequency of floods and the occurrence of landslides is expected. , Since 1925, the Black Sea level has already risen by 0.7 cm, and the Black Sea in some areas has covered the coast with a width of 3.5 km. The calculation results showed that in 2050 the Black Sea level in the Rioni delta is expected to increase by 20-30 cm, which

will lead to catastrophic consequences (SNCU NFCCE, 2009; Kutaladze et al. 2005; Zhang et al. 2005; Matchatashvili and dr. 2006).

References to Chapter 1

1. Aguilar E., Auer I., Brunet M., Peterson T.C., J. Wieringa. Guidelines on climate metadata and homogenization (WMO-TD No. 1186, WCDMP No. 53), World Meteorological Organization, Geneva, Switzerland (2003), p. 55
2. Andreas K., Huggel C.and L.Fischer, 2006, Remote Sensing Technologies for Monitoring Climate Change Impacts on Glacier- and Permafrost-Related Hazards, 2006ECI Conference on Geohazards,Lillehammer,Norway, pp.67-78
3. Beritashvili B., Kapanadze N. 2011. Fuatures of climate change in the second half of the past century at the territory of Georgia / *Transactions of the Institute of Hydrometeorology of GTU* : 124 p.p 91-96
4. Braithwaite R. J., and O. B. Olesen, 1989. Calculation of glacier ablation from air temperature, West Greenland *In J. Oerlemans (Ed.), Glacier Fluctuations and Climatic Change*, Kluwer Academic Publisher, 1989, pp.124-135
5. Chen J. and A. Ohmura, 1990. Estimation of Alpine glacier water resources and their change since 1870s. In H. Lang and A. Musy (Eds.), Hydrology in Mountainous Regions I, Volume 193, 1990, pp. 172–135. IAHS.
6. Davitashvili T and A. Khantadze, 2008. On climate, desertification and water pollution problems for the territory of Georgia" Netherlands: Springer-Verlag,,2008,pp.453-469.
7. Davitashvili T, Khantadze A. and Kh. Sharikadze. 2002. Influence of Non-linear Heat sources on Climate Change". *Reforts ofVIAM.* Vol.17. N3, 2002, pp.21-29.
8. Davitashvili T., Khvedelidze Z., Khantadze A., Tavartkiladze K. and I.Samkharadze, 2008. Investigation of Some Climate Singularities on the territory of Georgia by Mathematical Modeling",- *Transactions of the Institute of Hydrometeorology* Vol.115, pp. 7-19.
9. Dyurgerow A. and S. Meier, 1997. Mass balance of mountain and subpolar glaciers: A new global assessment for 1961– 1990, *Arct. Alp. Res*., 29, 1997a, pp.379–391.
10. Elizbarashvili E.Sh.,Varazanashvili O.Sh., Elizbarashvili M.E., Tsereteli N.S., 2011. Light frosts in the freeze free period in Georgia. Russ.Meteorol.Hydrol. 36, 399–402. http://dx.doi.org/10.3103/S1068373911060069.
11. Elizbarashvili E. Sh., Tatishvili M.R., Elizbarashvili M.E., Elizbarashvili Sh.E., Meskhiya R.Sh., 2013. Air temperature trends in Georgia under global warming conditions. Russ. Meteorol. Hydrol. 38, 234–238. http://dx.doi.org/10.3103/ S1068373913040043.
12. Elizbarashvili E.Sh., Meskhiya R.Sh., Elizbarashvili M.E., Megrelidze L.D., Gorgisheli V.E., 2009a. Frequency of occurrence and dynamics of droughts in 20th century were studied based on the observational materials of 20 meteorological stations of Eastern Georgia. Russ.Meteorol.Hydrol. 34, 401–405. http: //dx.doi.org/10.3103/S1068373909060107.
13. Gigineishvili V.M. hail in eastern Georgia.L., 1960 (Russian).
14. Gogishvili K.S. The study of circulating factors genesis of the climate of Georgia. Tb., 1974 (Russian).
15. Gorgijanidze S., Tsintsadze N., 2007, Geography of dam lakes created by the glaciers stepping back, Transactions of the Hydrometeorological Institute, V.111, p. 43-49 (Georgian)

16. Huggel C., Haeberli W., Kääb A., Ayros E.and C.Portocarrero, 2003, Assessment of glacier hazards and glacier runoff for different climate scenarios based on remote sensing data: a case study for a hydropower plant in the Peruvian Andes. EARSel eProceedings, 2, pp.22-33.
17. Huggel C., Kääb A., and N. Salzmann, 2004, GIS-based modeling of glacial hazards and their interactions using Landsat TM and Ikonos imagery. Norwegian Journal of Geography, 58, pp.61-73.
18. IPCC, 2007. Climate Change 2007: Synthesis Report. Pachauri, R.K. and A. Reisinger (eds.), Contribution of Working Groups I, II and III to the Fourth Assessment. Report of the Intergovernmental Panel on Climate Change. IPCC, Geneva, Switzerland. 104 pp.
19. IPCC,2013.Edited by Stocker T.F., Qin D.,Plattner G-K., Tigner M.M.B. Allen S.K. https://www.ipcc.ch/site/assets/uploads/2018/03/WG1AR5_SummaryVolume_FINAL.pdf
20. Javakhishvili Sh. Atmospheric precipitation on the territory of Georgia. Tb., 1981(Georgian).
21. Keggenhoff I., Elizbarashvili M., King L. Recent changes in Georgia's temperature means and extremes: Annual and seasonal trends between1961and 2010. Weather and Climate Extremes 8, (2015), 34–45
22. Kondratyev K.Ya and, I. Galindo, 2002.*Contemporary stage of civilization development and its perspectives*, Univ. of Colima Press.
23. Kordzakhia G., Shengelia L., Tvauri G., and M.Dzadzamia, 2015. The Research of Devdoraki Glacier Based on Satellite Remote Sensing Data and Devdoraki Glacier Blockage Analysis in Historical Context, Report of ICAE 7-10 May, 2015, Tbilisi-Batumi, pp.56-65
24. Kutaladze N., Kartvelishvili L., Kordzakhia G., Shavishvili N. and L.Megrelidze, 2005. Reccurence ofextreme temperature events inGeorgia on background of climate change. Bullit. of GeorgianAcademy of sciences 171, N3, pp.489-480.
25. Levitus S.,J. Antonov L. and J. Wang,2001. Anthropogenic warming of Earth's climate system. *Science,* vol. 292, N 5515, 2001, pp. 267-270.
26. Matchatashvili T.,,Kutaladze N.. Japaridze P., Megrelidze L. and D.Mikautadze 2006. Trends and long Range correlation in Daily Temperature Records in Georgia. Bullit. of Georgian Academy of sciences 173, N1, pp.95-98.
27. Meier M. F. and D. B. Bahr, 1996: Counting glaciers: Use of scaling methods to estimate the number and size distribution of the glaciers of the world In S. C. Colbeck (Ed.), Glaciers, Ice Sheets and Volcanoes: a Tribute to Mark F. Meier, Hanover, New Hampshire, pp. 89–94. CRREL Special Report 96-27: U. S. Army.
28. Mindorashvili A. 2002, Urgent problems of Georgian's population protection with drinking water and its quality monitoring. *Transactions of the Institute of Hydrometeorology*: 108 p.p 91-96
29. Oerlemans J., 1997. A flowline model for Nigardsbreen, Norway: Projection of future glacier length based on dynamic calibration with the historic record, *Annals of Glaciology*, 24, 1997, pp. 382-389.
30. Oerlemans J., Anderson B. Hubbard A., Huybrechts Ph., Johannesson T., Knap W.H., Schmeits M., Stroeven A.P., Van de Wal R.S.W., Wallinga V. and Z. Zuo, 1998. Modelling the response of glaciers to climate warming, *Climate Dynamics*.14, 1998, pp.267-274.

31. Podozersky E.T., Catalogue of Glaciers, 1911(in Russian).
32. Schneeberger Ch., Glaciers And Climate Change: A Numerical Model Study,*2006 Diss. ETH No. 14743,* A dissertation submitted to the Swiss Federal Institute Of Technology Zurich.
33. Second National Communication to the United Nations Framework Convention on Climate Change. Ministry of Environment Protection and Natural Resources, Republic of Georgia. 2009, www.unfccc.int, p.240
34. Shahgedanova M., Hagg W., Hassell d., Stokes C.R. and V. Popovin, 2009. Climate Change, Glacier Retreat, and Water Availability in the Caucasus Region, *In Book Threats to Global Water Security*, Editors: J. Anthony A. Jones, Trahel G. Vardanian, Christina Hakopian,Publisher Springer Netherlands, 2009, pp. 131-140.
35. Shea J. M., Immerzeel W. W., Wagnon P., Vincent C., and S. Bajracharya, 2015, Modelling glacier change in the Everest region, Nepal Himalaya, The Cryosphere, 9, 1105-1128,
36. Shengelia L. Kordzakhia G., Tvauri G., Davitashvili T., and N.Begalishvili, 2012. Possibilities of the use of remote sensing technologies for the estimation of modern climate change impact on the Caucasus glaciers, *Georgian National Academ y of Sciences, Monthly Scientific-Reviewed Magazine, "Science and Technologies"*, Vol.4-6, 2012, pp. 25-30.
37. SNCUNFCCC-*Second National Communication to the United Nations Framework Convention on Climate Change*; Ministry of Environment Protection and Natural Resources, Republic of Georgia. 2009, www.unfccc.int, p.240
38. Summary of Analytical Report by IPCC. *Bulletin of WMO*, vol.1, No. 1., 1991.
39. Svanidze G. and V.Tsomaia, 1999, Assessment of vulnerability of Georgian glaciers to expected climate change, Georgian National Bulletin of the UNFCCC, No 8(E), pp. 52-60
40. Svanidze G., Tsomaia V. et.al, 1988: Water Resources of Trancaucasia. Leningrad: Gidrometizdat Press.
41. Sylvén M., Reinvang R. and Z. Andersone, 2008, WWF overview report, Climate Change in Southern Caucasus: Impacts on nature, people and society, p.35
42. Third National Report of Georgia, 2006. On The Implementation of the UN Convention to Combat Desertification, May, 2006, Tbilisi, Georgia, p.24
43. Tielidze L.G. and R. D. Wheate, 2018. The Greater Caucasus Glacier Inventory (Russia, Georgia and Azerbaijan), The Cryosphere, 12, 81–94, https://doi.org/10.5194/tc-12-81-2018
44. Tsomaia V. and R. Meskhia, 2007, The dynamic of glacial flow in Georgia according to the modern climate change conditions, Transactions of the Hydrometeorological Institute, V.111, p. 26-29 (Georgian)
45. Van de Wal R. S. W. And M. Wild, 2001. Modelling the response of glaciers to climate change by applying vloume-area scaling in combination with a high resolution GCM, *Climate Dynamics* 18(3-4), 2001, Dec. pp.359–366.
46. Westphal M. I., Mehtiyev M., Shvangiradze M. and V. Tonoyan, 2011, Regional Climate Change Impacts Study for the South Caucasus Region, p.63.
47. World Bank, 2006. Drought: management and mitigation assessment for Central Asia and the Caucasus (Regional and Country Profiles and Strategies).World Bank, Washington DC,USA.

48. Zhang X., Aguilar E., Sensoy S., Melkonyan H., Tagiyeva U., Ahmed N., Kutaladze N. and all, 2005: Trends in Middle East climate extreme indices from 1950 to 2003, Journal of Geophisical Researchs, V. 110, D22104, 12 PP., doi:10.1029/2005JD006181
49. Zuo, Z. and J.Oerlemans,1997. Numerical modelling of the historic front variation and the future behaviour of the Pasterze glacier. *Ann Glaciol* 24, 1997, pp.234-241.

Chapter 2. SOME FEATURES OF CLIMATE CHANGE IN WESTERN GEORGIA

Currently, the global cycle of climate warming is the result of a number of natural factors and is especially a consequence of anthropogenic activities. Indeed, in addition to natural factors (eruptions of volcanoes and geysers, forest fires, desert storms (sulfur dioxide emissions with other gases and particles), mists (ice fog, steam fog), exudates), anthropogenic aerosol and greenhouse gas emissions (water vapor, oxide carbon, methane, etc.) enhance the global warming cycle. The Accumulation of the anthropogenic aerosols and greenhouse gases in the lower atmosphere (h=6km) plays the role of the scum, which enhances the solar warming of the atmosphere (significantly reduces the long-wave flux sent from the Earth into space) (Bulletin of WMO 1991 [1]). Indeed, in a physical system with strong nonlinear thermal parameters (heat content, thermal coefficient of turbulent exchange, coefficient of heat inflow and loss, etc.), the system becomes dependent on temperature and the nonlinear thermal process (over a certain time), causes an increase in the characteristic temperature of the system over time and it creates a "greenhouse effect" in the system (Ramathan 1989 [17], Bulletin of WMO 1991 [1]).

Currently, non-linear heat sources are already operating in the atmosphere, and their intensity may increase in the future. The “greenhouse effect”" is a direct result of the accumulation of “radiation” gases caused by human activities (the rapid development of industrialization of oil, gas, coal, and other types of organic resources). This process was followed by the accumulation of combustion products (radiation gases): carbon dioxide (CO_2), nitrogen, peroxide (N_2O), methane (CH_4), freons $CFCL_3, CF_2CL_3$, ozone (O_3) in the lower atmosphere. Against the backdrop of global climate change, climate change in Georgia is characterized by pronounced regional features. In Georgia, both warming and cooling are observed. Namely, statistical processing of data on average climatic temperature for 1905-2005, showed a sharp process of warming in eastern Georgia and a cooling of the climate in western Georgia. Microregions were also identified where the average climatic temperature did not change with time (SNCU NFCCE 2009 [20]). The indicated climate variability throughout Georgia corresponds to the picture of global climate change obtained as a result of observations carried out in accordance with the global climate research program and model calculations of the global climate (Krapivin et al. 2002b [16]).

2.1. Influence of thermal and advective-dynamic factors on climate change

Since the climate cooling process occurs mainly on the territory of Western Georgia, it is necessary to find permanent thermal and advective-dynamic sources there that will be periodic in time, its frequency will be of the order of a year, and the characteristic horizontal and vertical scales will be 200-300 km and 3 -4 km. The magnitude of the indicated spatial scales for Western Georgia is determined by the average values of longitude and latitude, as well as the distribution zone of thermal and advective-dynamic sources along the troposphere. The vertical scale of closed circular flows generated by these sources is less than the height at which the “greenhouse effect” usually appears. According to international experts, this height reaches 6-8 km from the Earth in the troposphere, but for the surface of the mountain it is 4-5 km (Bulletin of

WMO 1991 [1]). Among the many atmospheric circulation processes occurring in Western Georgia, only the monsoon circulation is characterized by such spatial and temporal parameters that are associated with irregular warming of the Black Sea and Kolchi lowland during the year(Shuleikin, 1968 [19]). This circulation (which cannot exist in Eastern Georgia) should be caused by the action of two constantly operating heating mechanisms, in which the Kolchi lowland plays the role of heating, and the Black Sea plays the role of a refrigerator in summer, but conversely during a winter (Kolchi lowland is a refrigerator and the Black Sea is a heating). Naturally, against the background of changes in global climatic parameters, this alternation of sources leads to changes in the temperature of the region with an annual period. The diversity of the general circulation of the Earth's atmosphere and the failure of zonal regularity due to heat and cold sources (ocean-land), well known as "second-order" thermal machines, in the thermodynamics of the atmosphere (Shuleikin 1968 [19]). Studies indicate the existence of a monsoon type circulation in Georgia (Kordzakhia 1981 [14]; Davitashvili et al. 2002 [5]), but it should be noted that the horizontal component of the monsoon velocity (whose value does not exceed 1-3 m/s) is insignificant as compared to the dominant winds (5-10 m/s) and its exposure requires statistical processing of climatic parameters for a long time. Unfortunately, Georgian experimental meteorologists have not yet conducted large-scale research in this direction. Since the reality of the existence of sources generating monsoon circulation in Western Georgia has no alternative (only daily sources of circulation of breeze, valleys and mountains are similar), we a priori assume the existence of such circulation in Western Georgia (a real exposition and a detailed description of which should be relevant subject of future research of Georgian weather forecasters).The monsoon type circulation, which is the largest among the daily circulations existing in Western Georgia, can easily cover the entire territory of Western Georgia, including the Likhi ridge. This circulation, rotating clockwise in winter and having an upward flow over the Black Sea (rather far from the coast), is characterized by descending flows over the Likhi ridge (Kordzakhia 1981 [14]). In summer, the circulation has the opposite direction of rotation, and the ascending flows over the Likhi ridge change downstream over the Black Sea. The distance between the ascending and descending flows depends on the contrast (intensity) of the summer and winter circulations during the year (Javakhishvili, 1988 [11]).

Considering that at the Likhi Summit (in a mountain valley) and on the Black Sea, breeze circulation causes intense precipitation (Kordzakhia 1961 [14]; Javakhishvili 1981 [10]), it can be assumed that the latent heat of condensation caused by precipitation production contributes to the monsoon circulation, the velocity of the vertical component of which W can reach 1.5-3 cm/s. In this case, from the following continuity equation

$$\frac{\partial U}{\partial x}+\frac{\partial W}{\partial z}=0, \tag{2.1.1}$$

we get a fundamental result for the width characteristic of the movement of monsoons:

$$H \approx L\frac{W}{U} \approx 3 \div 4{,}5\,\text{km}, \tag{2.1.2}$$

where $L \approx 200 \div 300\,\text{km}$ is the characteristic horizontal length of the monsoon motion, $W \approx 1{,}5 \div 3\,\text{cm/s}$, $U \approx 1 \div 2\,\text{m/s}$ are accordingly its vertical and horizontal velocity components.

Relation (2.1.2) justifies the magnitude of vertical scale and the existence of the circulation of closed type, which we postulated above.

Let us show that the thermal and advective – dynamic factors characteristic of this region should play an important role in generating the monsoon flow in Western Georgia. Namely, the thermal factor, caused by the baroclinity of the atmosphere (as a result of irregular heating of the Black Sea and Kolchi lowlands in summer and winter), causes the intersection of isobaric and isothermal surfaces and the intensification of this circulation in the region mentioned above. The effect of baroclinity on air circulation is described by V. Berknes formula (Gandin et al. 1989 [8]):

$$\frac{d\Gamma}{dt} = -\int \frac{dP}{\rho} = R(T - T_0)\rho_n \frac{P}{P_0}, \tag{2.1.3}$$

where Γ is the circulation of velocity of the atmospheric particle along a closed curve, P_0, T_0, P, T are the pressure and temperature on the land and sea surface, respectively.

The Berknes formula (2.1.3), which theoretically well describes the mechanism of circulation generation and its amplification in time, gives irrational results in numerical estimates. Indeed, if we put the values of P_0, T_0, P, T in this formula and assume that the length of the closed curve is $400 \div 600$ km, we get that after 1-1,5 hours the magnitude of wind velocity in the monsoon flow should reach the magnitude of the velocity of the storm $(50 \div 100 m/s)$, that practically never occurs.

This fact shows that the Burknes formula numerically describes the unreal monsoon flow. In particular, this formula does not take into account two important factors existing in the atmosphere:

1. The amplification of wind in the monsoon flow, caused by baroclinity and decreases the temperature difference between land and sea and, accordingly, reduces circulation;
2. The Berknes formula does not take into account turbulent friction between the atmospheric layer and the Earth's surface, which also reduces the circulation flow.

If we denote by $B(\Gamma)$ the magnitude of these two factors that reduce circulation, the Berknes formula will take the following form (Davitashvili et al. 2002, [5]):

$$\frac{d\Gamma}{dt} = A - B(\Gamma), \tag{2.1.4}$$

If we expand $B(\Gamma)$ function in Taylor series and take only first two members of the series, we get:

$$B(\Gamma) = B(0) + \alpha\Gamma = \alpha\Gamma, \tag{2.1.5}$$

where $B(0) = 0$, since the function B, which takes into account the factors mentioned above, identically equals to zero when the circulation does not exist. The value of α parameter depends on the intensity of the factors mentioned above.

If we insert (2.1.5) into (2.1.4), we get:

$$\frac{d\Gamma}{dt} = A - \alpha\Gamma . \tag{2.1.6}$$

The Baroclinity A caused by the thermal factor varies in time more slowly than $\alpha\Gamma$ term in equation (2.1.6), and in the first approach we can consider A to be constant. Then a non-stationary solution of equation (2.1.6) with the Cauchy condition ($\Gamma = 0$, when $t = 0$) takes the following form

$$\Gamma = \frac{A}{\alpha}\left(1 - e^{-\alpha t}\right), \tag{2.1.7}$$

and from (2.1.7) for small time intervals we obtain

$$\Gamma = At . \tag{2.1.8}$$

Expression (2.1.8) shows that after the generation of monsoon circulation, baroclinity increases circulation over time. After adding to this process the factors of slowing down the monsoon flow, the circulation becomes stationary

$$\Gamma_{st} = \frac{A}{\alpha} . \tag{2.1.9}$$

where two opposite processes are balanced: baroclinity A, which increases the circulation and the advective – dynamic factors $B = \alpha\Gamma_{st}$, which decrease the circulation by the friction force.

According to Prigozin (Prigozin and Nikolis 1979 [16]), in stationary circulation, as in an organized structure, there is always a joint (coordinated) action of two internal sources. In particular, the intensity with which the first source increases the circulation is equal to the intensity with which the second source reduces it during cooperation. We do not consider the case when the function $B(\Gamma)$ is nonlinear and the existing wind circulation affects the monsoon circulation. This complex problem is the subject of a separate study and, in addition, theoretical analysis requires studying the stability of monsoon circulation using the Lyapunov method (Prigozin and Nikolis 1979 [16]).

The presence of monsoon circulation in the atmosphere practically proves its stability, and therefore we can consider formula (2.1.9) as a mathematical test of the first approximation of monsoon circulation for Western Georgia. This formula describes the effect of constantly acting factors in the territory of this region. Among these factors, surface water cooling of 1 °C along the Black Sea coast in Georgia over the past 80 years can be noted. However, as the first calculations show, this factor can play an important role in the process of cooling the climate in Western Georgia (Davitashvili et al. 2002, [5]).

2.2. Numerical modeling of zonal air flow over the Caucasus region

As we mentioned above, the monsoon-type circulation is the largest among other circulations existing in Western Georgia. This airflow can play an important role in the climate change process in Western Georgia, and therefore it is reasonable to study the nature of this airflow, using reliable methods such as mathematical modeling. To conduct such a study, first of all, it is necessary to review all types of basic synoptic processes that dominate in Georgia.

The classification of the main synoptic processes observed over the territory of Georgia, and the nature of the weather caused by these processes, were well studied by Georgian synoptic-meteorologists (Kordzakhia 1961 [14]; Javakhishvili 1981 [10], 1988 [11]). The analysis of large-scale synoptic processes carried out in these studies showed that the following six atmospheric processes prevail in Georgia:

- Western atmospheric processes (with zonal transfer of atmospheric masses towards latitude, with a frequency of about 54%) ;
- Eastern atmospheric processes (with a frequency of about 21% per year);
- Anticyclone processes at high pressure (about 7% per year);
- Wave mixing in Georgia (mainly originate from the southern regions of the Caucasus- about 4% per year);
- Southern atmospheric processes (invasion of a warm front from the south - about 9% per year);
- Mutual atmospheric processes (invasion from the west and east at the same time - about 1.5% per year).

It should be noted that cases of invasion of cold (warm) air masses from the north are very rare. Indeed, as can be seen from Figure 1, the high ridges of the Main Caucasian Range, located along latitude, are a natural obstacle for air masses arriving from the north. Therefore, as a rule, northern atmospheric currents bypass around the Main Caucasian Range and invade on the territory of Georgia from the northwest or northeast (Javakhishvili 1981 [10]). As mentioned above, atmospheric currents coming from the south make up only 13%, while western and eastern atmospheric processes (with zonal transport of atmospheric masses from the Black Sea to the Caspian Sea and vice versa) account for about 75%. That is why, for a better understanding main reasons of climate cooling in Western Georgia, it is necessary to study the structural variability of meteorological fields in the lower atmosphere when atmospheric flows are transferred from the Black Sea to land and vice versa.

The studies showed that climate formation on the territory of Georgia is the result of joint actions of large-scale synoptic and especially local processes, which are mainly due to the complex orography of the Caucasus (Khvedelidze and Davitashvili 1978 [12]; Davitashvili and Janelidze 1979 [4]; Davitashvili 1996 [2]). In addition, the geographical location plays an important role in the formation of the regional climate in Georgia (Kordzakhia 1961 [14]; Javakhishvili 1981 [10], 1988 [11]). Indeed, on the one hand, the location of Georgia between the Black and Caspian Seas, and on the other hand, its location between the ranges of the Main and Lesser Caucasus, play an important role on spatial-temporal redistribution of meteorological fields in Georgia. Observation of the territory of the Caucasus from near space shows that in Georgia formed a natural channel for the transfer of atmospheric masses from west to east and back (see Fig. 1). Indeed, Fig. 1 shows that there is a convenient passage, between the Main and Lesser Caucasus, with a single obstacle (the Likhi Mountain Range that connects the ridges of the Main and Lesser Caucasus Ranges and located in the central part of Georgia) for possible transfer atmospheric masses between the Black and Caspian Seas. To the west of the Likhi Range, the relief gradually becomes lower, forward to the Black Sea coast (Colchis Lowland). On the eastern side of the Likhi Range is the Kartly Plain, which extends along the Kura River to the border of Azerbaijan. Figure 1 shows that the Black Sea and the mountains of the Main and Lesser Caucasus with the Likhi Range can play an important role in shaping the climate in Western Georgia. Studies have shown that large-scale synoptic processes in Georgia are unsteady in nature, and their alternation significantly affects the pattern of

circulation of mesoscale air currents (Javakhishvili 1988, [11]). In the process of studying this issue, the question arises of how much mesoscale flows are subjected by the variability of large-scale processes in complex orography. Such studies were partially carried out for the territory of Georgia using 2 and 3-D hydrostatic models in (Demetrashvili 1979 [6]; Demetrashvili and Davitashvili 2013 [7]; Davitashvili and Demetrashvili 2015 [3]).

This chapter is devoted to a numerical study of the structural variability of meteorological fields in the lower atmosphere when atmospheric masses are transported from the Black Sea to land and vice versa and are influenced by unsteady large-scale background flows and an orographically inhomogeneous earth's surface. To achieve this goal, we use a three-dimensional hydrostatic non-stationary model designed for a "dry atmosphere" (Davitashvili and Demetrashvili 2015, [3]).

Consider the air mass moving in the troposphere, which is bounded below by an inhomogeneous underlying earth surface $\delta(x, y)$, and above, at the height of the tropopause, by a free surface *H(x,y,t)*, the variability of which is determined by the integration of model equations (Fig. 2.1). For simplicity, at the first stage, let's neglect the condensation and radiation processes taking place in the atmosphere.

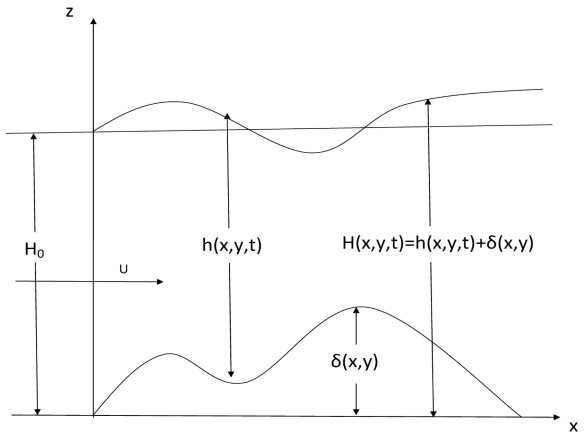

Fig. 2.1. Schematic vertical section of the modeling area

According to the ideas proposed in (Kibel 1964, [13], Gutman 1972, [9]), using simplifications of the theory of free convection, the problem of transporting atmospheric masses in the troposphere is formulated in terms of deviations from the background values of meteorological parameters. After transition from Cartesian coordinate system (x, y, z) (the axes x, y and z are directed eastward, northward and vertically upward, respectively) to the terrain-following system x_1, y_1, ζ, where

$$x_1 = x,\ y_1 = y,\ \zeta = \frac{z - \delta(x,y)}{h(x,y,t)},$$
$$h = H(x,y,t) - \delta(x,y)$$

the model system of equations get the following form (Davitashvili and Demetrashvili 2015 [3]):

$$\frac{du}{dt} = -\Theta_0 \frac{\partial \varphi'}{\partial x} + \lambda \vartheta' \left(\zeta \frac{\partial h}{\partial x} + \frac{\partial \delta}{\partial x} \right) + l\,\mathrm{v} + \mu \Delta u + F_u, \qquad (2.2.1)$$

$$\frac{d\,\mathrm{v}}{dt} = -\Theta_0 \frac{\partial \varphi'}{\partial y} + \lambda \vartheta' \left(\zeta \frac{\partial h}{\partial y} + \frac{\partial \delta}{\partial y} \right) - lu + \mu \Delta \mathrm{v} + F_v, \tag{2.2.2}$$

$$\Theta_0 \frac{\partial \varphi'}{\partial \zeta} = \lambda \vartheta' h, \quad \varphi = c_p (p/1000)^{R/C_p}, \tag{2.2.3}$$

$$\frac{d\,\vartheta'}{dt} + Sw = \mu \Delta \vartheta' - u' \frac{\partial \Theta}{\partial x} - \mathrm{v}' \frac{\partial \Theta}{\partial y}, \tag{2.2.4}$$

$$\frac{\partial h}{\partial t} = e^{\sigma h} \int_0^1 E\, e^{-\sigma h \zeta} d\zeta, \quad \tilde{w} = \frac{1}{h} \left[e^{\sigma h \zeta} \int_0^{\zeta} E e^{-\sigma h \zeta} d\zeta - \zeta\, e^{\sigma h} \int_0^1 E\, e^{-\sigma h \zeta} d\zeta \right], \tag{2.2.5}$$

$$w = \zeta \frac{\partial h}{\partial t} + u \left(\zeta \frac{\partial h}{\partial x} + \frac{\partial \delta}{\partial x} \right) + \mathrm{v} \left(\zeta \frac{\partial h}{\partial y} + \frac{\partial \delta}{\partial y} \right) + \tilde{w} h, \tag{2.2.6}$$

$$E(x, y, t) = \sigma u h \left(\zeta \frac{\partial h}{\partial x} + \frac{\partial \delta}{\partial x} \right) + \sigma \mathrm{v} h \left(\zeta \frac{\partial h}{\partial y} + \frac{\partial \delta}{\partial y} \right) - \frac{\partial u h}{\partial x} - \frac{\partial \mathrm{v} h}{\partial y}. \tag{2.2.7}$$

where,

$$\frac{d}{dt} = \frac{\partial}{\partial t} + u \frac{\partial}{\partial x} + \mathrm{v} \frac{\partial}{\partial y} + \tilde{w} \frac{\partial}{\partial \varsigma}, \quad \Delta = \frac{\partial}{\partial x^2} + \frac{\partial}{\partial y^2},$$

$$\mathrm{u} = \mathrm{U} + \mathrm{u}', \ \mathrm{v} = \mathrm{V} + \mathrm{v}', \ \mathrm{w} = \mathrm{w}', \ \vartheta = \Theta + \vartheta', \ \varphi = \Phi + \varphi',$$

$$\mathrm{F_u} = -\mathrm{lV} + \frac{\partial \mathrm{U}}{\partial \mathrm{t}}, \ \mathrm{F_v} = \mathrm{lU} + \frac{\partial \mathrm{V}}{\partial \mathrm{t}}, \ \mathrm{S} = \frac{\partial \Theta}{\partial z},$$

$$\frac{\partial \Theta}{\partial x} = \frac{l}{\lambda} \frac{\partial V}{\partial z}, \quad \frac{\partial \Theta}{\partial y} = -\frac{l}{\lambda} \frac{\partial U}{\partial z}.$$

where the following notations are used: u, v and w are the air velocity components in the Cartesian coordinate system along the axes x, y and z, respectively; $\tilde{w}$ is the analogue of the velocity vertical component in the terrain-following coordinate system; ϑ' and φ' are deviations of the potential temperature and analogue of the pressure from the corresponding background values Θ and Φ, respectivally; U and V are the background velocity components along the axes x, y, respectively; g, Θ_0, l are the gravitational acceleration, the average potential temperature and the Coriolis parameter, respectively; c_P, R, λ are the specific heat capacity at constant pressure p, the gas constant for dry air and the buoyancy parameter; σ is the parameter describing reduction of the density with height; F_u and F_v are given functions of time and space describing the influence of the large-scale synoptic process on the meso-scale process.

The system of equations (2.2.1)-(2.2.7) is solved under the following boundary and initial conditions:

$$\widetilde{w} = 0\,,\ (w = u\frac{\partial \delta}{\partial x} + v\frac{\partial \delta}{\partial y}, z = \delta(x,y))\ \text{if}\ \varsigma = 0\,, \tag{2.2.8}$$

$$\widetilde{w} = 0 \quad (w = \frac{\partial H}{\partial t} + u\frac{\partial H}{\partial x} + \mathrm{v}\frac{\partial H}{\partial y}, \quad z = \delta(x,y)), \quad \varphi' = 0, \ \text{if}\ \varsigma = 1 \tag{2.2.9}$$

$$\frac{\partial u}{\partial x} = 0, \quad \frac{\partial \mathrm{v}}{\partial \mathrm{x}} = 0, \quad \frac{\partial \vartheta'}{\partial x} = 0, \quad \frac{\partial h}{\partial x} = 0, \ \text{if}\ \ x = 0, \ L_x\,, \tag{2.2.10}$$

$$\frac{\partial u}{\partial y} = 0, \quad \frac{\partial \mathrm{v}}{\partial \mathrm{y}} = 0, \quad \frac{\partial \vartheta'}{\partial y} = 0, \quad \frac{\partial h}{\partial y} = 0, \quad \text{if}\ \ y = 0, \ L_y\,, \tag{2.2.11}$$

$$u = u^0, \ \mathrm{v} = \mathrm{v}^0, \vartheta' = \vartheta'^0, \ h = H_0 - \delta\,(x,y)\,, \ \text{if}\ \ \mathrm{t} = 0, \tag{2.2.12}$$

where H_0 is the initial height of the free surface; L_x and L_y are horizontal scales of the calculated domain along x and y, respectively. The basic requirement to the lateral conditions (2.2.10) and (2.2.11) consists that they should provide passing of perturbations, generated inside the solution domain, through lateral boundaries without essential reflection.

The equations (2.2.5) for definition $\widetilde{w}$ and h are obtained from the continuity equation

$$\frac{\partial h}{\partial t} + \frac{\partial uh}{\partial x} + \frac{\partial \mathrm{v}h}{\partial y} + \frac{\partial \widetilde{w}h}{\partial z} = \sigma wh\,,$$

with use of boundary conditions (2.2.8) and (2.2.9) for $\widetilde{w}$.

Thus, the problem is reduced to solution of the equations (2.2.1)-(2.2.7) with the use of the boundary and initial conditions (2.2.8)-(2.2.12) in the rectangular parallelepiped M($0 \le \varsigma \le 1$, $0 \le x \le L_x\,, 0 \le y \le L_y$). The problem is solved numerically by the two-step Lax-Wendroff method (Richtmayer and Morton 1972 [18]).

2.2.1. Airflow modeling over an isolated obstacle

Before conducting numerical experiments to simulate air flow over real topography, consider air flow over an isolated circular obstacle. The shape of the obstacle is given by the formula (Demetrashvili and Davitashvili 2013 [7])

$$\delta(x,y) = \begin{cases} a_0(1 - r^2/r^2{}_0)^3, r = \sqrt{(x - x_0)^2 + (y - y_0)^2} \le r_0 \\ o, \qquad\qquad r > r_0, \end{cases}$$

where a_0 and r_0 are maximum heights and half-width of the obstacle, x_0 and y_0 are the horizontal coordinates of the top.

On a vertical 21 levels were taken by regular vertical steps $\Delta\varsigma = 0.05$. On each level there were 46 x 66 grid points with a grid step 10 km. Other parameters had the following numerical values: a_0=1km, r_0=75km, H_0 = 12 km, $S = 0.003\,K/m$, $\sigma = 10^{-4}\,\text{m}^{-1}$, $l = 10^{-4}\,\text{s}^{-1}$, $\lambda = 0.033\,\text{m/s}^2\text{K}$, $\Theta_0 = 300K$. The time step $\Delta t = 60$ s.

In the numerical experiment the uniform undisturbed background current was directed along the axis x and it changed in time as follows: the background current arose at t = 0 and within two hours reached 12 m/s. After that it did not change up to t = 10 h.

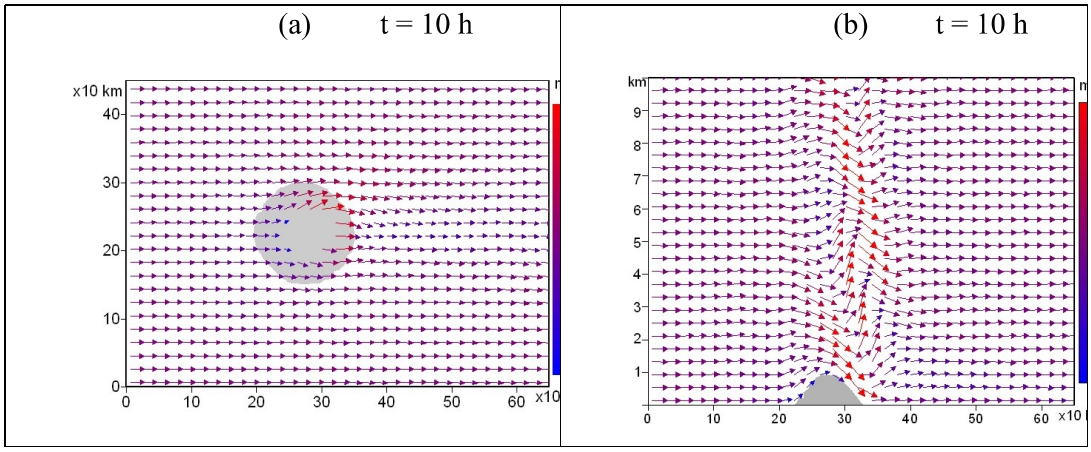

Fig. 2.2. View of the transformed meso-scale airflow at an altitude of z = 500 m, at t=10 h, (a) and view of the meso-scale flow in the vertical (j = 23), at t=10 h, (b).

This numerical experiment was performed to study the nature of mesoscale flow over an obstacle. Fig. 2.2 (a). illustrates the transformation of air flow over the isolated obstacle at the horizon z = 500 m, and in Fig. 2.2 (b) - in the vertical plane zx (passing through the center of the obstacle). Analysis Fig. 2.2 (a) shows that within 10 hours the movement of mesoscale air is disturbed in the horizontal plane and the flow is significantly transformed. In particular, from fig. 2.2 (a) it is clearly seen that during this time the air flow velocity in the obstacle zone increases with the tendency to form vortices in the horizontal plane near the obstacle (Fig. 2.2 (a)). Besides, analysis Fig. 2.2 (b) shows that the amplitudes of the wave current above the obstacle increase significantly throughout the troposphere, and the wave current is gradually converted into an eddy current above the obstacle. It is important to note that almost a similar result was obtained in the framework of the two-dimensional model (Demetrashvili 1979, [6]).

2.2.2. Airflow modeling over the real Caucasus topography

Some numerical calculations were carried out on the basis of equations (2.2.1) - (2.2.7) with boundary and initial conditions (2.2.8) - (2.2.12) taking into account the real relief of the Caucasus. In particular, numerical experiments took into account the matrix data obtained from topographic maps of the Caucasus and its environs using some parameters of the elevations of the terrain and its inclines, with a grid spacing of 10 km, respectively (Fig. 2.3). Comparison of Fig. 2.3 with Fig. 1 shows that Fig. 2.3 satisfactorily describes features of the rather complex and original topography of the Caucasus and is especially good at representing the corridor of atmospheric flows in the territory of Georgia.

For numerical calculations, the considered region M with horizontal dimensions of 830 x 690 km was covered with a grid having 30 levels in the vertical direction and 84 x 70 points on each horizon, with a grid step of 10 km. The time step was $\Delta t = 60$s. Other parameters had taken the following numerical values: H_0 = 12 km, $S = 0.003 K/m$, $\sigma = 10^{-4}$ m^{-1}, $l = 10^{-4}$ s^{-1}, $\lambda = 0.033$ m/s^{2}K, $\Theta_0 = 300K$.

In the numerical experiments the uniform undisturbed background current was directed along the axis ox and it had changed in time as follows: the background currents arose at t = 0 and within two hours have reached 12 m/s. After that it did not change up to t = 10h.

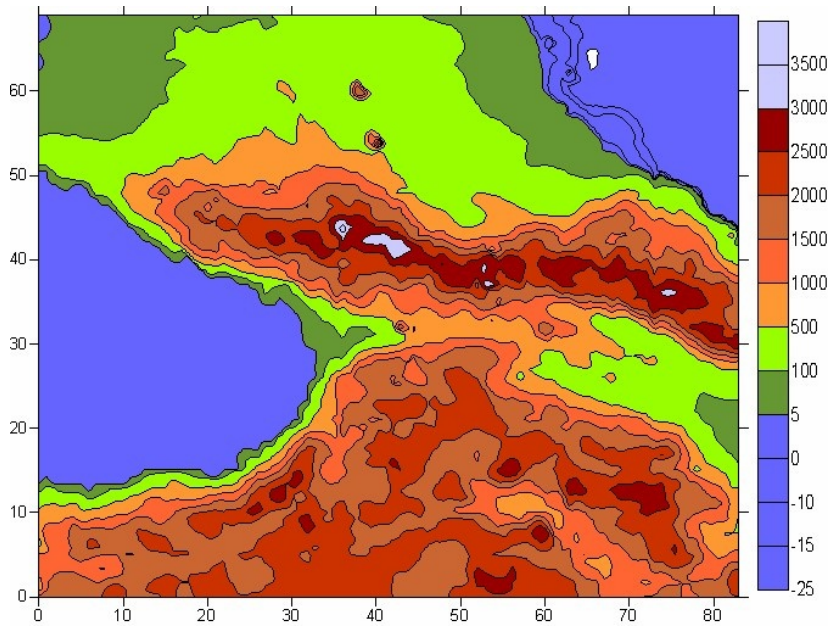

Fig. 2.3. Digital map of the Caucasus (in meters from sea level) used for numerical calculations

Some results of numerical calculations carried out on the basis of equations (2.2.1) - (2.2.7) with boundary and initial conditions (2.2.8) - (2.2.12) are presented by Fig. 2.4. In Fig. 2.4 are presented the disturbed fields of western air currents over the territory of the Caucasus at different heights z = 200, 1500, 3000 and 5000 m (above sea level) at time t=10h. From Fig. 2.4 it is clearly seen that the western flow undergoes significant changes under the influence of orography at time t=10h. Namely, on the shores of Abkhazia and Adjara, which are characterized by rather high mountain systems, the air flow is directed to the north. It is also clearly seen that the bulk of the western air stream avoids the Caucasus Mountains and spreads throughout the northern Caucasus. In addition, the analysis of the flow at z = 200 m shows the formation of a wind vortex counterclockwise over the Colchis Lowland, at velocities of about 12-16 m/s, due to the impact of the orography of the Likhi Range (Fig. 2.4 a), while the analysis of the air flow at z = 1,500 m shows that instead of the formation of wind vortex over the Colchis Lowland, there are some weak formations of air vortices over the Main Caucasus Range (Fig. 2.4 b). Analysis Fig. 2.4 (c, d) clearly shows that with increasing height (from z = 3000 m to z = 5000 m), the influence of the mountains of the Main Caucasus weakens, and the direction of the air flow gradually returns to its background direction, but, nevertheless, the effect of orography to the moving air flow is clearly traced by the

deviation of the air flow path and by the increase in air flow velocity (maximum wind speed reaches about 26 m / s) over the mountains of the Main Caucasus Range.

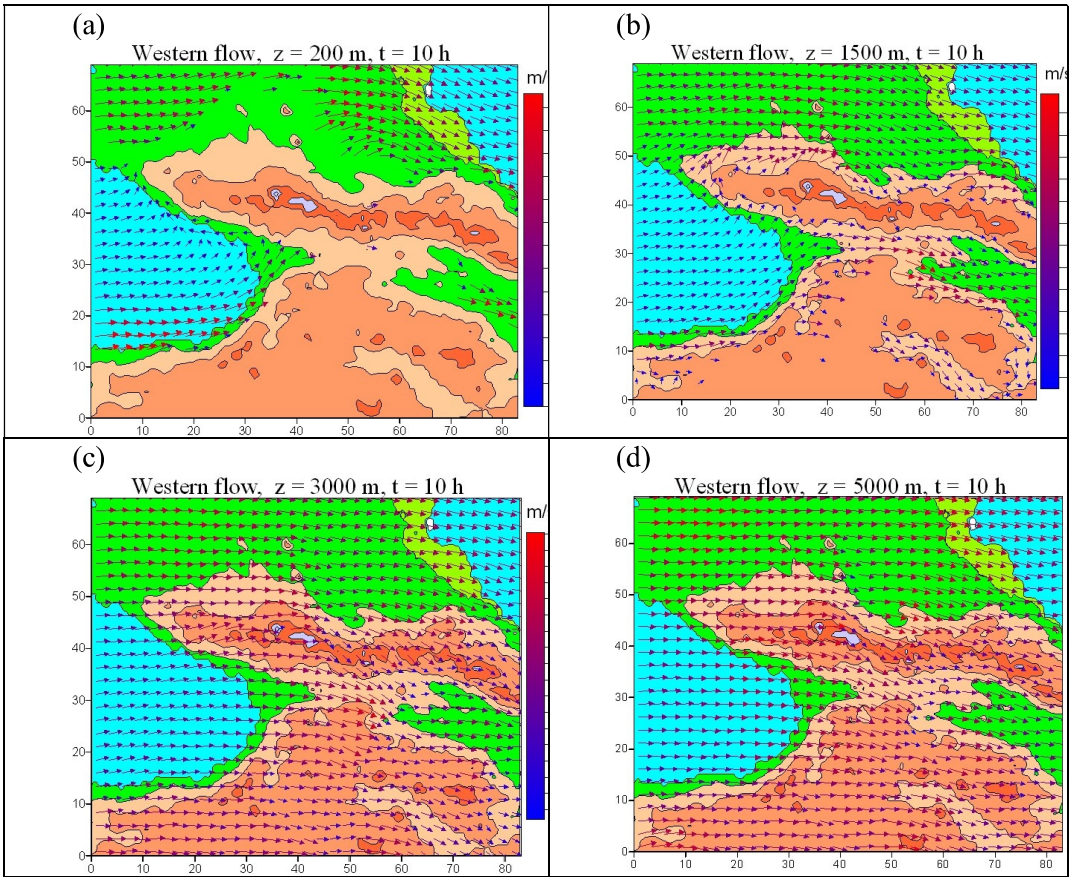

Fig. 2.4. Simulated fields of western air currents over the territory of the Caucasus at time t = 10h for the following heights (a) z = 200 m, (b) z = 1500 m, (c) z = 3000 m, (d) z = 5000 m.

The study of the behavior of mesoscale air flow in Georgia (in Western Georgia), when the western background air flow (directed from the Black Sea to the Caspian Sea) is changed by the eastern background air flow (directed from the Caspian Sea to the Black Sea) is of great research interest, since such phenomena often occur in Georgia. Therefore, to simulate the air flow over the real topography of the Caucasus, numerical calculations were performed when the western background flow at a velocity of U = 12 m /s was converted into an eastern flow with U = -12 m / s. The time variability of the background flow up to t = 12 h was the same as in previous numerical experiments based on equations (2.2.1) - (2.2.7) with boundary and initial conditions (2.2.8) - (2.2.12).

In Fig.2.5 the disturbed flow fields on height z = 200 m (above the Black Sea level) are shown at different time moments, when transformation of background flow was taking place. The numerical experiment showed that during reduction of speed of a background flow from 12 m/s up to 0, orographycaly disturbed flow undergoes significant changes. In particular, above the Kolchis lowland and the east part of the Black Sea turn of a wind counter-clockwise and tendency of generation of vortical formation are clearly observed.

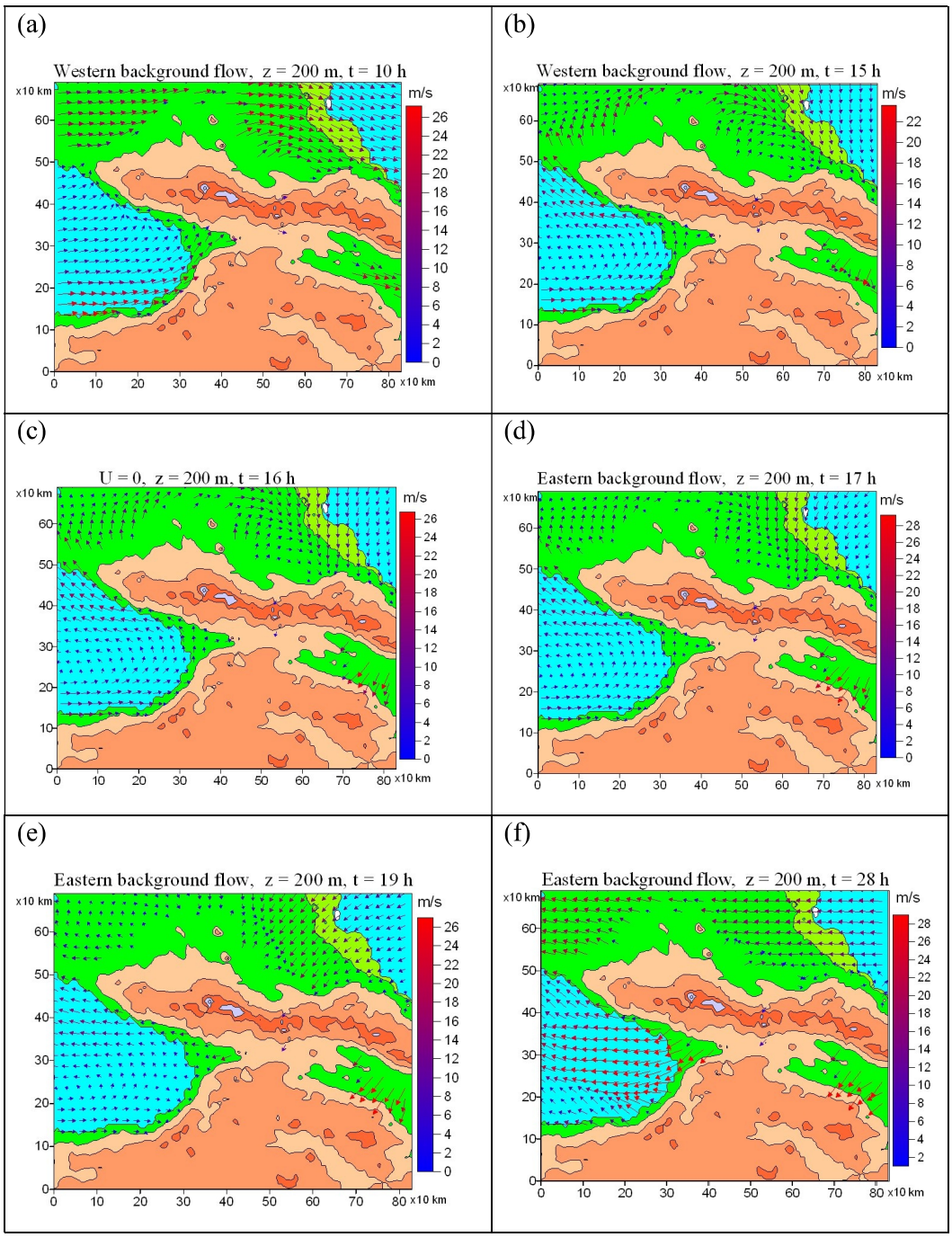

Fig. 2.5. Simulated air current fields over the Caucasus on z = 200 m at the following times: (a) – 14 h, (b) – 15 h, (c) – 16 h, (d) – 17 h, (e) – 19 h , (f) – 28 h.

As in case of the air flow over an isolated circular obstacle, there is very interesting phenomenon, when the disturbed meso-scale current exists in that case, when the background current is absent (Fig. 2.5 c). Analysis of the flow patterns show that despite lacking background current, in the surface layer the significant winds with speeds approximately 12-16 m/s can be kept. After disappearance of the background current, existence of meso-scale movement over orographically inhomogeneous

underlying surface is caused by disturbances of a pressure field, because of what the meso-scale movement is kept at absence of background pressure gradient.

After t = 16 h, when the eastern background flow arises and reaches speed -12 m/s during 16-22 h, the meso-scale flow is gradually transformed and during the certain time the structure of such current is formed which corresponds to the eastern background flow (Fig. 2.5 d-f).. The analysis of the flow patterns on different horizons showed that character of response of the disturbed flow to non-stationary transformation of large-scale processes differs in the lower and upper layers of the troposphere. In the lower layer, where orographyc factor is very significant, the time of the response of the meso-scale flow to changability of synoptic processes is more than in the upper layers of the troposphere and maso-scale flow not at once reacts to changes of the background current.

The analysis of results in a vertical plane has shown, that as well as in case of air flow over an isolated circular obstacle, above the real relief the significant growth of amplitudes of wave current in the all troposphere and formation of vortical structures is observed during approach of the background state of the atmosphere to calm conditions (see Fig. 2.5).

2.3. Conclusion

The air flow over an isolated obstacle and over the real relief of the South Caucasus under the conditions of non-stationary large-scale background processes is modeled on the basis of a three-dimensional hydrostatic mesoscale model. An analysis of the results of numerical experiments showed the occurrence of some orographic effects in the troposphere, at significant transformations of the unsteady background flow. In particular, during the damping of the motion of the synoptic scales, the amplitudes of the mesoscale flow of the vertical directions and the deviation of the velocity from their average value increased significantly (the maximum values of wind speed reached 26 m / s, when the speed of the unperturbed background air flow was 12 m / s). In addition, it was shown that even in the absence of a background current, an atmospheric wind may exist with significant speeds over mountainous areas. Besides, the calculation results showed that over the Caucasus ridges (as in the case of the modeled relief), there is a significant increase in the amplitudes of atmospheric currents throughout the troposphere and the existence of vortex structures even when the background flow approaches the state of calm. These results were first obtained by numerical modeling and are in good agreement with meteorological observations.

Since the inertia of the aerosol flow is greater than the inertia of the greenhouse gases, the monsoon flow in the Western Georgia more easily inflates greenhouse gases than aerosols, due to which the abundance of aerosols (which is a characteristic and constant factor in Western Georgia) can lead to cooling in the atmospheric layers over the territory of Western Georgia. Greenhouse gases (inflated by closed circulation), in the case of a summer monsoon with the influence of precipitation (caused by breeze circulation), are easily washed off the Black Sea far from the coast (10 - 31 km), but in the case of a winter monsoon, they are washed near the Likhi ridge (under the influence of the circulation of mountains and valleys). Such atmospheric processes seem to contribute to the reduction of greenhouse gases and contribute to the cooling of the climate in Western Georgia.

As our conception about climate cooling has the general form, climate cooling must take place in other regions of the Earth, particularly, where the monsoon flow and the advective – orographic factors are sharply expressed. For verification of this conception

we can consider the picture of global climate warming, which has a mosaic structure. Cooling and warming regions of the Earth caused by big variety of the regional factors are given.

It should be noted that the existing fact of climate cooling in Western Georgia may become an important concept of the policy of the Georgian government. It would be strategically reasonable if in the future the development of industry (related to greenhouse gases) will occur more actively in Western Georgia for the balance of greenhouse gases in Georgia.

References to Chapter 2

1. Bulletin of WMO, Summary of Analytical Report by IPCC, 1991, vol.1, No. 1.
2. Davitashvili T. Regional nested grid numerical model for baroclinic atmosphere forecast-. *Journal of Georgian Geophysicsal Sociate* vol. 2. 1996 p. 43-50.
3. Davitashvili T., Demetrashvili D. 2015. Numerical Modeling of Air Flow above the Caucasus Region, Proceedings of the Tbilisi International Conference on Computer Sciences and Applied Mathematics (TICCSAM 2015), March 21-23, 2015, Tbilisi, Georgia, pp. 175-185.
4. Davitashvili T., Janelidze P. On the prediction of short-term Geopotential, using complete equations of hydrodynamics with account of orography. *Bulletin of the Academy of Sciences of the Georgian SSR,* 96, No. 1, 1979 (Russian)
5. Davitashvili T., Khantadze A. and Kh. Sharikadze. Influence of Non-linear Heat sources on Climate Change. Reforts of Enlarged Session of VIAM, Vol.17. N3, 2002, pp. 21-29.
6. Demetrashvili D. I. A nonstationary problem of meso-scale processes in the free atmosphere over orographically inhomogeneous Earth's surface, Izv. AN USSR, Atmospheric and Oceanic Physics, 1979, t.15, N 7, p. 609-709 Russian).
7. Demetrashvili D., Davitashvili T. A modeling study of mesoscale air flow over the mountainous relief with variable in time large-scale background flow. *Bulletin of the Georgian National Academy of Sciences,*Vol.7, No 2, 2013, pp.57-64.
8. Gandin L.S., Laikhtman L.T., Matveev L.T. and M.I. Judin. *Fundamentals of Dynamical Meteorology* L., Gidrometeoizdat, 1989 (Russian).
9. Gutman L. N. *Introduction to the nonlinear theory of mesoscale meteorological processes*, Jerusalem, 1972, 293 p.
10. Javakhishvili Sh., *Atmospheric precipitations on the territory of Georgia,* Tbilisi, 1981, p. 182 (Georgian).
11. Javakhishvili Sh., *Georgian Climate Description by the Months*. Publishing House "Ganatleba. Tbilisi, 1988, pp.153. (in Georgian).
12. Khvedelidze Z., Davitashvili T. Effect of the changeability of the Coriolis' force and Geopotential variation in availability of mountains. *J. Meteorology and hydrology* No. 3. 1978. pp. 36-40. (Russian).
13. Kibel I. A., Trudy MMTS, 1964, Vol.3, pp. 3-17 (in Russian).
14. Kordzakhia M., *Climate of Georgia*. Tbilisi, 1961, (in Georgian).

15. Krapivin V., K.Kondratyev, 2002, Environmental Global Change: Ecoinformatics, 476*, Gidrometeoizdat Press.*
16. Prigozin I. and G.Nikolis, *The Self –organization in Non-balanced Systems*. M., Publ. House, Mir, 1979, (Russian).
17. Ramathan I. The Green-house Effect, Change and Ecological Systems. Report of MSNS, WMO and UNEP to the UN. L. 1989.
18. Richtmayer R. and K. Morton, *Raznostnye metody resheniya kraevykh zadach,* 1972, M., 418 p. (Russian).
19. Shuleikin, V.V. *Physics of Sea*. M., Publishing House of Acad. Sci. USSR, 1968. (Russian).
20. SNCU NFCCE Georgia's Second National Communication to the United Nations Framework Convention on Climate Change, Tbilisi, 2009.

Chapter 3. ON DROUGHT AND DESERTIFICATION IN EASTERN GEORGIA

Against the background of accelerating climate change, caused by growing anthropogenic factors, the problems of drought and desertification are of particular importance in Georgia. As mentioned in previous chapters, the climate of Georgia varies widely from subtropical (on the Black Sea coast) to continental with cold winters and hot summers in the extreme east (with arid lands). Against the backdrop of the hot summer, the activity of anthropogenic factors led to a significant change in the area of the underlying surface in Eastern Georgia. Namely, there is a reduction in the following units (due to increased production and construction): mowing, arable land, unused land, shrubs and forests. Converting a structural unit of one type to another naturally leads to climate change in some regions of Georgia.

3.1. Some features of the drought processes in Eastern Georgia

Droughts in Georgia are characterized by special weather conditions, with high temperature, low humidity and lack of rainfall for a long period of time (2-3 months, when the daily rainfall is less than 1 mm). In general, the genesis of droughts is determined by numerous natural phenomena, but hot atmospheric currents play a special role in Georgia. This occurs when air currents invade from the eastern or southeastern regions and bring dry air masses to the territory of Georgia. Namely, under the influence of the Asian depression, a summer thermal cyclone invades from the southeast, as a result of which masses of dry and hot air form in Georgia, in which case the minimum temperature in the lowland does not fall below + 20 ° C and the daily maximum exceeds + 38 ° C. The recurrence of such phenomena is highest in July (25.1%), when the invasion of hot and dry air masses is very dangerous for the development of droughts in Georgia. For example, in the steppe valley of the Gardaban region, lack of precipitation (the period of dry weather) is observed 3-4 times a year (when the land requires watering), while in the coastal regions of the Black Sea the period of dry weather is observed only once every 10 years. Recently, in the arid regions of eastern Georgia, a period of 15–20 days of dry weather is observed 5–6 times a year, and sometimes the period of dry weather even exceeds 80–100 days (Elizbarashvili et al. 2002 [8]).

It is known that the most arid regions in Georgia are the Lower Kartli and the Eldar Lowland, where the likelihood of severe drought is high and averages about 40%. For example, in the most arid regions of eastern Georgia in Shiraki it is 39%, and in Gardabani - 44% (SNCU NFCCE, 2009 [18]). Studies have also shown that, over the course of the 20th century, every ten years, the average annual temperature increased by an average of about 0.02-0.070 ° C, which is close to the rate of global average annual temperature increase (Elizbarashvili et al. 2002 [8], Papinashvili 2002 [15]). Studies have shown that in lower Kartli and in the Shiraki Valley, the average annual temperature from the mid-19th to the beginning of the 20th century increased slightly. Later, until 1980, this growth was oscillatory. Namely, from 1920 to 1940 the temperature value increased by 0.3-0.40° C, and from 1940 to 1955 the temperature value decreased on average by 0.25-0.290° C. From 1955 to 1960. it increased by 0.21-0.340° C and from 1960 to 1980 the temperature dropped by 0.26–0.30° C (Elizbarashvili et al., 2002 [8]). Further, from 1985 to the present, the average annual temperature is rapidly increasing at a rate of 0.32–0. 4° C every 10 years (Davitashvili et al. 2008 [4], 2012 [7]).

The occurrence of desertification depends on the interaction of a large number of factors. Among other things, a decrease in total rainfall in arid and semi-arid areas may increase the total area of arid land, and therefore a significant portion of the land is potentially at risk of desertification. In addition, in recent years, many arid regions are faced with increasingly rain showers, combined with wind erosion and drying up of water resources, which lead to an increase in temperature in such regions. Besides, such areas also suffer land degradation due to over-cultivation, over-grazing, deforestation and inefficient irrigation methods. The analysis of perennial research materials and the data of observations made in Georgia shows that there exists very close dynamic connection between activation of desertification processes and the mean perennial index of precipitation. Namely, when the amount of precipitation is about 700 mm, then the activation of desertification processes remains at the general background level. With atmospheric precipitation of about 500 mm, there is a tendency to intensify desertification processes, but with precipitation of less than 200 mm, a catastrophic development of desertification processes begins (Papinashvili 2002 [15]; Elizbarashvili et al. 2002 [8]).

3.2. On one simple thermodynamic model of desertification process

Desertification takes one of the important places in the cycle of global warming, but, since the nature of desertification is rather complicated, it is currently less studied by mathematical modeling. The conditions that cause the degradation of the surface layer are so diverse that their simultaneous consideration in the general mathematical model of desertification encounters insoluble difficulties. So, when discussing this problem with mathematical modeling at the first stage, it is necessary to highlight the main factors that substantially determine the desertification of the surface layer. As in other physical studies, the problem of desertification should be reduced to the creation of a certain theoretical model of desertification, in which the basic physical mechanism that causes desertification will be preserved. To find out what physical process occurs during exposure of the soil surface, it is necessary to proceed from the concept of soil as a physical medium.

According to (Marshal et al. 1996 [14]; Khrgian 1978 [11]) any simple soil fraction represents a conglomerate of elementary particles composing the soil. Since these particles have irregular geometrical shape, their direct contact with each other occurs merely in certain points or on very small areas. Therefore, elementary soil particles are mainly connected with each other by air layer or a water film. The richer the soil with water contact, then more particles is connected with each other by water layer. Since the air is a bad heat conductor in comparison with water (air heat conductivity coefficient is $\lambda = 5{,}6 \cdot 10^{-5} \frac{cal}{cm.s.\deg.}$, for water $\lambda = 1{,}3 \cdot 10^{-3} \frac{cal}{cm.s.\deg.}$) these particles connected with each other by air layer badly transmit heat, obtained through solar radiation to each other, while between particles connected by water film intense heat exchange is taking place and temperature gradients between them are rapidly decreasing. While decreasing vegetation and precipitation (these two factors may be conditioned by many reasons) radiation load upon soil active layer is intensifying. Number of particles connected by air layer is intensively increasing and each particle becomes the source of heat accumulation due to bad air heat conductivity. This time so called “greenhouse effect” develops in the active layer, when soil has a function of semi conduction: it actively gets heat through solar radiation and extremely passively gives it out. This physical phenomenon occurring in the active soil layer may be safely called as a soil

desertification process and the following consideration may be made. In fact, soil desertification process of a specific region starts due to precipitation decrease and degradation of vegetation cover. At this time, average annual intensity of solar radiation action in the given region sharply increases, causing drying (aridity) of soil active layer and gradual change of its structure. In particular, soil physical parameters such as density ρ, specific heat capacity C_p, transfer soil heat – conductivity coefficient λ, become dependent upon temperature (otherwise, changing of soil structure and its transformation into a new fraction will not occur) and a heat transfer mechanism in the soil gets a non-linear nature, as a result of which strong a heat accumulation and growth of temperature in time are observed in the active soil layer during the entire desertification process. This process, as already mentioned, is a "greenhouse effect", continues until arid soil structure gets quite a new appearance, with new physical parameters (e. g. heat conductivity coefficient of one the soil fractions, that of moist sand at $+10^0 C$ is equal to $\lambda = 3{,}71 \cdot 10^{-5} \frac{cal}{cm.s.\deg.}$ and dried out sand to $\lambda = 0{,}7 \cdot 10^{-5} \frac{cal}{cm.s.\deg.}$). This completes the desertification process and in the new fraction its physical parameters p, C_p and λ become dependent upon temperature and a heat transfer mechanism gets the form of the traditional linear Fourier problem (Davitashvili and Kantadze 2004 [2], Davitashvili et al. 2002 [5], Khrgian 1978 [11]).

If under the influence of external factors (degradation of vegetation, decrease of precipitation, drought, erosion, advection, etc.) a radiation load on the soil intensifies and on the active layer of soil the structural changes begins (desertification process with physical parameters, dependent upon temperature) then the heat conductivity mechanism gets a non-linear nature. In this case, the superposition principle no longer is observed and generation of various harmonics (their intensified interaction with each other), increase of heat process in the soil (i.e. “greenhouse effect” occurrence) take place, accelerating structural process in the active layer of the soil. Therefore, “greenhouse effect”, which, in fact, represents a growing thermal process in limited time interval, is stipulated by a non-linear mechanism of heat conductivity. If radiation loads upon the soil decreases, heat transfer process will get a linear nature and the “greenhouse effect” disappears. Following to the articles (Samarski et al. 1975 [17]; Rose 2004 [16]), one should mind that it is impossible to measure by means of experimental methods the soil intrinsic parameters (p, c, λ) that structurally change during the desertification process.

The soil temperature is the only, main characteristic parameter, which submits to accurate measurement. It should be mentioned that in normal conditions (in terms of vegetation coverage and adequate amount of precipitation) in the active soil layer the water content functions as the complex parameter q, which prevents the sharpening of the radiation processes and origination of “greenhouse effects”. Meanwhile, heat obtained from the solar radiation intensively scatters among the elementary soil particles that are linked to each other with water pellicle and the stationary temperature field forms with the stationary temperature T_{st}. The relationship between the stationary temperature Tst of the soil and the q parameter can be easily arranged for different types of soil (in natural terms) in case if the water content evaporates per unit of the soil It is no exaggeration to note that such work for soils in the eastern part of Georgia should be a precondition for studying the desertification process.

In natural conditions, the value of the parameter q decreases significantly, and the thermal activity of the soil increases due to structural changes in internal parameters. Under these conditions, only by means of artificial, soil-conservational methods is it possible to raise the parameter q to such a value, that in the given geographical and climatic conditions is necessary for conducting thermal processes in the same way as it proceeded before the origination of the desertification process.

The parameter q can be defined as: water mass m_b per soil unit divided by sum of the soil and water masses in the same volume: $q = \frac{m_b}{m_n + m_b}$, where m_n is the soil mass per unit of volume, thus q represents dimensionless parameter and is always below 1 in soil.

As it was mentioned, the parameter q prevents the sharpening of the desertification process in the soil, while the structural change of the internal soil parameters causes heat accumulation, origination of "greenhouse effect" and its further development. Thus in natural conditions the process of desertification always proceeds on the basis of two opposite processes: the first one promotes the growth of the "greenhouse effect" in the soil according to the time (p, c, λ) and the second one disturbs it and causes extinction of the "greenhouse effect" q.

Below we will review a real case when the thermal sources resulting in desertification are located in the soil active layer.

If we generally mark the heat flow and loss functions by $Q(t)$ and $R(t)$ functions, the equation of soil heat conductivity formula will look as (Khrgian 1978 [11]; Landau et al. 1988 [13]):

$$pc = \frac{\partial T}{\partial t} = \frac{\partial}{\partial z}\lambda\frac{\partial T}{\partial z} + Q(T) - R(T). \qquad (3.2.1)$$

where p, c, λ parameters represent the power functions of temperature T (Khrgian 1978 [15]).

Generally the equation (3.2.1) is solved with the initial and the boundary conditions:

$$T(0,t) = \varphi(t) * T(z,0) = f(z), \qquad (3.2.2)$$

where the quantities $\varphi(t)$ and $f = (z)$ represent the functions depended on the solar radiation and the intensity of Earth radiation.

Certainly, the temperature change caused by the solar radiation at the considerable depths of the soil $(z \to \infty)$ should tend to zero.

Let us consider a thermal function of volume and the heat conductivity coefficient (Khrgian 1978 [11]; Landau et.al. 1988 [13]):

$$du = pcdT; \qquad f = \frac{\lambda}{pc} = au^n, \qquad (3.2.3)$$

The result of equation (3.2.1) and the relation (3.2.2) gets the following form:

$$\frac{\partial u}{\partial t} = \frac{a}{n+1}\frac{\partial^2 u^{n+1}}{\partial z^2} + Q(u) - R(u). \tag{3.2.4}$$

$$U(0,t) = \Phi(t): \quad U(z,0) = F(z), \tag{3.2.5}$$

where $a = f_0 u_0^{-n}$; $f_0 = \frac{\lambda_0}{p_0 c_0}$; the coefficient n shows the nonlinear character of desertification process; ρ_o, C_{po} and λ_o are values of density and heat transfer coefficients, respectively, when $T = T_0$.

3.2.1. Analytical consideration of the process

In order to solve (3.2.4)-(3.2.5), the thermal sources should be identified. Let us consider the case when the difference between heat flow and loss functions represents the power function of the u function

$$Q(u) - R(u) = \alpha u^{\sigma}, \tag{3.2.6}$$

where α and u^{σ} are the parameters of the thermal function.

The representation of thermal functions $Q(u)$ and $R(u)$ in (3.2.6) by means of power formula of u function is justified by the fact that they represent the complex temperature function in the thermodynamic tasks of the soil. The aforementioned appropriateness changes from the appropriateness of Newtonian thermal function ($\sigma = 1$) to the appropriateness of the Boltsman thermal function ($\sigma = 4$) according to the value $\Delta T = T - T_e$, where T_e is the temperature of environment. According to the relation (5.1), equation (3.2.4) takes the following form:

$$\frac{\partial u}{\partial t} = \frac{a}{n+1}\frac{\partial^2}{\partial z^2} u^{n+1} + \alpha u^{\sigma}. \tag{3.2.7}$$

The first term in the right part of the equation (3.2.7) expresses the nonlinear heat transfer process, and the second member marks the action of the nonlinear thermal sources in the soil.

An exact solution of equation (3.2.7) was obtained by us in case when $\alpha = 0$ (Davitashvili and Khantadze 2004 [2]). It is easy to demonstrate that considering the thermal source the equation (3.2.7) preserves the mechanism of "greenhouse effect" in case when we assume that $\sigma = n+1$. Consider also that the α parameter must include the effect of the thermal activity, resulted by the change of internal soil parameters (p, c, λ). The intensification of this thermal activity effect promotes the sharpening of "greenhouse effect", and the growth of the parameter q, which prevents the development of "greenhouse effect" in the soil. Out of the aforementioned let us introduce the parameter α as a two members difference

$$\alpha = \alpha_1(p, c, \lambda) - \alpha_2(q) \tag{3.2.8}$$

and rewrite the equation (3.2.7) in the following way:

$$\frac{\partial u}{\partial t} = \frac{a}{n+1}\frac{\partial^2 u^{n+1}}{\partial z^2} + (\alpha_1 - \alpha_2)u^{n+1}. \qquad (3.2.9)$$

By direct insertion it is possible to show that the nonlinear solution of the equation (3.2.9), which includes the "greenhouse effect" will look like (Khantadze et.al.1997 [10]; Davitashvili 2006 [3]):

$$u(z,t) = u(0,0)\cos^{\frac{2}{n}}\left(\frac{\pi}{2}\frac{x}{|\Delta|}\right)\cdot\left(1 - n\frac{t}{|t_f|}\right)^{-\frac{1}{n}}, \qquad (3.2.10)$$

where $|\Delta|$ and t_f are defined by the formulas:

$$|\Delta| = \frac{\pi}{n}\sqrt{n+1}\sqrt{\frac{f_0}{|\alpha_1 - \alpha_2|}}; \quad |t_f| = \frac{2(n+1)}{(n+2)}\frac{u_0^n}{u^n(0,0)|\alpha_1 - \alpha_2|}. \qquad (3.2.11)$$

The formula (3.2.10) shows that desertification process develops in time in three stages:

1. If the water content q is sufficient to satisfy the condition $\alpha_1(p_1, c_1, \lambda_1) = \alpha_2(q_1)$ then $|\Delta| \to \infty$, $|t_f| \to \infty$ is obtained from (3.2.11) formulation, and the stationary temperature distribution can be obtained from the formula (3.2.10):

$$u = u(0,0), \quad that\ is \quad T = T_{st}^{(1)}. \qquad (3.2.12)$$

This kind of thermal condition of the soil takes place before the desertification process begins, when the vegetation coverage and the precipitation amount is sufficient for normal functioning of the thermally active soil layer;

2. If the thermal activity coefficient is higher than the heat loss coefficient, which represents the water content function q, than the following equation will be obtained from $|\Delta| = \Delta > 0$, $|t_f| = t_f > 0$ and formula (3.2.10):

$$u(z,t) = u(0,0)\frac{\cos^{\frac{2}{n}}\left(\frac{\pi}{2}\frac{z}{\Delta}\right)}{\left(1 - n\frac{t}{t_f}\right)^{1/n}}, \qquad (3.2.13)$$

which includes the "greenhouse effect" - thermal process that is space limited ($z < \Delta$) and grows by time for the interval $t < \frac{t_f}{n}$. This type of appropriateness of soil temperature field should take place in desertification process.

3. If by human active interference in the desertification process the water content q grows up so as to satisfy the condition $\alpha_1 < \alpha_2$ then, $|t_f|_f$ in the (3.2.11) formulation will be negative and equal to and imaginary $|\Delta|$ to $|\Delta| = i\Delta$. Therefore (3.2.10) solution will have the following form:

$$u(z,t)=u(0,0)\frac{\cos^{\frac{2}{n}}\left(\frac{\pi}{2}\frac{z}{\Delta}\right)}{\left(1+n\frac{t}{t_f}\right)^{1/n}}, \qquad (3.2.14)$$

The (3.2.14) formula demonstrates that the thermal function of soil will be space limited in this case as well ($|z|\le\Delta$), and will have the form of time reducing function.

This kind of thermal process will develop in the soil under the soil-conservation methods, accomplished by a man. At this time the function $u\left(u^t\right)$ achieves zero for a long-term interval and the "greenhouse effect" extinct. From the above mentioned it may be concluded, that analytical formula (3.2.10) quantitatively well describes the three stages of desertification process and includes the basic physical mechanism which is the basic reason of desertification. This physical mechanism proceeds in cooperation of two opposite process (sharpening of the "greenhouse effect" because of the structural change of the soil and thermal activity on the one hand and the weakening of the process resulted by man's active interference).

3.3. Evaluation of the desertification process in the Shiraki Valley using one statistical method

First of all, we looked for arid lands, which in recent years have been characterized by an increased frequency of droughts and then possession of long-term climate observation data in the zone of searching. Such an area with an observation station was selected in Shiraki. Using the data of the selected weather station, we examined changes in soil surface temperature, precipitation, and some established climatic parameters, which are considered as the beginning of desertification process. To identify the most pronounced increase in surface temperature (in the area of searching), we mainly studied the anomalous change in the average monthly soil surface temperature from January 1936 to December 1990 (since climate monitoring stations in eastern Georgia stopped working since 1990 due to the beginning civil war). Changes in temperature throughout the year and season occur differently (Tavartkiladze et al. 1998 [19]). The warming process is well characterized by an increase in temperature in the cold season. But it should be noted that the desertification process is mainly well characterized by changes in temperature (precipitation) in the warm periods of the year. Therefore, it is necessary to study as changes in temperature in the cold and warm season, as well as changes in average annual temperatures and soil surface temperatures whicg are of great interest too. In order to study these concepts, an autocorrelation matrix for the Shiraki Valley was compiled and normalized (see Table 3.1) in accordance with the soil surface temperature and average annual and seasonal temperature and precipitation anomalies (Davitashvili et al., 2008 [4], 2012 [7]).

Table 3.1. Normalized correlation matrix for Shiraki, according to the soil surface temperature and average annual and seasonal precipitation anomalies

		1	2	3	4	5	6
Average annual temperature	1	1	0.83	0.67	-0.34	-0.06	-0.3
Cold season's temperature	2		1	0.14	0.01	-0.06	0.31
Warm season's temperature	3			1	-0.6	-0.07	-0.58
Total of the annual precipitation	4				1	0.24	0.89
Total of the Cold season's precipitation	5					1	-0.22
Total of the Warm season's precipitation	6						1

Table 3.1 shows that the anomalies in the average annual temperature of the soil surface are well pronounced in the cold season (correlation coefficient -0.83), but the warm season also has a rather large share (correlation coefficient -0.67) in the temperature increase. As for the change in precipitation, it occurs almost completely in the warm season (correlation coefficient - 0.89). A relatively high correlation between temperature and precipitation anomalies is found in the warm season (correlation coefficient -0.6), which is another indicator of the development of desertification in the Shiraki Valley.

3.4. Drought, desertification and its mitigation in Eastern Georgia

Challenges facing the scientific community mainly include both a better understanding of the soil surface and meteorological processes that lead to desertification, and determining how new technologies and methods can be used to reduce the risk of desertification. Solving these problems usually involves mapping hazardous areas of drought, and then trying to predict the likelihood of drought and its associated consequences. To achieve this goal, scientists use advances in satellite remote sensing and other data sets (satellite digital elevation maps, satellite information on land cover, soil characteristics and precipitation with high resolution). The combination of these approaches potentially provides information on "where" (exposure) and "when" (rainfall) during desertification, dangerous droughts can be expected.

The drip irrigation method requires 3 times less water compared to surface natural irrigation, which provides up to 67% savings in water for irrigation (Chikvaidze et al., 2002 [1]), which is very important against the backdrop of the melting of the Caucasus glaciers. Therefore, the introduction of this method in river basins with a shortage of irrigation water can be considered an important measure against drought in the arid regions of Georgia.

In addition, the risk of atmospheric, hydrospheric and biospheric disasters associated with climate change on a regional scale has recently increased. Therefore, it

becomes necessary to strengthen the Integrated Environmental Monitoring Services, one of the directions of which is the early warning system (Keburia 2002 [9]). To coordinate scientific research, it is necessary to create a Scientific Center, which will summarize environmental monitoring information obtained from various sources, analyze it and create models of atmospheric, hydrospheric and biospheric catastrophic processes that could serve as the basis for the creation sustainable development program.

3.5. Conclusion

The simplified mathematical model of desertification discussed above indicates that in order to stop the desertification process, it is first necessary to stop the non-linear thermal process occurring in the soil, causing its structural changes as a result of the "greenhouse effect". To achieve this goal, it is necessary to take measures that reduce the load of solar radiation on the soil, which, of course, leads to the disappearance of the "greenhouse effect" in its active layer. For this, it is necessary to use a drip irrigation system and well-known hydroponic methods based on many years of experience from scientists from Israel and other countries (Davitashvili et al. 2008 [6]). In the conditions of arid lands of Georgia, this will allow to obtain the maximum irrigation effect with minimal water use and get vegetation due to drip water rich in various salts necessary for the soil. At the same time, it is necessary to sow heat-resistant wild plants that form the vegetative cover of the soil, are characterized by deep and branched roots and even when burning their upper part, retain viability and biological activity (Davitashvili et al. 2008 [6], Krapivin and Kondratiev 2002 [12] , Tavartkiladze et al. 1998 [19]). In addition, in combination with a drip irrigation system, it is necessary to carry out automatic measurements of the intensity of the radiation load on the soil surface to enrich the soil with salts (necessary for the soil by the hydroponic method) and biological nutrients. This, in our opinion, will lead to a suspension of the desertification process and the disappearance of the "greenhouse effect" in the active soil layer. Finally, it should be noted that the development of a common model to combat desertification and effective recommendations for combating desertification should be carried out in close cooperation meteorologists, biologists, mathematician, physicist and irrigation specialists (Davitashvili et al. 2002 [5], Krapivin.and Kondratyev 2002 [12], Tavartkiladze et al. 1998 [19]).

References to Chapter 3

1. Chikvaidze G., Shavelidze O., Geladze I., Devdariani N., N. Arhkielidze, 2002: Introduction of Dripping Irrigation as an Anti-drought Measure and Basis for Rational Uses of Water Resources:*Transactions of the Institute of Hydrometeorology:*-V.107.pp. 218-222. (Georgian).
2. Davitashvili T. and A.Kantadze, 2004: Research of Conditions of the climate Change in Georgia in view of Regional Antropogenie Factors., *Journal Geography and Natural Resorses,* pp. 302-308, Russian Academic Publishers.
3. Davitashvili T., 2006: Oil Filtration in Soil: Problems of the Georgian Section of TRACECA and Their Numerical Treatment. *ARW/NATO*, pp. 56-69, Springer, Netherland Press.

4. Davitashvili T., Khantadze A., K.Tavartkiladze, 2008: Mathematical Modeling of Some Peculiar Properties of Regional Climate Change.*Applied Mathematics, Informatics And Mechanics*, Vol. 13, No.2, pp. 40-56
5. Davitashvili T., Khantadze A., Kh.Sharikadze.2002: Influence of Non-linear Heat sources on Climate Change. *Reforts of VIAM* Vol.17, No3, p.21-29.
6. DavitashviliT., Khantadze A., and K. Tavartkiladze, 2008: Mathematical Modeling of Some Peculiar Properties of Regional Climate Change, *Applied Mathematics, Informatics And Mechanics*, Vol. 13, No.2, 2008. p.p 40-56
7. DavitashviliT., Khantadze A., and K. Tavartkiladze, 2012: On Some Aspects of Climate Change, Drought and Mitigation of Risk of Desertification in Arid Regions of Georgia, Int. Journal Natural resource management and study of the impact of climate change with geographic information systems, science and space technologies. Geosciences magazine,Tunisia; Vol.5, 2012, pp. 67-75 http://magazine.geotunis.org/2012/01/05/1596.html
8. Elizbarashvili M., Aladashvili T., N. Sulxanishvili 2002: Climate Current Variation and Expected Climate Seevarios for Arid Regions in Georgia, *Transactions of the Institute of hydrometeorologe* v. 107 p. 175-178 (Georgian).
9. Keburia G., 2002: On the problem of environmental monitoring in Georgia *Transactions of the Institute of Hydrometeorology:*V.107.-p.230-233 (Georgian).
10. Khantadze A.. Gzirishvili T., G. Lazriev, 1997: On the Non-linear Theory of Climatic Global Warmin. *Bulletin of CRNC.* No 6, pp. 3-33
11. Khrgian A.,1978: Physics of Atmosphere, *Gidrometeoizdat Press*.
12. Krapivin V. and K. Kondratyev, 2002: Environmental Global Change: Ecoinformatics, 476*, Gidrometeoizdat Press.*
13. Landau L., E. Lifshits. 1988: Hydrodynamics, 347,Nauka Press.
14. Marshal T., Holmess J., and C. Rose, 1996: Soil Physics, 3rd edn, *Cambriddge: Cambriddge university Press.*
15. Papinashvili L., 2002: Drought in Georgia: *Transactions of the Institute of Hydrometeorology*, 107, 28-33 (Georgian).
16. Rose C., 2004: An Introduction to the Environment Physiscs of Soil, Water and Watersheds, *Cambriddge: Cambriddge university Press.*
17. Samarski A., Zmitenko N., Kurdiumov S.and A. Mikhalkov, 1975: The Effect of Meta-Stabile Localities of Heat within Non-Linear Heat Conductivity. *Report. A.N. USSR,*Vol 233, No 6.
18. SNCU NFCCE Georgia's Second National Communication to the United Nations Framework Convention on Climate Change, Tbilisi, 2009.
19. Tavartkiladze K., Elizbarashvili E., Mumladze D., G.Vachnadze, 1998: Empiriuli model of temperature field of Georgia. Tbilisi, p. 128 (Georgian).

Chapter 4. MODELLING TRANSPORTATION OF DESERT DUST TO THE SOUTH CAUCASUS

Aerosol is one of the main sources of uncertainty in modern climate variability (IPCC, 2007 [23]). Recently, against the backdrop of climate change, aeolian dust aerosol has become the subject of a special study in the North Caucasus (Kutuzov et al., 2014, 2016 [29], [30]). Observations show that dust aerosol is one of the main pollutants in Georgia, although the question of its origin and its effect on the regional climate has not been properly studied (SNCUNFCCC 2009 [48], Davitashvili et al. 2018, 2019 [7], [9]). Therefore, the study of the causes of an increase in the concentration of dust aerosol in Georgia and the study of the possibility of transfer of aeolian dust from deserts to the South Caucasus (Georgia) based on numerical modeling is an urgent issue.

4.1. Aeolian mineral dust transportation

Dust (mainly originated from deflation of erodible sediments and deserts' storms) and smoke (chiefly originated from biomass burning and anthropogenic pollution) are main sources of atmospheric aerosol (Choobari et al. 2014 [6]). Mineral dust (principally originated from deserts' storms) is the leader among natural aerosols, since 75% of the global mass of aerosols is mineral dust (Ginoux et al., 2012 [15]). The role of mineral dust in the Earth's climate system is enhanced by its active participation in physical, chemical and biogeochemical processes of all scales (Shao et al., 2011b; Shao et al., 2011a [45]; Rizza et al., 2017 [40]). Namely, Aeolian Dust Aerosol (ADA) scatters and absorbs shortwave and longwave radiation, affects the radiation and energy balance of the atmosphere and the Earth's surface, reduces visibility and affects precipitation (Charlson et al.1992 [3]; Kim et al. 2001 [27]). Besides, dust particles can rearrange the molecular and ionic structures of the polluted atmosphere due to chemical reactions (Andreae and Rosenfeld, 2008 [1]). Passing through contaminated areas, desert dust (covered with sulphur due to chemical reactions) can serve as a giant Cloud Condensation Nuclei (CCN), which enhances the collision and coalescence of droplets and therefore, increases the formation of warm precipitation (Charlson et al., 1992 [3]). However, satellite, aerial and laboratory observations have shown that mineral dust can prevent precipitation (Rosenfeld et al., 2001 [42]). Although the effect of mineral dust on precipitation is less than that caused by smoke, nevertheless, during and after a desert storm, a very large amount of dust in the atmosphere becomes a significant factor for precipitation (Rosenfeld et al. 2001 [42]). Thus due to chemical reactions and physical affects the ADA impacts on dust chemistry and on atmospheric composition. In case of settled onto or into clouds ADA condenses cloud's nucleus, alters clouds albedo and particles size, changes the optical propertied of clouds, put obstacles in the way of clouds and precipitations normal formation (indirect effect) and thereby impacts on climate formation (Andreae and Rosenfeld 2008 [1]; Twomey et al. 1974 [51]). As a rule, arid and semi-arid areas adjacent to deserts are most often affected by dust storms; however, remote areas are also not protected from severe dust storms (Huang et al., 2010 [21]). Indeed, studies show that strong winds from African and Asian deserts carry large amounts of dust into the atmosphere and, therefore, about 30% are deposited in deserts, 20% are transported on a regional scale, and about 50% are transported across the Atlantic and Pacific oceans from the outside. (Zhang et al., 1997 [54]; Huang et al., 2010 [4]). Regional-level ADAs have a significant impact on drought, desertification processes and, in general, on climatic conditions in mountainous and semi-arid regions

(Han et al., 2008 [20]; Wang et al., 2008 [52]). Studies show that the territory of the Caucasus is one of the regions affected by ADA, transferred from the deserts of Africa and the Middle East by strong winds (Shahgedanova et al., 2013 [44]; Kutuzov et al. Al., 2014 [29]). According to the National Environmental Agency (NEA) of Georgia, dust aerosol (DA) is one of the main pollutants in Georgia. A number of studies have focused on the origin, chemistry, and physical effects of long-travelled desert dust (LTDD) deposited in the European Alps (Schwikowski et al.,1999 [43]; Grousset et al., 2003 [19]; Sodemann et al., 2006 [49]), in West and Central Asia (Eghbali et. al. 2016 [12]; Dong et al., 2009 [10]; Prasad et al. 2009 [38]), in the Himalayas and Tibetan Plateau (Kang et al., 2010 [26]; Li et.al., 2011 [32]; Prasad et al.,2009 [38]), in the Mediterranean region (Erel et.al., 2006 [13]), in the Caucasus (Shahgedanova et al. 2013 [44]; Kutuzov et al. 2014 [29]; Mikhalenko et al. 2015 [35]; Kutuzov et al. 2016 [30]). Issues of the origin, chemical composition, and physical effects of LTDD deposited in the Caucasus were mainly studied by ice cores extracted from the Mt. Elbrus in 2009, 2012 and 2013 years (Kutuzov et al. 2014 [29], Shakhgedanova et al. 2013 [44], Kutuzov et al. 2016 [30], Mikhalenko et al. 2015 [35]) and only once by ice cores extracted from Mt. Kazbeg which is located in Georgia (Kutuzov et al. 2016 [30]). Based on these studies, it was found that desert dust precipitates on the glaciers of the Caucasus 3–7 times a year and comes mainly from the deserts of the Middle East and less often from Northern Sahara (Kutuzov et al. 2014 [29]).

The main goal of this study is to study for the first time possible routes for transporting aeolian dust from deserts to the territories of the South Caucasus (Georgia) by numerical modelling. To study this problem, two numerical models, WRF-Chem / Dust and HYSPLIT, are used. The ability of WRF-Chem/Dust and HYSPLIT to model dust transfer (temporal spatial evolution) is assessed by the observational data set (PM10) and satellite products CALIPSO and MODIS. In this study, from the results of numerical simulations performed from December 2017 to November 2018, only two of them, which took place on March 22-24 and July 25-26, 2018, are presented and discussed.

4.2 .Materials and methods

4.2.1. Study area

As mentioned in Chapters 1,2, the Main Caucasus Ridge prevents air advection from the north, the Lesser Caucasus Ridge disturbs the weather fronts moving from the south, but the natural air transport corridor, stretched from the Black Sea to the Caspian Sea (Fig.4.1 (a)), is a convenient passage for transporting atmospheric flows (with dust aerosols) from west to east and back (Kordzakhia 1961 [28], Javakhishvili 1988 [25]).

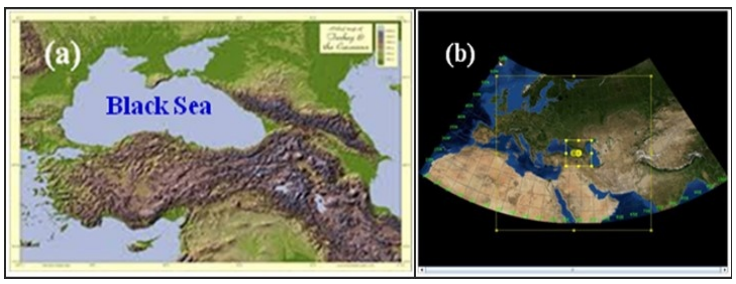

Fig. 4.1. Physical map of the Caucasus region - (a), location of the nested domains in the WRF Chem model - (b)

Transportation of LTDD to the Caucasus (Georgia) is associated with the low- and mi-tropospheric flows from Africa (through the Mediterranean Sea), from the Central Asia regions (through the Caspian Sea) and by warm advection from the Middle East (Kutuzov et al. 2013 [44], Shahgedanova et al. 2016 [30], Kutuzov et al. 2014 [29], Mikhalenko et al. 2015 [35], Davitashvili et al. 2018 [9], Davitashvili 2018, 2019 [8], [7]).

4.2.2. Model and method

The Weather Research and Forecasting (WRF) model is a real-time numerical weather forecasting system in which the atmosphere modeling system includes the regional climate modeling, air quality modeling, atmosphere-ocean coupling and idealized simulations (Skamarock et al. 2005, [4]). In WRF there are two dynamics solvers: the Advanced Research WRF (ARW) solver (Eulerian mass or "Em" solver) developed primarily at the National Center for Atmospheric Research's, and the NMM (Nonhydrostatic Mesoscale Model) solver developed at National Centers for Environmental Prediction. The ARW dynamics solver is based on compressible, non-hydrostatic Euler equations, which in the vertical mass coordinate (following the terrain), in the flux form using variables that have conservation properties have the following form (Skamarock et al. 2005, [4]):

$$\frac{\partial U}{\partial t}+(\nabla\cdot Vu)-\frac{\partial}{\partial x}(P\frac{\partial\phi}{\partial\eta})+\frac{\partial}{\partial\eta}(P\frac{\partial\phi}{\partial x})=F_U, \tag{4.2.2.1}$$

$$\frac{\partial V}{\partial t}+(\nabla\cdot V_V)-\frac{\partial}{\partial y}(P\frac{\partial\phi}{\partial\eta})+\frac{\partial}{\partial\eta}(P\frac{\partial\phi}{\partial y})=F_V, \tag{4.2.2.2}$$

$$\frac{\partial W}{\partial t}+(\nabla\cdot V_w)-g(\frac{\partial P}{\partial\eta}-\eta)=F_w, \tag{4.2.2.3}$$

$$\frac{\partial\theta}{\partial t}+(\nabla\cdot\theta)=F_\theta, \tag{4.2.2.4}$$

$$\frac{\partial\mu}{\partial t}+(\nabla\cdot V\ )=0, \tag{4.2.2.5}$$

$$\frac{\partial\phi}{\partial t}+\left[(V\cdot\nabla\phi)-gW\right]=0, \tag{4.2.2.6}$$

along with the diagnostic relation for the inverse density

$$\frac{\partial\phi}{\partial\eta}=-\alpha\mu, \tag{4.2.2.7}$$

and the equation of state

$$P=P_o(R_d\theta/P_o\alpha)^\gamma, \tag{4.2.2.8}$$

In (2.1.2.1) – (2.1.2.6), used the following denotations,

$$\nabla \cdot Va = \frac{\partial(Ua)}{\partial x} + \frac{\partial(Va)}{\partial x} + \frac{\partial(\Omega a)}{\partial x},$$

$$V \cdot \nabla a = U\frac{\partial a}{\partial x} + V\frac{\partial a}{\partial y} + \Omega\frac{\partial a}{\partial \eta},$$

where η is terrain-following hydrostatic-pressure vertical coordinate and defined as $\eta = (P_h - P_{ht}/\mu)$, $\mu = P_{hS} - P_{ht}$, and $\mu(x, y)$ represents the mass per unit area within the column in the model domain at (x, y), Ph is the hydrostatic component of the pressure, and Phs and Pht refer to values along the surface and top boundaries, respectively. $V = \mu v = (U, V, W)$, $\Omega = \mu\eta^{\cdot}$, $\Theta = \mu\theta$. $v = (u, v, w)$ are the covariant velocities in the two horizontal and vertical directions, respectively, while $\omega = \dot{\eta}$ is the contravariant 'vertical' velocity, u,v,w are the axis components of wind velocity along axis x, y, z, t – is time, θ is the potential temperature, $\varphi = gz$ (the geopotential), p (pressure), and $\alpha = 1/\rho$ (the inverse density). a represents a generic variable. $\gamma = Cp/Cv = 1.4$ is the ratio of the heat capacities for dry air, R_d is the gas constant for dry air, and P_0 is a reference pressure. The right-hand-side terms F_U, F_V, F_W, and F_Θ represent forcing terms arising from model physics, turbulent mixing, spherical projections, and the earth's rotation.
System of equations (4.2.2.1)- (4.2.2.8) is solved by the open lateral boundary conditions using one-way nesting (Skamarock et al. 2005, [4], Davitashvili 2019 [7]). Boundary and initial conditions for outer domain were extracted from ECMWF ERA-Interim data (with 0.75 degree resolution), available every 6 h. Outer, a mother domain consisting of 128 x 128 cells with a 37.2 km resolution (it covers all of the regions, taking part in the formation of the atmospheric processes over the Caucasus region, namely: the most of south and east Europe, Ural and Siberian Region, Middle East and Central Asia) and a nested domain consisting of 81 x 81 cells with a 12.4 km resolution (centered at 41°72'N, 44°78'E) has been used in order to capture dust storms above the arid regions of North Africa, Middle East and West Asia arid regions (see Fig.4.1 (b)). The model's vertical structure for both domains includes 32 layers covering the whole troposphere. For the coarse domains we use time step 60 sec. and for the nested ones - 10 sec.

4.2.2.1. The WRF-Chem/Dust model

The WRF model, online fully coupled with chemistry community module (WRF-Chem), is widely used to predict air quality and to model the transport and dispersion of dust aerosols over long distances (Grell et al. 2005 [18]). This study uses the WRF-Chem v. 3.6.1 (with its dust research module (Chem) simulating the outbreak of dust aerosols in the desert and its transportation to the South Caucasus (Georgia)), applying two nested domains (Fig.4.1. (b)). All performed simulations, using the WRF-Chem v.3.6.1 model, were performed on the GRENA cluster (one computing node with 15 cores of Intel Xeon CPU E5-2670 @2.60GHz). The WRF-Chem model (version 3.6.1) includes the DUST-GOCART, DUSTGOCART / AFWA and DUSTUOC mineral dust emission modules. A comparison between the modern DUST-GOCART / AFWA and DUSTUOC schemes showed that the GOCART / AFWA emission scheme caused an excessive prediction of dust concentration and the DUSTUOC scheme - lower (Rizza et al. 2016 [41], Fountoukis et al. 2016 [14]). Therefore, in this study, we chose the easy-to-use DUST-GOCART scheme, but with seven mass output types of aerosols (Chin et al. 2000 [5]). In the DUST-GOCART scheme (dust_opt = 1) module_gocart_dust, the amount of dust emissions into the atmosphere depends on the surface wind speed, soil

characteristics, threshold fraction velocity, horizontal salinity flow, and vertical flow distributed into 5 sizes bins (Grell et al. 2005 [18]). As described in Ginoux et al. (2001 [16]), the GOCART scheme calculates the dust emission flux G as

$$G = C * S * S_p * U^2_{10m}(U_{10m} - U_t) \tag{4.2.2.9}$$

where C is an empirical proportionality constant, S is a source function which defines the potential dust source regions and comprises surface factors, such as vegetation and snow cover, S_p is a fraction of each size class of dust in emission, $U_{10\,m}$ is the horizontal wind speed at 10 m, U_t is the threshold wind velocity below which dust emission does not occur and is a function of particle size, air density, and surface moisture.

In (4.2.2.9), the source function S, is the fraction of alluvium available for wind erosion, is prescribed as in Ginoux et al. (2001 [16]) as:

$$S = \left(\frac{Z_{\max} - Z_i}{Z_{\max} - Z_{\min}} \right)^5 \tag{4.2.2.10}$$

Formula (4.2.2.10) shows that the source function determines the potential areas of the dust source. Namely, the source function indicates the probability of accumulation of precipitation in grid cell i with height Z_i, where Z_{max} and Z_{min} are the maximum and minimum elevations in the surrounding of grid cell i, respectively.

4.2.2.2. Physical parameterizations

As summarized in Table 4.1, the following physical parameterization schemes of WRF-Chem were used to conduct dust experiments: The Purdue Lin scheme (Lin et al. 1983 [33]) with parameterization of saturation and ice deposition (Chen and Sun 2002 [4]) was used to interpret microphysical processes; The 3D scheme of the Grell and Devenyi ensemble was used to process cumulus convection over land and ocean (Grell and Devenyi 2002 [17]); The model of fast radiation transfer (RRTMG) with both short-wave and long-wave radiation was used to take into account the effect of direct radiation (Iacono et al. 2008 [22]); The parameterization of the turbulent kinetic energy Mellor–Yamada–Nakanishi and Niino (MYNN) (level 2.5) was used to describe the planetary boundary layer (Nakanishi and Niino 2009 [36]); The Janjic Eta Similarity Surface Layer scheme (Janjic 2002 [24]) and the RUC land surface model (Benjamin et al., 2004 [2]) were chosen to represent the physics of the surface layer and the interaction of the surface layer to the earth. In experiments with dust collectors, was activated only dust tracers - 4 dust bins scheme a scheme of 4 dust collectors was used.

Table 4.1. Namelist of physical parameterization schemes used in WRF-Chem model

Physical options	Option number	Namelist variable	Model
Microphysics	2	mp_physics	Purdue Lin
PBL model	2	bl_pbl_physics	MYNN level 2.5
Cumulus convection	5	Grell 3D	Tiedtke

scheme over the land and the ocean		Ensemble Scheme	Grell 3D Ensemble Scheme
Land surface	3	sf_surface_physics	RUC model
Surface similarity	1	sf_sfclay_physics	MM5 similarity scheme
Shortwave radiation	4	ra_sw_physics	RRTMG
Long-wave radiation	4	ra_lw_physics	RRTMG
Dust only dust tracers	1	dust_opt/	DODT
Aerosol mixing rules	2	aer_op_opt	Maxwell–Garnett
Chem	401	chem_opt	

4.2.3. Model validation

To validate the model, comparisons between the WRF-Chem v.3.6.1 model outputs and the different types of satellite observation data, obtained from the Moderate Resolution Imaging Spectroradiometer (MODIS-(http://modis.gsfc.nasa.gov/), Cloud Aerosol Lidar and Infrared Pathfinder Satellite Observation (CALIPSO-(http://eosweb.larc.nasa.gov/)) and ground based in situ measurements obtained from the National Environmental Agency (NEA) of Georgia were performed. Also the Hybrid Single-Particle Lagrangian Integrated Trajectory (HYSPLIT (http://ready.arl.noaa.gov/HYSPLIT.php)) model was used for computing air masses dispersion, pollutants (aerosols) trajectories and deposition from local to global scales.

4.2.3.1. In situ data

One of the areas of activity of the NEA of Georgia is the preparation and dissemination of warnings in case of expected natural, hydro-meteorological disasters, adverse events and extreme environmental pollution (in order to ensure state security and safety of the population). To carry out these activities, in particular, there are nine automatic air monitoring stations in Georgia (four in the west and five in the eastern part of Georgia), and four of them are located in the capital of Georgia, Tbilisi (http: // nea). .gov.ge / o / o / o-we / 2). In this study, we used PM10 data obtained from air monitoring stations located in Batumi and Kutaisi (Western Georgia) and from four air monitoring stations located at different areas in Tbilisi (Eastern Georgia).

4.2.3.2. CALIPSO data

Both day and night, the Cloud-Aerosol Lidar and Infrared Pathfinder Satellite Observation (CALIPSO) provides a wealth of data throughout the region to study the effects of clouds and aerosols on the radiation balance and climate of the Earth since 04/04/2006. The CALIPSO satellite contains 3 instruments: cloud aerosol lidar with orthogonal polarization (CALIOP), infrared radiometer (IIR) and wide-angle camera (WFC). CALIOP is the main tool on the CALIPSO satellite, since it provides significant information on the vertical and horizontal distribution of clouds and aerosols (Winker et al. 2007 [53]). CALIOP receives vertical profiles of elastic backscattering at two wavelengths (532 nm and 1064 nm) in both day and night phases at an altitude of 705 km of the orbit and also provides linear depolarization profiles at 532 nm, which makes it possible to distinguish between ice and water clouds, as well as to identify non-

spherical aerosol particles (Winker et al., 2007 [53]). CALIPSO detects dust aerosols using the volume depolarization ratio (perpendicular to the parallel component of the received lidar signals) at 532 nm (Omar et al., 2009 [37]). In this study, profiles of the Vertical Feature Mask, Aerosol Subtype and Total Attenuated Backscatter from CALIPSO version 3.40 level 2 are used to obtain information about the sources and routes of dust event transportation.

4.2.3.3. MODIS data

The Moderate Resolution Imaging Spectroradiometer (MODIS) is a key instrument aboard NASA's on both Terra (since February 2000) and Aqua (since June 2002) satellites, which daily monitor Earth in a wide spectral range. MODIS plays a pivotal role in developing models of the Earth system that can accurately predict global changes in the environment (Li and Sokolik, 2018 [31]). MODIS Terra and Aqua in orbits with a height of 705 km make it possible to cover a swath width of 2,330 km, obtaining data for 36 spectral wavelengths from 0.41 to 14 μm, and these measurements are used to obtain the parameters of the spectral optical thickness of the aerosol and the parameters of aerosol size above ground every two days (Remer et al. 2005 [39]). This article used data from MODIS: satellite images of Red Green Blue (RGB) with a resolution of 500 m and Aerosol Optical Depth (AOD) - 0.55 microns, obtained from the Aerosol Product of MOD04 level 2. These data were used to assess calculated dust clouds and to detect large sources of emissions of dust and dust clouds. Potential dust cells were determined based on the AOD values extracted and obtained by the MODIS sensor (Draxler et al. 2010 [11]).

4.3. Results and Discussion

Between December 2017 and November 2018, nine cases of dust transfer were recorded in the South Caucasus (Georgia). Two have been modeled and are discussed in this article.

4.3.1. Dust storm in the Sahara March 22, 2018

A strong dust storm burst out in Eastern Sahara (northeastern Libya), which on March 22, 2018, from Libya moved to Crete and the southeastern Aegean islands and the island of Rhodes (Solomos et al. 2018 [50]). This dust belt gradually stretched to the northeast during the day, and then moved in the direction of Turkey, to the Black Sea and reached both South Russia (Krasnodar Territory) and the coastal regions of Georgia. Indeed, red-brown snow and rain were recorded in Sochi (the Russian Black Sea coast), in Tbilisi (the capital of Georgia), and surroundings on March 23, 2018.

4.3.1.1. WRF-Chem/Dust model results

The results of numerical calculations performed by the WRF-Chem / Dust v.3.6.1 model are presented in Fig. 4.2. Namely Fig. 4.2 (a) shows that a strong wind blows over the Black Sea, transferring dusty air masses from the south to the southeastern coastal zone of the Black Sea at 18:00 on March 23, 2018. At the same time, a large dust cloud is observed on the territory of eastern Georgia (apparently imported from the southeast). Thus, Fig. 4.2 (a) shows that there is a simultaneous bilateral invasion of air masses from the southwest and southeast on the territory of Georgia (which is rare and accounts for 1.1% of all major synoptic processes). Figure 4.2 (b) shows that fairly

strong atmospheric currents carry dust clouds from Turkey to the south-west coast of Georgia, and at the same time, dust clouds are removed (disappear) from the territories of eastern Georgia at 20:00 on March 23. 2018. Over the next 2 hours, dust clouds from Turkey reached the western coast of Georgia (see Fig. 4.2 (c)), and then dust clouds were delivered by air currents to the territory of Eastern Georgia at 00:00. March 24, 2018 (see Fig. 4.2 (d)). Over the next 2 hours, dust clouds cross the ridge of the Great Caucasus and spread throughout the southern territory of Russia (Fig. 4.2 (e)). From Fig. 4.2 (f) it is clear that at 12 noon a new portion of dust clouds appear in the waters of the Black Sea (stretching from Turkey to Abkhazia), moving in the direction of Russia (to the mountains of Sochi and the Great Caucasus). Further calculations showed that dust clouds left both the waters of the Black Sea and the territory of Georgia at 22:00 on March 24, 2018.

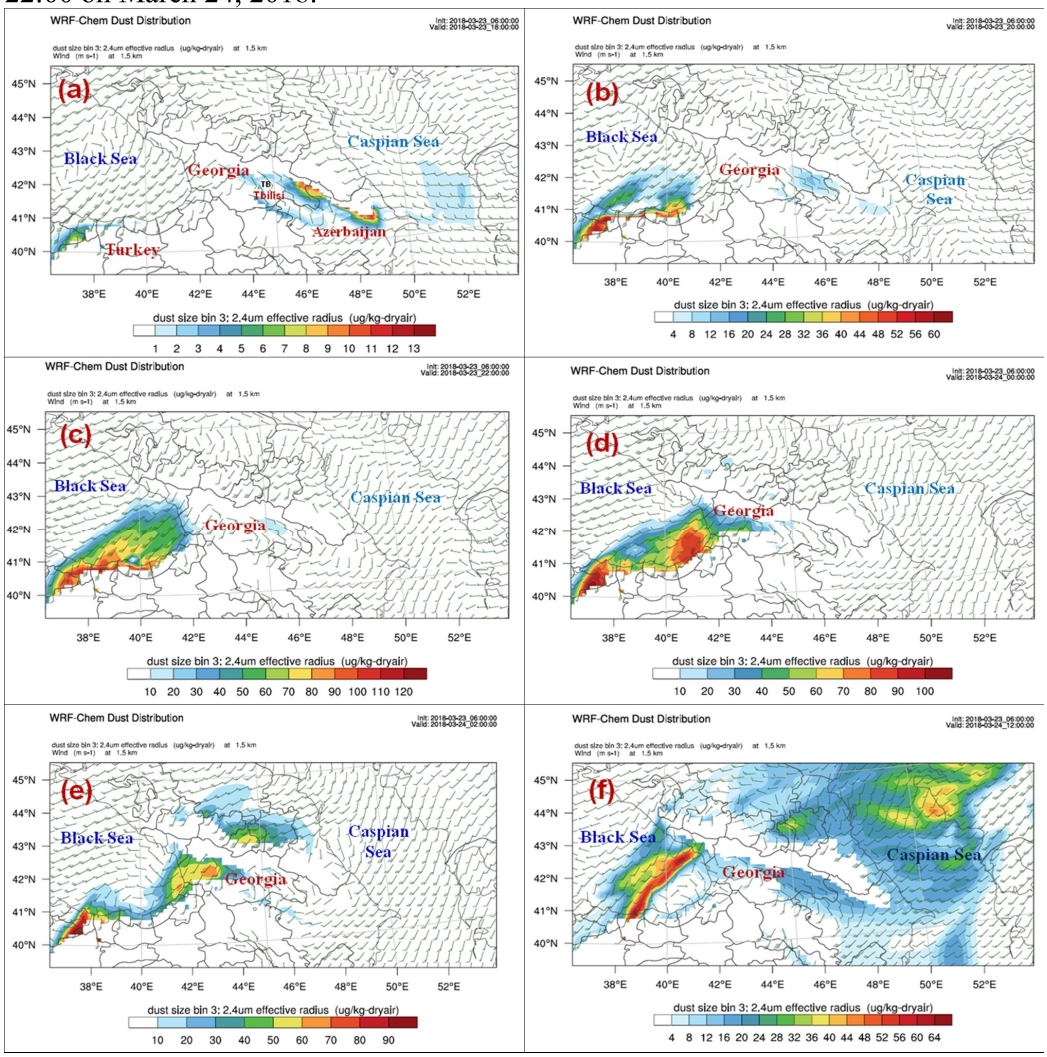

Fig.4. 2. The results of numerical calculations according to the WRF-Chem v.3.6.1 model, performed in the nested domain with a resolution of 12.4 km, obtained for the following time instants: (a) - at 18:00 on March 23; (b) at 20:00 on March 23, 2018; (c) - at 22:00 on March 23; (d) - at 00:00 on March 24; (e) - at 02:00 on March 24; (e) – at 12:00 on March 24th.

4.3.1.2. HYSPLIT model calculation results

Determining the trajectories and location of the dust source is important when studying dust storms, and the HYSPLIT model is a good tool to study this issue. Therefore, in this study, the HYSPLIT model is used to study the location of the source of dust storms and the trajectories of precipitated dust clouds in Georgia (Tbilisi (41 ° 72 'north, 44 ° 78' east) and Batumi (41 ° 38 'north, 41 ° 38 'East longitude)) from March 22 to March 24, 2018.

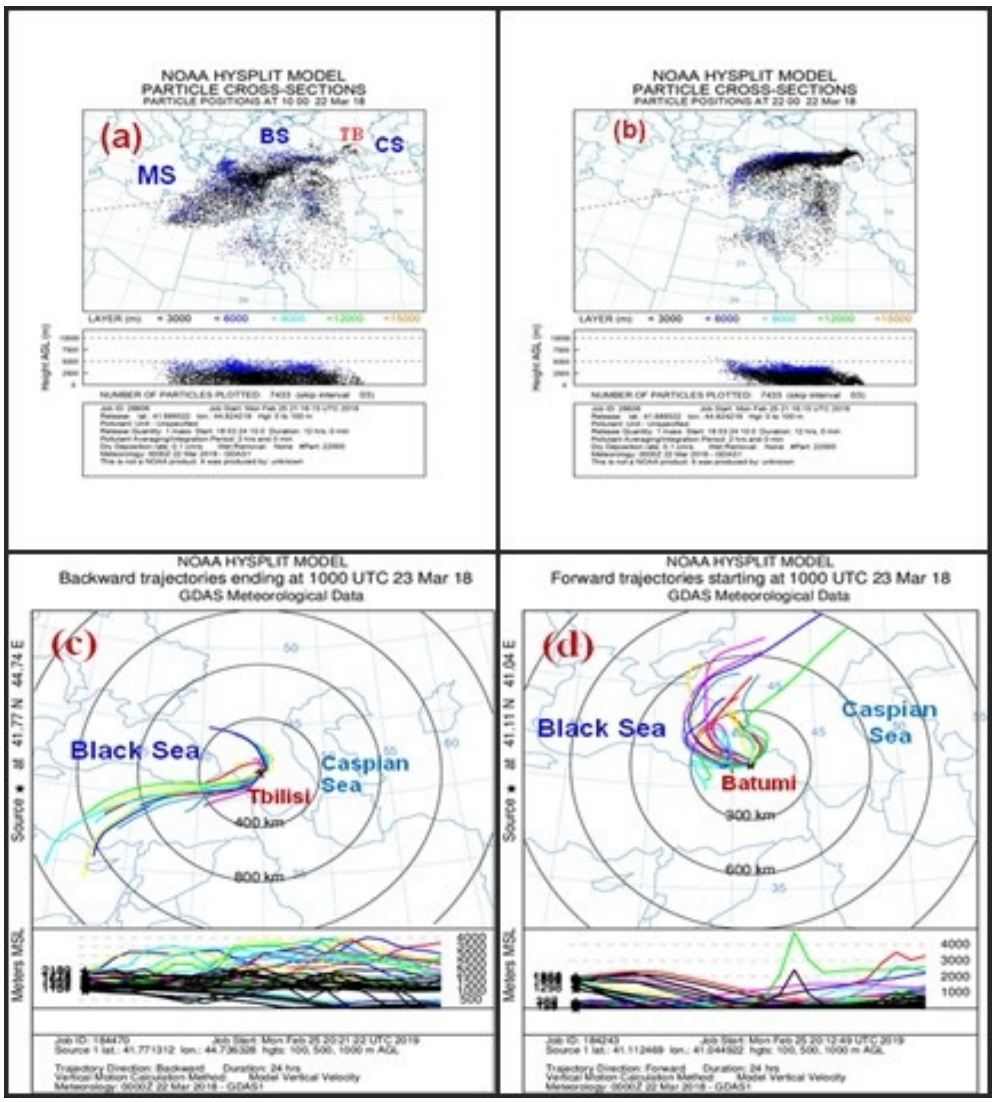

Fig.4.3. The results of calculations by the HYSPLIT model, performed (a)at 10:00 on 22nd of March 2018; (b) at 22:00 on 22nd of March 2018; (c) at 10:00 on 23rd of March 2018; (d) at 10:00 on 23rd of March 2018, based on GDAS meteorological data (in Fig.5.3.(a): (MS)-the Mediterranean Sea; (BS)-the Black Sea; (CS)-the Caspian Sea; TB-(Tbilisi))

Some results of calculations of the HYSPLIT model performed to determine the sources and forward and backward trajectories are presented in Fig. 4.3. Namely, in Fig. 4.3. (a) and (b) show cross sections of particles obtained using the HYSPLIT model at

10:00 and 22:00 on March 22, 2018, respectively. Analysis of Fig. 4.3 (a) shows that a dust storm occurred as a result of an outbreak of dust in the desert in Libya, the maximum concentration of dust aerosol is observed above the waters of the Mediterranean Sea, and the dust plume is completely contained in a 5-km layer in the vertical direction, while the bulk of the dust aerosols is limited by height 2.5 km. Comparison of Fig. 4.3 (b) (received after 12 hours) with Fig. 4.3 (a) shows that the bulk of the dust particles moved from the Mediterranean to Turkey, and the dust cloud from Turkey (through the waters of the Black Sea) invaded Georgia. It should be noted that in both cases, the dust plume transported from the source areas inside the boundary layer, which, as a rule, causes more precipitation due to gravitational sedimentation. In Fig. 4.3, (c) shows the reverse trajectories obtained by the HYSPLIT model (ending at 10:00 UTC on March 23, 2018), and in Fig. 4.3, (d) shows the direct trajectories (starting at 10:00 UTC on March 23, 2018). Analysis Fig. 4.3 (c) shows that the reverse paths (the source is located in Tbilisi at altitudes of 100, 500, 1000 m above sea level, the calculation time is 24 hours) pass through the territories of Georgia, the Black Sea, Turkey and the Mediterranean Sea. In Fig. 4.3 (d) it can be seen that direct trajectories (a source located in Batumi) pass from Georgia through the Black Sea to the territory of Russia (Sochi, Krasnodar Territory). Thus, according to the calculations of the HYSPLIT model, a dust-flash cloud located on the southern coast of the Mediterranean Sea reached the southern territories of Russia (Krasnodar Territory) and the territory of Georgia, which is in good agreement with the results of the WRF-Chem model and with observational data.

4.3.1.3. Validation of calculation results

First of all, the results of numerical calculations were evaluated by ground-based PM10 measurements (obtained from NEA). In situ observations presented in Table 4.2 confirms the numerical calculations performed by the WRF-Chem and HYSPLIT models and show the existence of high PM10 concentrations in Tbilisi. Namely, the 24-hour averaged distribution of PM10 concentrations in various districts of Tbilisi from March 22 to March 25, 2018 exceeded the corresponding maximum permissible concentrations (MPC) (50 μg/m^3) in all areas of Tbilisi. For example, PM10 concentrations exceeded the MPC on Tsereteli Avenue by 4.76 times, on Kazbegi Avenue by 4.58 times, in Varketili area by 3.62 times and in Vashlijvari by 4.92 times.

Table 4.2 . 24-hours averaged PM10 concentrations distribution in different districts of Tbilisi from March 22 to March 25, 2018 and 24-h average bias error (BE) and the root mean square error (RMSE) calculated against average PM_{10} observations.

PM_{10} (mkg/m^3)	Tsereteli Avenue	Kazbegi Avenue	Varketili District	Vashlidjvari District	Average	BE	RMSE
22/3/2018	49.0	57.0	42.0	41.0	47.25	-	-
23/3/2018	**238.0**	**229.0**	**181.0**	**246.0**	**223.5**	**-31.01**	**44.79**
24/3/2018	**178.0**	**174.0**	**126.0**	**195.0**	**168.25**	**-37.23**	**52.67**
25/3/2018	75.0	69.0	58.0	84.0	71.5	-	-

Then, the calculation results obtained by the WRF-Chem and HYSPLIT models were evaluated using data received from the Cloud-Aerosol Lidar and Infrared Pathfinder Satellite Observation (CALIPSO).

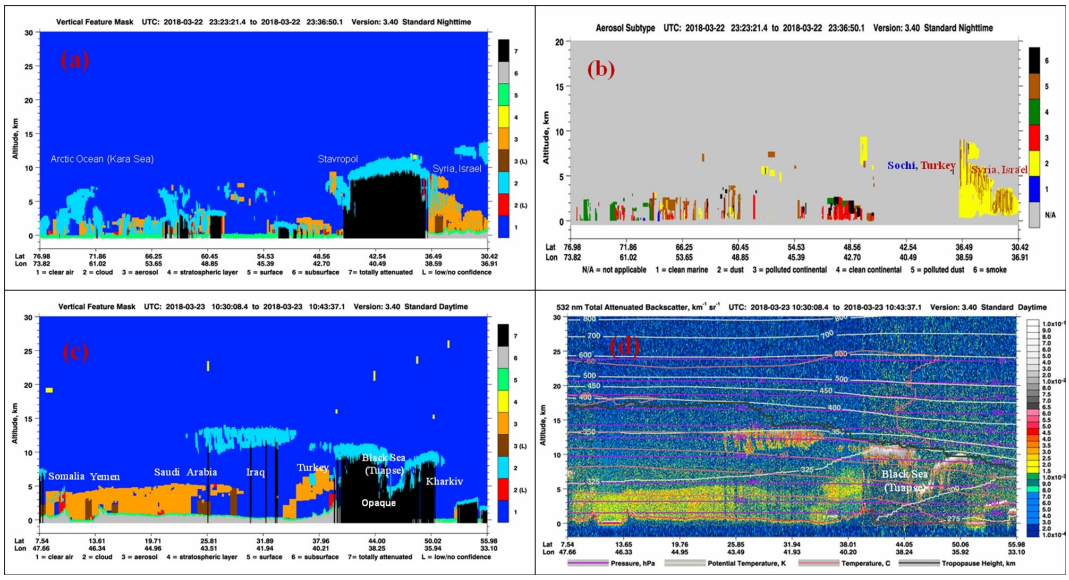

Fig.4.4. The altitude-orbit- cross–section measurements obtained from CALIOP version 3.40: (a)-vertical feature mask and (b)-aerosol subtype were obtained at standard nighttime from 23:23 to 23:36 on 22nd March; (c)-vertical feature mask and (d)-total attenuated backscatter were obtained at standard daytime from 10:30 to 10:43 on 23 March 2018.

Fig. 4.4. (a) shows the vertical arrangement of all atmospheric layers, detected by a level 2 processing code, that stretch horizontally for a thousand kilometres from the Arctic Ocean (Kara Sea: Lat: 71^0.86 ', Lon: 61^0.02') to Israel (Lat: 30^0, 42 ', Lon: 36^0.91'). Fig.4. 4 (a) shows that vertically the aerosols (orange) are mainly located below 5 km, and an increase in the number of aerosol plumes on the right side of Figure 4.4 (a) is especially observed (in the territories of Israel and Syria). It should be noted that, there is observed a totally attenuated area from the town Ain Issa (Lat: 36^0.49', Lon:$38^0$59', the North of Syria), until Stavropol (Lat: 46^0.06 ', Lon: 42^0.22', Russia), due to the presence of huge clouds at an altitude of 10 km. Figure 4.4. (b) shows subtypes of aerosols: dust, contaminated continental and contaminated dust, which are colored yellow, red and brown, respectively. Fig. 4.4. (b) confirms that the territories of Israel and Syria are covered with strong dust plums, but the territories of our interest, such as Crete, Rhodes, Turkey, are inaccessible for CALIOP observations. The following two slides in Figure 4.4 ((c) depicts the vertical mask and (d)- general attenuated backscatter), obtained at standard daytime-from 10:30 to 10:43 UTC (14:30~14:43 LGT) on 23 March 2018, depict aerosol plumes in Somalia, Yemen, Saudi Arabia, Iraq, Turkey, the Black Sea waters (Tuapse), Russia (Krasnodar Territory) and Ukraine (Kharkov). Analysis Fig. 4.4 (c) and (d) show that the territory of Turkey is covered with aerosol clouds, but the waters of the Black Sea, the coastal regions of Georgia and the Krasnodar Territory (Sochi) are not accessible for CALIOP observations.

4.3.2. Dust storm in Turkmenistan July 25-27, 2018

An unusually strong dust storm was recorded in the capital of Azerbaijan, Baku, on July 26, 2018, causing a strong yellow haze (like of tobacco smoke) and reducing visibility (see Fig.4.5). The Ministry of Ecology and Natural Resources of Azerbaijan officially announced in the press that a moderate north-west wind brought dust from neighboring Turkmenistan across the Caspian Sea and a dust storm completely covered the Absheron peninsula and raised humidity and air temperatures. On July 27, 2018, dust fog was fixed in Tbilisi and its environs and the NEA of Georgia has announced that the dust cloud was coming from Turkmenistan via Azerbaijan.

Fig. 4.5. The capital of Azerbaijan, Baku, painted yellow with dusty aerosols on July 26, 2018

4.3.2.1. WRF-Chem/Dust model results

The results of calculations obtaned on a coarse mesh using the WRF-Chem model, simulating the transfer of a dust storm from Turkmenistan, are presented in Fig. 4.6 (a) - (d). An analysis of Fig. 4.6 shows that initially there are two large dust clouds at an altitude of 800 m (a.s.l.) in the Karakum desert and in addition two more small dust clouds are observed over Syria and Iraq at 06:00 on July 26, 2018 (Fig. 4.6 (a)). Fig. 4.6 (b) shows that over time, the Karakum dust cloud moved west to the Caspian Sea, and at the same time a larger dust cloud appeared over the Arabian Peninsula, which shifts toward the Indian Ocean at 08:00. 26 July. From Fig. 4.6 (c) it can be seen that the Karakum dust cloud occupied the territory of Azerbaijan and moves west to the territory of Georgia at 16:00 on July 26. Indeed, from Fig. 4. 6 (d) it is clear that the Karakum dust cloud reached the territory of Georgia and further tends to move north-west towards Russia, at 06:00 on July 27.

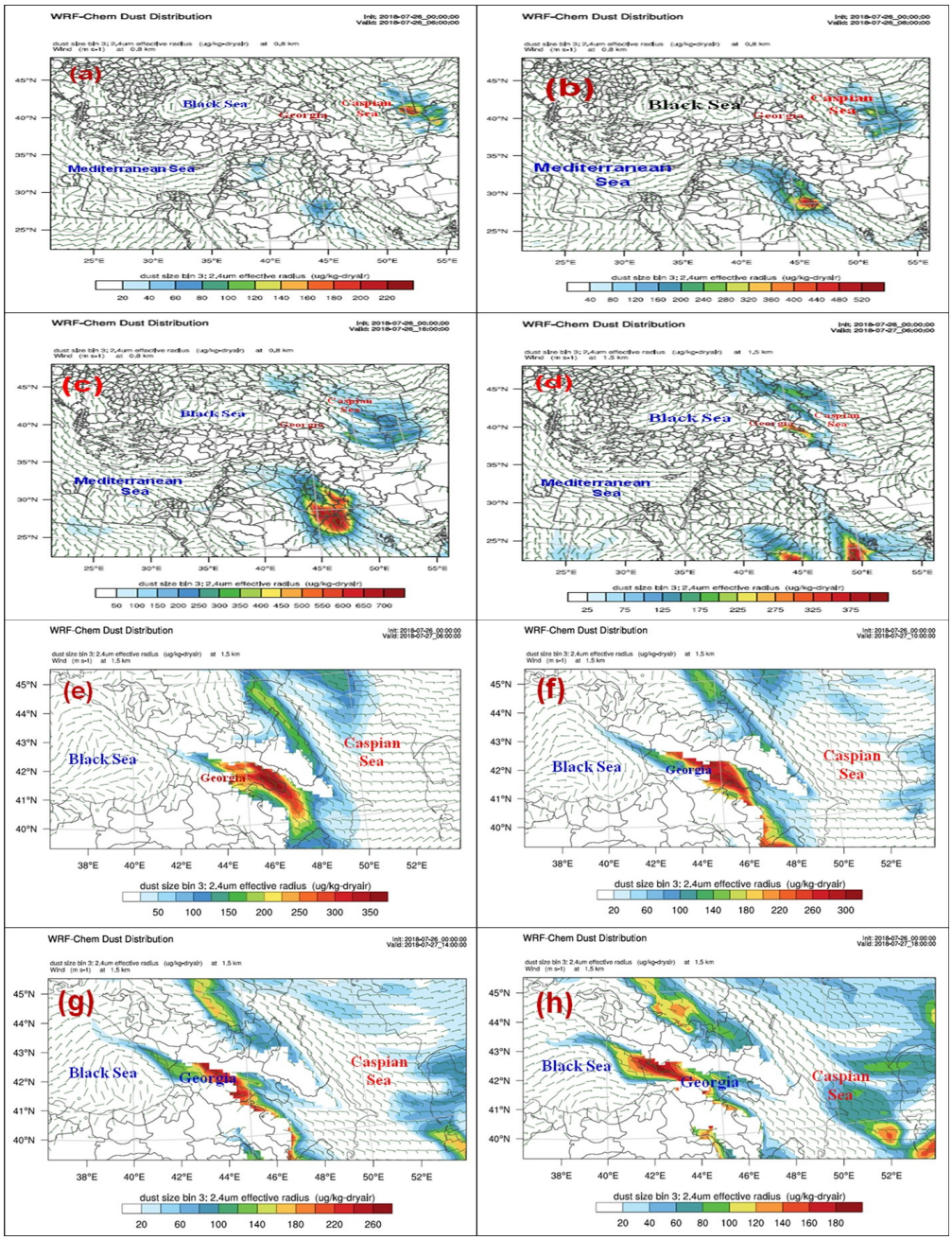

Fig. 4.6. The results of numerical calculations of the model WRF-Chem v.3.6.1, executed on a coarse (a) - (d) and fine resolution grids (e) - (h) a) at 06:00 on July 26, 2018; b) at 08:00 on July 26, 2018; c) at 16:00 on July 26, 2018; d) at 06:00 on July 27, 2018; e) 06:00 July 27, 2018; e) 10:00 on July 27, 2018; g) 14:00 on July 27, 2018; (h) 18:00 on July 27, 2018.

The results of calculations performed by WRF-Chem on a fine mesh at an altitude of 1,500 m (a.s.l.) are presented in Fig. 4.6 (e) - (h). In contrast to Fig. 4.6 (d), Fig. 4.6 (e) clearly shows that the Karakum dust cloud reached the territory of Western Georgia at 06:00 on July 27, 2018. The next slide (see Fig. 4.6 (f)) shows that the Karakum dust cloud reached the Black Sea coastal zone at 10:00 on July 27, and Fig. 4.6 (g) shows

that the dust cloud occupied almost the entire territory of Georgia (at an altitude of 1.5 km above sea level) and it reached the Main Caucasian Range on July 27 at 14:00. From Fig. 4.6 (h) it can be seen that a part of the Karakum dust cloud (principally moved by air currents from the Caspian Sea to the Black Sea, through the Georgian transport corridor) overcomes the Likhi Range, occupied the territory of Western Georgia and the northeast coastal zone of the Black Sea at 18 : 00 July 27, 2018. It should be noted that dust clouds, which are observed in the territory of the North Caucasus (Russia) (see Fig. 4.6 (h)), were obviously delivered by another air flows blowing from the Caspian Sea in a north-westerly direction.

4.3.2.2. Validation of calculation results

The data for 24-hour averaged PM10 concentrations obtained using automatic meteorological devices located in different districts of Tbilisi from July 26 to 29, 2018 are presented in Table 4.3.

Table 4.3. The values of average daily concentrations of PM10, bias errors (BE), and root mean square errors (RMSE) in different districts of Tbilisi from July 26 to 29, 2018.

PM_{10} (mkg/m^3)	Tsereteli Avenue	Kazbegi Avenue	Varketili District	Vashlidjvari District	Average	BE	RMSE
26/7/2018	56.0	89.0	52.0	45.0	61.0	-	-
27/7/2018	**148.0**	**179.0**	**152.0**	**206.0**	**172.0**	**33.17**	**47.31**
28/7/2018	**78.0**	**74.0**	**76.0**	**95.0**	**81.0**	-	-
29/7/2018	52.0	53.0	54.0	55.0	54.0	-	-

Table 4.3 clearly shows that the remnants of the Karakum dust storm reached the territory of Tbilisi on 27/7/2018. Although dust concentrations are not as high as in Table 4.2, nonetheless, PM10 concentrations (averaged over 24 hours) in all areas of Tbilisi are several times higher than the corresponding MPCs from 27/7/2018 to 29/7/2018 of the year. Namely, the concentration values of PM10 as of 27/7/2018 exceed the MPC values on Tsereteli Avenue by 2.96 times, on Kazbegi Avenue by 3.58 times, in the Varketili area by 3.04 times and in the Vashlijvari area by 4.12 times , which is the easternmost district in Tbilisi. Table 4.3 shows that, in general, PM10 concentrations averaged over area and time were 3.44 times higher than the corresponding MPC (50 μg / m3) on July 27, 2018, and its values remained too high until July 30, 2018 in Tbilisi. The uneven distribution of PM10 concentrations in Tbilisi is due to the complex topography of Tbilisi and local circulation processes.

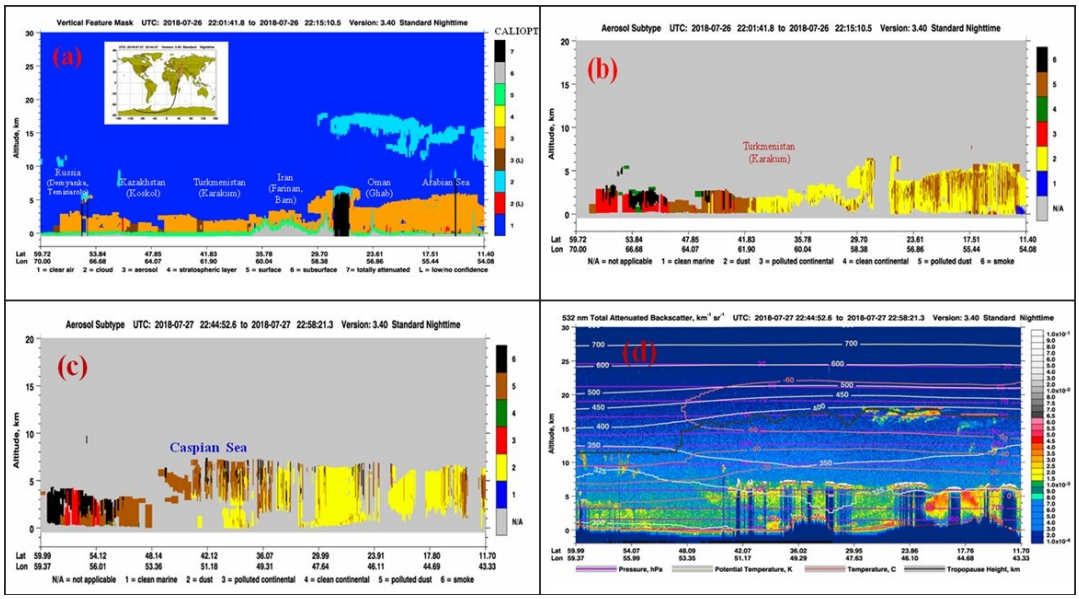

Fig. 4.7. The altitude-orbit- cross–section measurements performed by CALIOP version 3.40: (a)-vertical feature mask and (b)-aerosol subtype were obtained at standard nighttime UTC from 22:01 to 22:15 on 26th July; (c)-aerosol subtype and (d)-total attenuated backscatter were obtained at standard nighttime UTC from 22:44 to 22:58 on 27th July 2018.

The calculation results obtained by the WRF-Chem model, simulating the transfer of a dust storm from Turkmenistan, were evaluated using the altitude-orbit-cross–section measurements performed by CALIOP version 3.40 (see Fig. 4.7 (a)-(d)). Fig. 4.7 (a), representing a vertical feature mask of CALIOP, shows that the standard night satellite track (obtained at UTC standard night time from 22:01 to 22:15 July 26, 2018) is streached from Russia (Demynka (Lat:59^0.72', Lon:70^0.00') to the coastal zone of Oman (Lat:11^0.40', Lon:54^0.08') in the Arabian Sea), through the territory of Kazakhstan (Koskol), Turkmenistan (Karakum), Uzbekistan (Middle), Iran (Farima and Bam), Oman (Ghab (Lat: 23^0.57', Lon: 56^0.85')). Fig. 4.7 (a) shows that aerosol plumes are mainly contained in a 3-km layer from Russia to Iran (Kerman), including the Karakum desert and 6-7 km layer to the south (including the Arabian Sea). Fig. 4.7 (b), showing subtypes of aerosols (obtained at standard UTC night time from 22:01 to 22:15 on July 26), confirms that the territory of our interest, Turkmenistan (Karakum), is heavily polluted by dust, while the territories Russia and Kazakhstan are mainly contaminated with smoke and contaminated dust. In addition, territories from Iran to the Arabian Sea are contaminated with a mixture of dust and contaminated aerosol dust plumes. The following two figures representing the aerosol subtypes (Fig. 4.7 (c)) and the total attenuated backscatter (Fig. 4.7 (d)), were obtained at Standard UTC night time from 22:44 to 22:58, July 27, 2018. Fig. 4.7 (c) and Fig. 4.7 (d) (representing CALIOP measurements extending from Russia (Perm Lat: 59^0.59', Lon:59^0.37') to Saudi Arabia (Lat: 17^0.80', Lon: 44^0.89')) show that, over the Caspian Sea (in the upper3 -7 km layer), strong dust drains are observed, while in the lower 3 km layer dust drains are observed to a lesser extent and in the region of interest to us, in Eastern Georgia, unfortunately, is not in the field of view of the CALIOP detector device.

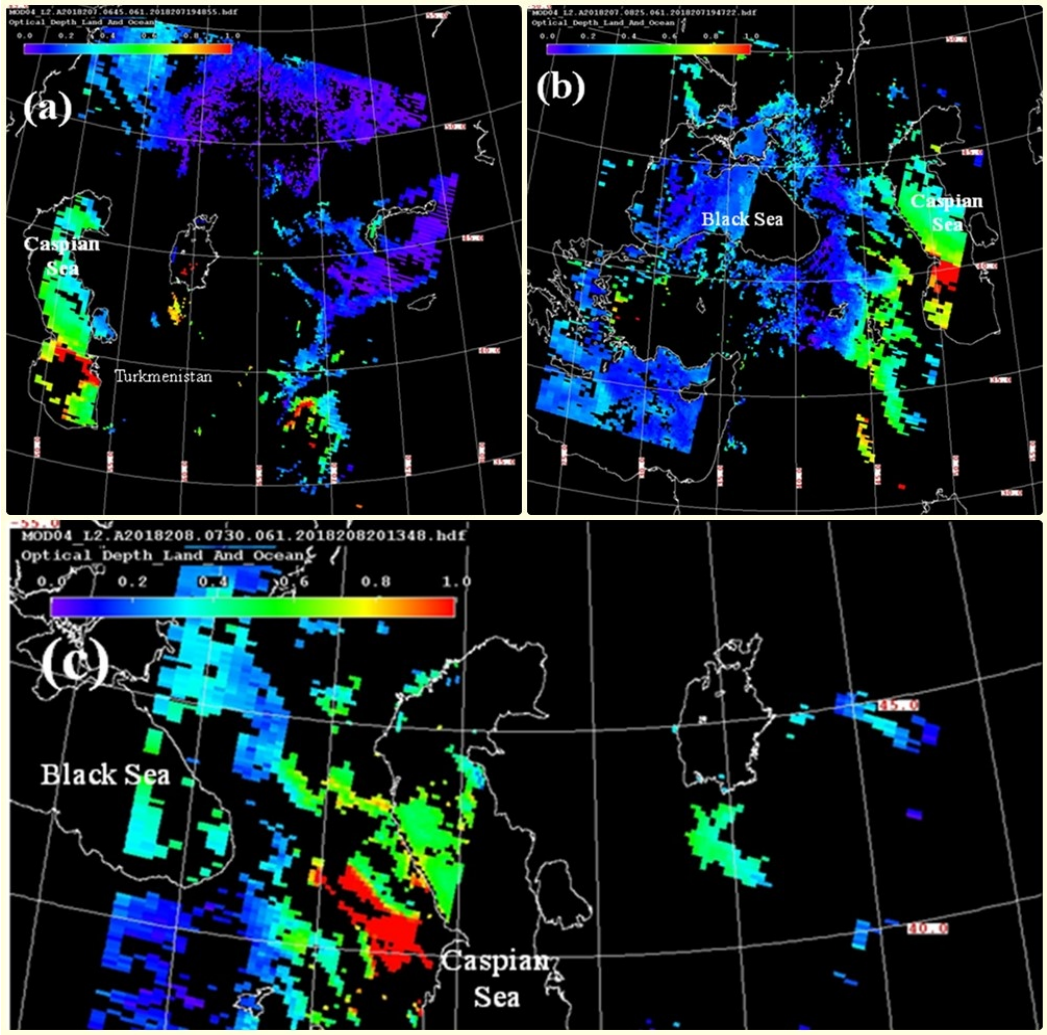

Fig.4.8. The maps of the altitude-orbit- cross–section horizontal measurements of aerosol optical thickness (AOT) obtained using MODIS version 3.40 at different points in time: (a)- at (UTC: 06:45) on 26 July 2018, (b)- at (UTC: 08:25) on 26 July 2018, (c)- at (07:30 UTC) on 27 July 2018.

With some exceptions, horizontal measurements of the optical thickness of the aerosol (AOT) obtained using MODIS v. 3.40, more clearly identify areas with a high concentration of dust in the deserts than using CALIPSO (Ma et al. 2013 [34]). Indeed, in Fig. 4.8 clearly depicted AOT MODIS products in Central Asia (Fig. 5.8 (a)) and in the Caucasus (Fig. 5.8 (b), (c)). In fact, in Fig. 4.8 (a) clearly shows the band with the maximum AOT value, stretched across the Caspian Sea (from Turkmenbush to Baku) at 6:45 on July 26, 2018. Fig. 4.8 (b) shows that two hours later this band completely occupied Baku and advanced west to the territory of Azerbaijan. From Fig. 4.8 (c) it can be seen that within 23 hours this strong band of dust completely occupied the territories of Azerbaijan and Eastern Georgia and reached the capital of Georgia, Tbilisi, on the morning of July 27, 2018.

4.4 Conclusion

In this study, numerical simulation together with remote sensing products is used for the first time to study dust transfer, dispersion and accumulation from deserts to the territory of the South Caucasus (Georgia). Namely, the WRF-Chem v.3.6.1 and HYSPLIT models, together with the CALIPSO and MODIS satellite-based observation tools, are used to study the transfer of intense dust storms from the Sahara and Sahel in Africa, from the Arabian deserts in the Middle East, from Kyzylkum and Karakum to Central Asia to the territory of the South Caucasus (Georgia). The results of calculations of the WRF-Chem model, performed from December 2017 to November 2018, showed that nine cases of dust transfer to the territory of the South Caucasus (Georgia) were simulated. Two of them, held on March 22-24 and July 25-26, 2018, were modelled and discussed in this chapter. Comparison of the calculation results of the WRF-Chem v.3.6.1 model with the observational data and the products of CALIOP and MODIS showed that the WRF-Chem model well simulated the transfer of dust aerosols from the Sahara and Kara-Kum deserts to the Caucasus in a complex terrain. In addition, calculations performed on nested grids showed that the use of a small-scale grid, with a horizontal resolution of 12.4 km, improved the results of numerical simulations. It should be noted that in our study, the WRF-Chem model was not able to record the transfer of dust storms from the Takli-Makan and Gobi deserts to the South Caucasus during our short-term (48-hour) calculations. But the Karakum and Kyzyl Kum deserts are closer to the Caucasus, and in our study, of the nine dust events detected, dust transfer to the Caucasus was observed three times from the Karakum and Kyzyl Kum deserts, and this fact was recorded in the first with the help of modelling. An analysis of the results showed that, in addition to dust storms, the background PM10 dust concentrations in Georgia were high (see Table 5.2 and Table 5.3), and therefore it can be concluded that dust aerosols have a strong effect on health, agriculture and the complex climate system of Georgia.

In short the results showed that: (i) WRF model was able to simulate dust aerosols transportation to the Caucasus well in conditions of a complex topography; (ii) dust aerosols were transported equally from the African, Middle east and Central (West) Asian deserts during the study period; (iii) using the fine resolution grid (12.4 km) improved the quality of the numerical simulations; (iv) dust aerosol is an important factor affecting the climate system of Georgia; (v) WRF-Chem model with HYSPLIT model can be taken as a testimonial in dust aerosol forecasting at Georgian National Environmental Agency in daily air quality service.

References to Chapter 4

1. Andreae M. O. and Rosenfeld D. 2008: Aerosol-cloud precipitation interactions. Part 1. The nature and sources of cloud-active aerosols. *Earth-Science Review*., 89: 13–41.
2. Benjamin S. G., Grell G. A., Brown J. M., et al. 2004: Mesoscale weather prediction with the RUC hybrid isentropic-terrain-following coordinate model. *Montly Weather Review,* **132**: 473-494.
3. Charlson R. J., Schwartz S. E., Hales J. M., et al. 1992: Climate forcing by anthropogenic aerosols. *Science,* 255 (5043): 423-430.

4. Chen S. and Sun W. 2002: A one-dimensional time dependent cloud model. J.Meteor.Soc. Japan., 80 (1): 99-18.
5. Chin, M., Rood, R. B., Lin, S.-J., Muller, J. F., and A. M.Thomspon: Atmospheric sulfur cycle in the global model GOCART: Model description and global properties, *J. Geophys. Res.-Atmos*., 105, 24671–24687, 2000.
6. Choobari O. A., Zawar-Reza P., Sturman A. 2013: The global distribution of mineral dust and its impacts on the climate system: *Atmospheric Research*., 138: 152–165.
7. Davitashvili T. 2019: Modelling transportation of desert dust to the South Caucasus using WRF Chem model, *E3S Web of Conferences* **99**, 03011 (2019) *CADUC 2019* https://doi.org/10.1051/e3sconf/20199903011.
8. Davitashvili T., 2018:. On Some Aspects of Climate Change in Georgia, *International Journal of Energy and Environment*, 12: 80-86.
9. Davitashvili T., Kutaladze N., Kvatadze R. et al. 2018:. Effect of dust aerosols in forming the regional climate of Georgia. *Scalable Computing: Practice and Experience*, 19 (2): 199–208.
10. Dong Zh., Li Zh., Xiao C., et al. 2009:. Characteristics of aerosol dust in fresh snow in the Asian dust and non-dust periods at Urumqi glacier no. 1 of eastern Tian Shan, China. *Environmental Earth Sciences*, 60: 1361–1368.
11. Draxler R. R., Ginoux P., and Stein A. F., 2010: An empirically derived emission algorithm for wind-blown dust. *J. Geophysics Research*., 115: D16212
12. Eghbali A., Mirrokni S. M., Memarian M. H., 2016: Dust storm simulation using WRF−Chem. (case study: West Asia), *International Journal of Recent Research and Applied Studies*, 28(1): 1-12.
13. Erel Y., Dayan U., Rabi R., et al. 2006: Transboundary transport of pollutants by atmospheric mineral dust, *Environmental Science Technology*., 40: 2996–3005.
14. Fountoukis C., Ackermann L., Ayoub M. A., Gladich I., Hoeh, R. D. and Skillern A.2016: Impact of atmospheric dust emission schemes on dust production and concentration over the Arabian Peninsula, Model. Earth Syst. Environ., 2, 1–6.
15. Ginoux P., Prospero J. M., Gill T. E. et al. 2012. Global-scale attribution of anthropogenic and natural dust sources and their emission rates based on MODIS Deep Blue aerosol products, *Review Geophysics*, 50, RG3005: 1-36 doi:10.1029/2012RG000388.
16. Ginoux, P., Chin, M., Tegen, I. Et. Al., Sources And Distributions of Dust Aerosols Simulated with the GOCART Model. Journal of Geophysical Research, Vol. 106, No. D17, Pages 20,255-20,273, 2001.
17. Grell G. A., Devenyi D. 2002: A generalized approach to parameterizing convection combining ensemble and data assimilation techniques. *Geophysics Research Letters*., 29**:**1693-1712.
18. Grell G. A., Peckham S. E., Schmitz R. et al. 2005: Fully coupled "online" chemistry within the WRF model. *Atmospheric Environment*, 39: 6957–6976.
19. Grousset F. E., Ginoux P., Bory A., et al. 2003: Case study of a Chinese dust plume reaching the French Alps. *Geophysical Research Letters*, 30 (6), 1277.

20. Han Y., Dai X., Fang X. et al. 2008: Dust aerosols: A possible accelerant for an increasingly arid climate in North China, *Journal of Arid Environment*., 72: 1476–1489.
21. Huang J., Minnis P., Yan H., et al. 2010:. Dust aerosol effect on semi-arid climate over Northwest China detected from A-Train satellite measurements. *Atmospheric Chemistry Physics.*, 10: 6863–6872.
22. Iacono M. J., Delamere J. S., Mlawer E. J., et al. 2008:. Radiative forcing by long–lived greenhouse gases: Calculations with the AER radiative transfer models. *Journal of Geophysical Research.*, 113: 1-8.
23. IPCC: Climate Change. 2007: The Physical Science Basis. Contribution of Working Group I to the Fourth Assessment Report of the Intergovernmental Panel on Climate Change, edited by: Solomon S, Qin D, Manning,M. et al. *Cambridge University Press*, Cambridge, UK and New York, NY, USA.
24. Janjic Z. I. 2002:. Nonsingular implementation of the Millor-Yamada level 2.5 scheme in the NCEP Meso model. NCEP Office Note.437:61.
25. Javakhishvili Sh. 1988: Georgian Climate Description by the Months,. Publishing House "Ganatleba". Tbilisi, 1988. (Georgian)
26. Kang S., Zhang Y., Zhang Y., et al. 2010: Variability of atmospheric dust loading over the central Tibetan Plateau based on ice core glaciochemistry, *Atmospheric Environment*, 44: 2980–2989.
27. Kim K. W., Kim Y. J., Oh S. J. 2001: Visibility impairment during Yellow Sand periods in the urban atmosphere of Kwangju, Korea. Atmospheric Environment. 35 (30): 5157-5167.
28. Kordzakhia M. Climate of Georgia. Tbilisi, 1961, (Georgian).
29. Kutuzov S. S., Mikhalenko V. N., Shahgedanova M. V. et al. 2014: Ways of far-distance dust transport onto Caucasian glaciers and chemical composition of snow on the Western plateau of Elbrus, *Lëd i Sneg,* 54 (3): 5-15, (Russian).
30. Kutuzov S. S., Mikhalenko V. N., Grachev A. M., et al. 2016: First geophysical and shallow ice core investigation of the Kazbek plateau glacier, Caucasus Mountains. *Environmental Earth Sciences*, 75 (23): 1-15.
31. Li L. and Sokolik I. N. 2018: Analysis of Dust Aerosol Retrievals Using Satellite Data in Central Asia, *Atmosphere,* 9: 288.
32. Li Z., Zhao S., Edwards R., et al. 2011: Characteristics of individual aerosol particles over U¨ ru¨mqi Glacier No. 1 in eastern Tianshan, central Asia, China. *Atmospheric Research*., 99:57–66.
33. Lin Y. L., Farley R. D., and Orville H. D. 1983: Bulk parameterization of the snow field in a cloud model, *Journal of Applied Meteorology and Climatology*, 22: 1065–1092.
34. Ma X., Bartlett K., Harmon K., Yu F. 2013: Comparison of AOD between CALIPSO and MODIS: significant differences over major dust and biomass burning regions, *Atmospheric Measurement Techniques*, 6: 2391–2401.
35. Mikhalenko V., Sokratov S., Kutuzov S., et al. 2015: Investigation of a deep ice core from the Elbrus western plateau, the Caucasus, Russia. *The Cryosphere*, 9: 2253–2270.

36. Nakanishi M. and Niino H. 2009: Development of an improved turbulence closure model for the atmospheric boundary layer, *Journal of the Meteorological Society of Japan*, 87 (5): 895–912.
37. Omar A. H., Winker D. M., Kittaka C. et al. 2009: The calipso automated aerosol classification and lidar ratio selection algorithm. *Journal of Atmospheric Ocean and Technology*., 26: 1994–2014.
38. Prasad A. K., Yang K-H. S., El-Askary H. M., et al. 2009: Melting of major Glaciers in the western Himalayas: evidence of climatic changes from long term MSU derived tropospheric temperature trend (1979–2008), *Annals of Geophysics*, 27: 4505–4519.
39. Remer L. A., Kaufman Y. J., Tanr´e, D. et.al. 2005: The MODIS algorithm, products and validation, *Journals of the Atmospheric Sciences*., 62: 947–973.
40. Rizza U., Barnaba F., Miglietta M, M., et al. 2017: WRF-Chem model simulations of a dust outbreak over the central Mediterranean and comparison with multi-sensor desert dust observations. *Atmospheric Chemistry Physics*., 17: 93–115.
41. Rizza, U., Anabor, V., Mangia, C., Miglietta, M. M., Degrazia, G. A., and Passerini, G. 2016: WRF-Chem Simulation of a saharan dust outbreak over the mediterranean regions, *Ciência e Natura*,Vol. 38, Special Edition, 330–336,, doi:10.5902/2179460X20249,.
42. Rosenfeld D., Rudich Y., Lahav R. 2001: Desert dust suppressing precipitation: A possible desertification feedback loop, *Proceedings National Academy Science*. USA, 98: 5975–5980.
43. Schwikowski M., Brütsch S., Gäggeler H. W., et al.1999: A high-resolution air chemistry record from an Alpine ice core: Fiescherhorn glacier, Swiss Alps. *Journal. of Geophysics Research.* 104 : 13709–13719.
44. Shahgedanova M., Kutuzov S., White K. H. et al. 2013: Using the significant dust deposition event on the glaciers of Mt. Elbrus, Caucasus Mountains, Russia on 5 May 2009 to develop a method for dating and "provenancing" of desert dust events recorded in snow pack. *Atmospheric Chemistry Physics*., 13: 1797–1808.
45. ShaoY., Ishizuka M., Mikami M and Leys J. F.2011a: Parameterization of size-resolved dust emission and validation with measurements, *Journal of Geophysics. Research*, 116, D08203: 1-19.
46. ShaoY., Wyrwoll K. H., Chappell A. et al. 2011b: Dust cycle: An emerging core theme in Earth system science, *Aeolian Research*., 2: 181–204.
47. Skamarock W. C., Klemp J. B., Dudhia J., Gill D. O., Barke D. M., Wang W. and J.G. Powers, 2005: A description of the advanced research WRF Version 2. *NCAR Tech. Notes. Natl. Cent. for Atmos. Res*., Boulder, Colorado.
48. SNCUNFCCC-*Second National Communication to the United Nations Framework Convention on Climate Change*; Ministry of Environment Protection and Natural Resources, Republic of Georgia. 2009, www.unfccc.int, p. 240.

49. Sodemann H., Palmer A. S., Schwierz C. et al. 2006: The transport history of two Saharan dust events archived in an Alpine ice core. *Atmospheric Chemistry Physics*, 6: 667–668.
50. Solomos S., Kalivitis N., Mihalopoulos N., et al. 2018: From Tropospheric Folding to Khamsin and Foehn Winds: How Atmospheric Dynamics Advanced a Record-Breaking Dust Episode in Crete, *Atmosphere*, 9: 240.
51. Twomey S.. 1974: Pollution and the planetary albedo. *Atmospheric Environment*, 8: 1251-1256.
52. Wang X., Huang J., Ji M. and Higuchi K. 2008: Variability of East Asia dust events and their long-term trend, *Atmospheric Environonment*., 4: 3156–3165.
53. Winker D., Hunt W., and McGill M. 2007: Initial Performance Assessment of CALIOP, *Geophysics Research Letters*., 34: L19803.
54. Zhang X. Y., Arimoto R., An Z. S. 1997: Dust emission from Chinese desert sources linked to variations in atmospheric circulation, *Journal of Geophysics Research*., 102: 28041–28047.

5. EFFECT OF DUSTY AEROSOLS IN THE FORMATION OF THE REGIONAL CLIMATE OF GEORGIA

5.1. Introduction

Dust aerosols in the form of tiny particles scatter and absorb solar and terrestrial radiation and, therefore, affect climate (Foster et al. 2007 [11]). In addition, dust aerosols raised from soils, rocks, plants, and anthropogenic pollutants into the atmosphere can reduce evaporation and, as a consequence, precipitation processes due to lowering the surface temperature of the earth (Miller et al. 2004 [29]). Studies have shown that anthropogenic activity on average leads to 30% of the dust load, while desert storms are the main sources of mineral dust load in the environment (Barnaba and Gobbi 2004 [4]). Indeed, the storms of the largest deserts in the world (the Sahara and Sahel in Africa, the Gobi, Kyzylkum, Karakum, Taklamakan in Central Asia) are usually the main sources of transport of mineral dust in the atmosphere, its deposition on the earth's surface and spread throughout Europe, Asia and Africa (Cavazos et al. 2009 [5], Forster et al. 2007 [11]). For instance, desert dust is the principal aerosol component over the Mediterranean basin and they strongly influence the Mediterranean climate (Barnaba and Gobbi 2004 [4]). For short or long periods of time, dust storms significantly affected the quality of the Earth's atmosphere, changed the microphysics of clouds, their optical properties, and had a strong influence on both regional and global climate systems (Cavazos et al. 2009 [5]). Indeed, dust storms affected the balance of radiation in the atmosphere, the albedo of the earth's surface, air quality and, consequently, human health and the entire biota (Zhao et al. 2010 [47] 2011 [46], Huang et al. 2011 [19]).

Numerical modeling of past, present and future climate processes is a good tool for studying the main factors affecting modern climate change. Several attempts have been made to study the ability of the global or regional climate models and to clarify the dynamic and physical mechanisms responsible for climate change in specific regions (Barnaba and Gobbi 2004 [4], Cavazos et al. 2009 [5], Zhao et al. 2010 [47], 2011 [46], Huang et al. 2011 [19], Kim et al. 2001 [21], Chen et al. 2004 [6], Aloysius et al. 2011 [2], Alexandri et al. 2015 [1]). For example, to assess the ability of the regional climate model and to model the patterns of surface solar radiation over Europe, the RegCM4.4 model was used (Alexandri et al. 2015 [1]). The results of calculations for 2000-2009 and their comparison with satellite observation data showed that the model has tendency slightly overestimate the surface solar radiation patterns in Europe. In recent decades, a better understanding of dust storm conditions and their migration trends continues to be an important area of research using global / regional climate models with satellite and in-situ monitoring networks (Kaskaoutis et al. 2012 [20]). In addition, the study of the life cycle of dust aerosols and the processes of dust – climate interactions using numerical climate models is widely appreciated in numerous studies (Nabat et al. 2012 [31], Zakey et al. 2006 [44], Shao and Wang 2003). [36], Zhang et al. 2009 [45], Zhao et al. 2014 [48]). Currently, the climatic effects of aerosols on a global scale are relatively well understood. Whereas there are a number of uncertainties in understanding these effects on a regional scale (Nabat et al., 2012 [31], Zakey et al., 2006 [44], Shao and Wang, 2003 [36] , Zhang et al., 2009 [45]). Studies show that the smallest dust particles of the desert, under threshold conditions of a near-surface wind, lifted up to high altitudes of the troposphere, and then are transported thousands of kilometers from the source areas (Mahowald et al., 2002 [28]).) That is why the influence of desert dust on the climate can be felt not only locally, but also in regions remote from sources (Zakey et al., 2006 [44]). Dust aerosols affect the thermodynamics

of clouds, change the microphysical and optical properties of clouds (number, size of cloud drops and ice crystals) by scattering and absorption of solar energy (Bangert et al. 2012 [3], Denjean et al. 2016 [10], Knippertz and Todd 2012 [22], Li et al. 2017 [25], Li 1998 [26], Mahowald at al. 2002 [27]; Myhre et al. 2007 [30], Tao et al. 2012 [41], Twomey 1997 [43]). Dust aerosol influences and responds to climate change mainly due to absorption shortwave radiation, that leads to surface cooling, especially over the arid and semi-arid areas (Zhao et al. 2014 [48]). To understand the degree of aerosol activity in the climate process, a regional climate model (RegCM). with a new dust aerosol scheme (including emissions, transport, calculation of gravity deposition and optical properties), was tested for various time scales, from episodic (several days) to seasonal (climatic regimes) (Zakey et al. 2006 [44]). The calculation results showed that the RegCM model was able to simulate the occurrence of strong dust outbreaks and the main areas of dust load in various regions of the Sahel. Several attempts have been made to study the ability of RegCM / Dust models for specific regions (Konare et al. 2008 [24], Nabat et al. 2012 [31], Das et al. 2013 [8], Tsikerdekis et al., 2016 [42]; Sun and Liu, 2016 [39]; Ozturk et al. 2017 [32]). So far, only a few attempts have been made to study the effect of dust aerosols on climate change processes in the Caucasus region, due to the accelerated melting of the Caucasus glaciers (Shahgedanova et al. 2009 [35], Shengelia et al. 2012 [37], Stokes et al. 2006 [38], Shahgedanova et al. 2013 [34]). Studies showed, that dust deposited on the Caucasus glaciers were originated by the products of decay of biogenic material, locally-produced mineral dust and long-travelled desert dust (Shengelia et al. 2012 [37], Stokes et al. 2006 [38]).

Until now, almost no attempts have been made to study the effect of dust aerosols on climate change processes in Georgia using regional climate models with a dust module (Davitashvili et al., 2018 [7]). In this chapter, the RegCM4.7 model (with a relatively high horizontal resolution (16.7 km)) in combination with the dust module is used to study the temporal / spatial distribution of dust aerosol in Georgia and its effect on some climate change parameters. Namely, the influence of dust aerosol on regional climatic processes is studied by the RegCM4.7-BATS model and investigated by comparing two 30-year simulations performed with and without dust emissions.

5.2. Model description and data

The study in Chapter 5 is based on the fourth-generation regional climate modeling system RegCM4.7 (Giorgi et al. 2012 [12]) combined with the Biosphere-Atmosphere Transfer Scheme (BATS) dust module, which among others can model emissions, transport and deposition of dust particles (Zakey et al. 2006 [44]). RegCM4 is a regional climate model in a sigma coordinate system with a dynamic core using the hydrostatic version of the PSU / NCAR Mesoscale MM5 model (Grell et al. 1994 [17]). The hydrostatic version of the RegCM dynamic core are given by the following (5.2.1)-(5.2.7) system of equations (Grell et al. 1994 [17]),

$$\frac{\partial P^* u}{\partial t} + m^2\left[\frac{\partial P^* uu/m}{\partial x} + \frac{\partial P^* vu/m}{\partial y}\right] + \frac{\partial P^* u\dot{\sigma}}{\partial \sigma} + mP^*\left[\frac{\sigma}{P}\frac{\partial P^*}{\partial x} + \frac{\partial \Phi}{\partial x}\right] = P^* fv + Du, \quad (5.2.1)$$

$$\frac{\partial P^* v}{\partial t} + m^2\left[\frac{\partial P^* uv/m}{\partial x} + \frac{\partial P^* vv/m}{\partial y}\right] + \frac{\partial P^* v\dot{\sigma}}{\partial \sigma} + mP^*\left[\frac{\sigma}{P}\frac{\partial P^*}{\partial y} + \frac{\partial \Phi}{\partial y}\right] = P^* fu + Dv, \quad (5.2.2)$$

$$\frac{\partial P^* T}{\partial t} + m^2\left[\frac{\partial P^* uT/m}{\partial x} + \frac{\partial P^* vT/m}{\partial y}\right] + \frac{\partial P^* T\dot{\sigma}}{\partial \sigma} = P^* \frac{\omega}{\rho c_p} + P^* \frac{Q}{c_p} + D_T, \quad (5.2.3)$$

$$\frac{\partial P^*}{\partial t} = -m^2 \int_0^1 \left[\frac{\partial P^* u/m}{\partial x} + \frac{\partial P^* v/m}{\partial y}\right] d\sigma, \quad (5.2.4)$$

$$\dot{\sigma} = -\frac{1}{P^*} + \int_0^\sigma \left[\frac{\partial P^*}{\partial t} + m^2\left(\frac{\partial P^* u/m}{\partial x} + \frac{\partial P^* v/m}{\partial y}\right)\right] d\sigma', \quad (5.2.5)$$

$$\omega = P^*\dot{\sigma} + \sigma\left(\frac{\partial P^*}{\partial t} + m\left(u\frac{\partial P^*}{\partial x} + v\frac{\partial P^*}{\partial y}\right)\right) d\sigma, \quad (5.2.6)$$

$$\frac{\partial \Phi}{\partial \ln(\sigma + P_t/P^*)} = -RTv\left[1 + \frac{q_c + q_v}{1 + q_v}\right]^{-1}, \quad (5.2.7)$$

where u *and* v are horizontal components of wind velocity, σ is terrain-following hydrostatic-pressure vertical coordinate and defined as $\sigma = (P - P_t)/(P_s - P_t)$, $P^* = P_s - P_t$, P_s and P_t =*const* are the surface and top pressures, respectively, $\dot{\sigma}$ is the vertical velocity in a σ coordinates, it is computed from (5.2.5) by vertical integration, t – is time, T is the potential temperature, Φ is geopotential, p is pressure, ρ is density), $C_p = C_{pd}(1 + 0.8q_v)$ is heat capacity for moist air at constant pressure, q_v is the mixing ratio for water vapor, C_{pd} is the heat capacity for dry air, $\omega = \frac{dP}{dt}$ and is calculated from (5.2.6), T_v is virtual temperature and is given by $T_v = T(1 + 0.608\ q_v)$, and q_c and q_r are the mixing ratios of cloud water and rain water, m is map scale factor defined as the ratio of the distance in computational space to the corresponding distance on the earth's surface,

System of equations (5.2.1)- (5.2.7) with BATS model has been widely used and tested to identify the main features of regional climatic changes and especially to study the effect of dust aerosols on regional climate formation (Zhao et al. 2014 [48], Zakey et al. 2006 [44], Giorgi et al. 2012 [12]). During the last decades, there has been a significant improvement in understanding of the dust sources properties, its transportation mechanisms and modeling capabilities (Sun et al., 2012 [39]).The coupled dust module of RegCM4.7 includes a dust emission scheme, successful behavior of which completely depends: on the value of simulated surface wind threshold friction velocity, on the land surface characteristics (surface roughness and soil moisture, provided by the BATS) and on the processes occurred in the boundary layer of atmosphere (Giorgi et al. 2001 [13], Qian and Giorgi 1999 [33]). Besides, the dust modulus simulates dust transfer (wet and dry removal), gravitational deposition, and optical properties of dust (Shengelia et al., 2012 [37]; Sun et al., 2016 [40]). The processes of transfer, deposition, and removal of dust have been studied in detail in a

number of articles (Giorgi et al. 2001 [13]; Qian and Giorgi 1999 [33]), so we will skip this question in this section. In our study, dust particles are divided into four sizes: small (0.01–1.0 μm), accumulated (1.0–2.5 μm), large (2.5–5 μm), giant (5.0– 20.0 μm), and we used the method of dust parameterization (four steps) proposed by Sun et al. (2012).

5.2.1. Dust parameters of satellite measurements

The simulated data of the Aerosol Optical Depth (AOD) was estimated using MODIS data obtained on a grid with a resolution of 1 ° × 1 °. MODIS is a key instrument aboard the Terra (originally known as EOS AM-1) and Aqua (originally known as EOS PM-1) satellites, from February 2000 and June 2002, respectively (Gkikas et al. 2013 [15], 2015 [16], 2016 [14]). For this reason, the AOD study was conducted since 2000 over 15 years.

The contours of volumetric dust concentration were obtained using the monthly average outputs of CALIPSO (2 ° × 5 °). CALIPSO products gave us the aerosol extinction coefficient at 532 nm, the optical depth of the aerosol in the column, and the properties of the aerosol layer in the global grid cells.

5.2.2. Meteorological data

The calculation results of the RegCM4 model are significantly affected by the boundary conditions (BCs). In our study the BCs for the model domain were derived from the ERA-Interim and the state-of-the-art global atmospheric reanalysis data developed by the European Centre for Medium Range Weather Forecasts (Dee et al. 2011 [9]). It should be noted that the observational data were combined with simulated information from the previous time step to build global atmospheric conditions. The calculation results were validated against the data from the Climate Research Unit (CRU) which represent a global climate database linked to a grid of monthly meteorological measurements from ground stations (Harris et al. 2014 [18]). Surface temperature measurements, among six data sets of meteorological variables, were interpolated into a 0.75 × 0.75 grid, which covered the entire Earth's surface

5.3. Experiments design and method

The studies of the influence of locally produced aerosols of mineral dust and desert mineral dust (displaced from long distances) on regional climate change in the Caucasus (Georgia) were very fragmented and focused only on the analysis of dust particles deposited on Mt. Elbrus (Russia) and on Mt. Kazbeg (Georgia) (Shakhgedanova et al. 2013 [34], Kokkalis et al. 2012 [23]). A regular and long-term impact of mineral dust aerosols on the regional climate for the territory of Georgia has not yet been studied, and the results of such studies (Davitashvili et al. 2018 [7]) are presented for the first time in this study.

The period from 1985 to 2014 with boundary conditions from ECMWF ERA-Interim data (with a resolution of 0.75 degrees) was selected for modeling. Our model uses a one way nesting of grids with a coarse domain with a resolution of 50 km (it covers all regions that are mainly involved in the formation of atmospheric processes over the Caucasus region, namely: most of the south and east of Europe, the Urals and Siberian region, the Middle East and Central Asia) and one nested domain (fully covering the Caucasus region) with a resolution of 16.7 km (see Fig. 5.1).

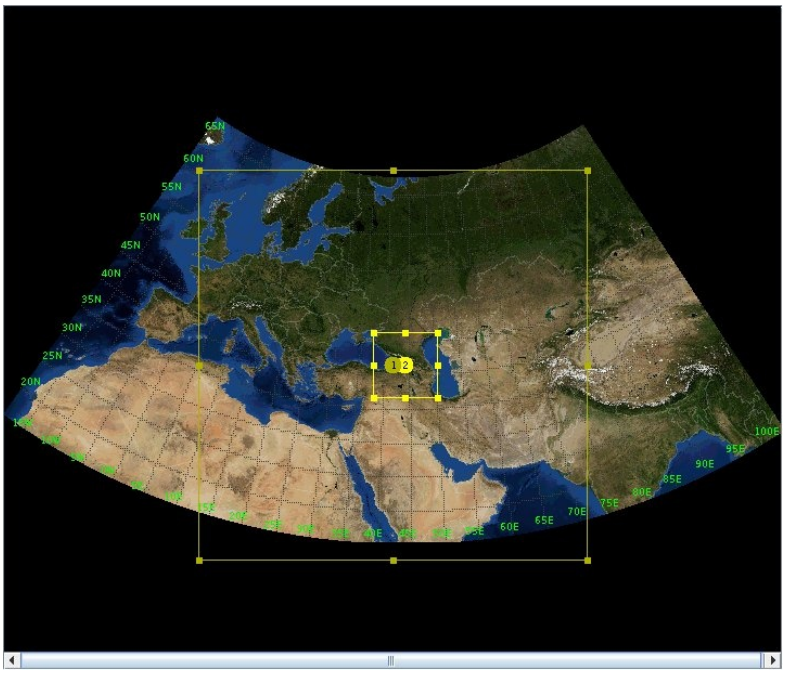

Fig. 5.1. Location of the study area with coarse and nested domains

The impact of dust on the regional climate was evaluated by comparing two numerical experiments in which the first was executed without dust and the second one was simulated through interactive dust inclusion. In order to explore the resolution effect each run was downscaled with nested simulation. For the coarse domains we use time step 100 sec. and for the nested ones - 30 sec. The coarse domains contain 128 grid points in each of the horizontal directions and 18 vertical levels and the nested domains - 64 and 18 correspondingly.

The same physical schemes were used for Dust and NoDust experiments:

Holtslag PBL Boundary layer scheme;

Tiedtke Cumulus convection scheme over the land and the ocean;

Explicit moisture scheme;

In the experiment with Dust only dust tracers - 4 dust bins scheme was activated and aerosol direct effects on radiation and dynamics of atmosphere were considered.

Simulations of the model without chemistry were performed on GRENA's (Georgian Research and Educational Networking Association) cluster (one computing node with 15 cores of Intel Xeon CPU E5-2670 @2.60GHz.) It took approximately 135 hours for the coarse domain and 70 hours for the nested one. For the simulations with chemistry more powerful computing resource - high performance computing cluster ARIS of GRNET (Greek Research and Technology Network) was used. The model run was performed on the 60 cores (it corresponds to the 3 nodes) of Intel Xeon CPU E5-2680 v2 @ 2.80GHz. It took approximately 84 hours for the coarse and 60 hours for the nested domains. In order to investigate the usage effect of two different computational resources on model results the same simulations were performed on GRENA and ARIS clusters, the results of calculations were the same.

5.4. Results and discussions

On the first stage, the simulations with dust were validated. Since in the South Caucasus region we do not have ground-based observations of stratospheric aerosols,

the only source for studying the concentration of dust in the air is data obtained from satellites. The simulated Aerosol Optical Depth (AOD) results were compared to MODIS (MISR, seawifs) data for the four seasons during the period 2000-2014. From the analysis of MODIS data, the AOD value is small in winter, since this period of the year is characterized by heavy snowfalls that prevent dust accumulation, and, therefore, its values above the Caucasus reach only 0.1-0.2 aerosol optical depths observed at a characteristic wavelength of 550 nm . The maximum values of the AOD occur in spring and at the beginning of summer season (March-June), when dust is uplifted and transported from the Sahara and Middle East across Mediterranean to the Black Sea's east coast and reaches the Caucasus regions (Shahgedanova et al. 2013 [34]). Indeed, in spring due to activation of dust transportation from Libyan and Egyptian deserts, the circulation process values of AOD increases and it reaches over Caucasus 0.5-0.6 at 550 nm. Besides, the observations have shown that the aerosol episodes are frequent during the dry period too, from June to October (Gkikas et al. 2013 [15]). In contrast, AOD is minimal in winter. From June to October the subtropical Atlantic high (Azores) prevails over the black sea basin, enhances and causes subsidence. Thus, it results in an extremely stable atmosphere and in absence of rainfall, conditions that favor the aerosol accumulation in the atmosphere. These variations related to synoptic meteorological conditions were investigated previously by authors (Shahgedanova et al. 2013 [34]; Gkikas et al. 2013 [15]; Ozturk et al. 2017 [32]).

The seasonal distribution pattern of simulated AOD's agrees well with MODIS data. It should be noted that in spring and summer sessions the simulated dust concentrations and corresponding AOD in the dust storm generation regions are overestimated, but for the Caucasus region calculated AOD values are very close to satellite data. For comparison the observed and simulated AOD are presented for summer period on the Fig. 5.2.

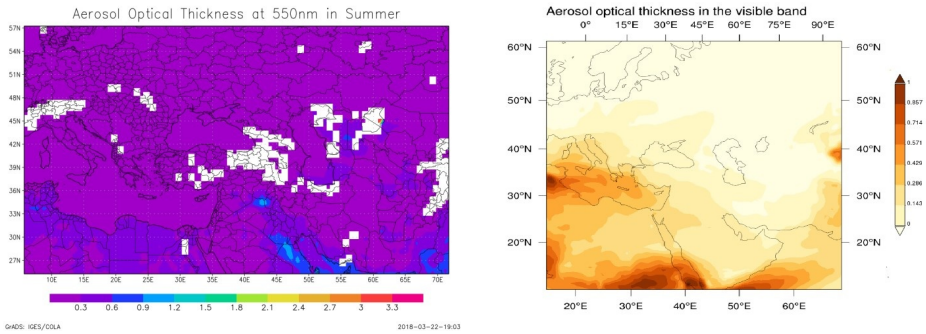

Fig. 5.2. Observed (seawifs) and simulated AOD of summer season for 2000-2014 periods.

To evaluate the impact of dust on the simulated 2 m temperature, all of the 4 runs have been interpolated on nested domain's grid and compared to the 0.5^0-resolution Climatic Research Unit (CRU) surface temperature (for land only) for annual and seasonal scale. On Fig. 5.3 observed and modeled summer and winter mean temperature plots are presented. From these plots difference between experiments with Dust (left on the Fig.5.3) and No Dust is evident, as well as difference between spatial resolutions. It depends on different sub-regions and is in agreement with CRU data.

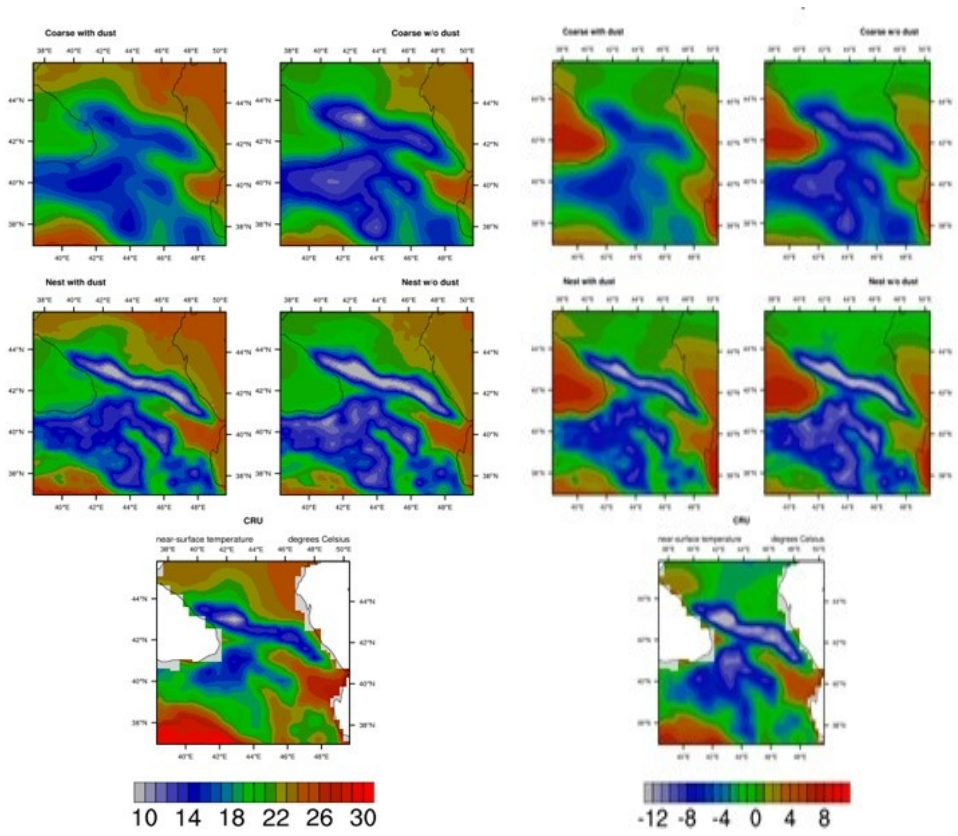

Fig. 5.3. Summer and winter mean surface temperatures observed (CRU) and simulated (with Dust and NoDust on different resolutions).

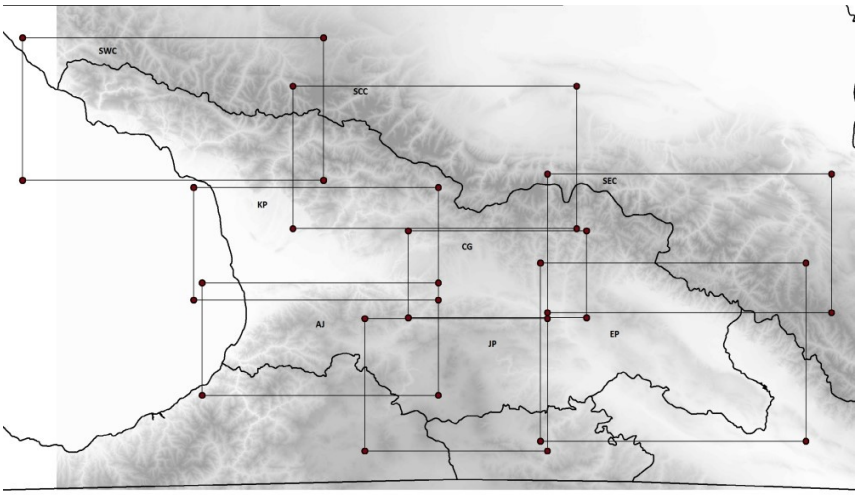

Fig. 5.4. The contours represent the terrain elevation (m). The boxes indicate the 8 sub-regions.

To examine the simulation performance across the experiments on different sub-regions of the South Caucasus nested domain was divided in 8 sub-regions (Fig.5.4). These regions mostly cover Georgia's territory but also include some other parts, according to the factors of local climate formation. On Fig. 5.4 location and names of

sub-regions are presented, where SCC is Central part of South Caucasus, SWC - Western part of South Caucasus, SEC - Eastern part of South Caucasus, EP - Eastern plane territory, KP - Kolkhety Down land, AJ - South mountainous part of Ajara, JP - Javakhety Plato, CP - Central part of Georgia including Likhi range.

The mean annual, as well as summer and winter temperatures bias, standard deviation and correlation coefficient in comparison with CRU data have been calculated from all of the 4 simulations and mean values across mentioned 8 sub-regions evaluated.

Table. 5.1 Mean Annual, Temperatures Bias, Standard Deviation and Correlation Coefficient for 8 sub-regions from 4 simulations.

	Dust			**NoDust**		
	BIAS	**STDV**	**CORREL**	**BIAS**	**STDV**	**CORREL**
SCC	1.91	1.79	0.987	-0.53	1.94	0.984
CG	-1.03	1.62	0.988	-2.79	1.66	0.986
SEC	2.00	1.90	0.990	-0.57	1.77	0.988
EP	-1.99	1.49	0.990	-3.15	1.47	0.989
JP	-0.81	1.57	0.987	-2.61	1.70	0.984
KP	0.57	2.11	0.984	-1.67	2.21	0.981
AJ	0.41	1.79	0.983	-0.99	1.93	0.981
SWC	0.60	1.48	0.987	-1.41	1.54	0.985
	Nested_Dust			**Nested_NoDust**		
	BIAS	**STDV**	**CORREL**	**BIAS**	**STDV**	**CORREL**
SCC	-0.57	1.95	0.984	-2.11	2.00	0.981
CG	-0.81	1.72	0.987	-1.99	1.71	0.985
SEC	-0.44	2.08	0.987	-1.72	1.89	0.987
EP	-1.21	1.61	0.988	-2.15	1.46	0.989
JP	-0.73	1.70	0.985	-2.07	1.77	0.983
KP	-1.03	2.16	0.983	-2.43	2.10	0.982
AJ	-0.41	1.93	0.980	-1.90	1.93	0.979
SWC	-0.52	1.57	0.984	-1.83	1.64	0.982

According to Table 5.1, annual negative bias appears in all sub-regions for the NoDust simulation, the biggest one is in **EP** sub-region, bias from Nested NoDust run is even bigger for the most of sub-regions. Dust simulation has evident benefit in reduction of mentioned cold bias, and in the western sub-regions produces warm bias. Nested_Dust run also improves performance. Namely for **EP** sub-region it continues the reduction of negative bias and smoothes bias in other regions produced from the course domain.

On the seasonal scale, Dust experiment improves winter mean temperature simulation for all sub-regions, and Nested_Dust run performance is better. But summer Dust experiment produces relatively large warm bias for south west sub-regions. The Nested_Dust run for summer has better results for some sub-regions than course run. But for others - mostly central regions Nested_Dust run simulation increases warm bias. These results are obtained after comparison with 0.5^0 resolution observations gridded

dataset. Comparing them with finer spatial resolution's observations will be useful to avoid mistakes raised from smoothing local effects.

5.5. Conclusion

In this chapter, the regular and long-term effects of dust aerosols on the variability of some climatic parameters in various sub-regions of Georgia are first investigated. The impact of dust aerosols on a regional climate was evaluated by comparing two numerical experiments (using the RegCM model with a dust module) performed by interactively switching on dust and not turning on dust. To study the effect of resolution, each run was downscaled using a nested simulation. To study the effectiveness of dusting in different sub-regions, the nested domain of the South Caucasus was divided into 8 sub-regions that completely covered the territory of Georgia.

Analysis of the results of calculations showed that on the seasonal scale, Dust experiment improved winter mean temperature simulation for all sub-regions, and Nested_Dust run performance was better. But summer Dust experiment produced relatively large warm bias for south west sub-regions. The Nested_Dust run for summer had better results for some sub-regions than course run. But for others - mostly central regions Nested_Dust run simulation increased warm bias.

AOD simulation results were compared with MODIS data (MISR, sea waves) for four seasons in the period 2000-2014. From winter analysis of MODIS data, the AOD values were small, since this period of the year was characterized by heavy snowfalls that prevented dust accumulation, and, therefore, its values over the Caucasus reached only 0.1-0.2. The maximum AOD values occurred in the spring and at the beginning of the summer season (March-June), when dust rose and transferred from the Sahara and the Middle East through the Mediterranean Sea to the eastern Black Sea coast and reached the Caucasian regions. It should be noted that the seasonal distribution model of the simulated AOD is in good agreement with the MODIS data.

To evaluate the effect of dust on the simulated 2-meter temperature in all 4 runs, CRU surface temperatures were used on an annual and seasonal scales. From a comparison of observational data (CRU) and simulated summer and winter average temperatures, the difference between experiments with and without dust was obvious. The simulated data on the average temperature in summer and winter varied depending on the sub-regions, but were in accordance with the CRU data.

References to Chapter 5

1. Alexandri G. et al. 2015: On the ability of RegCM4 regional climate model to simulate surface solar radiation patterns over Europe: an assessment using satellite-based observations, *Atmos. Chem. Phys*., 15, 13195–13216.

2. Aloysius M. et al. 2011: Role of dynamics in the advection of aerosols over the Arabian Sea along the west coast of peninsular India during pre-monsoon season: A case study based on satellite data and regional climate model, *J. Earth Syst. Sci.* 120, No. 2, 269–279.
3. Bangert M. et al. 2012: Saharan dust event impacts on cloud formation and radiation over Western Europe, *Atmos. Chem. Phys.,* 12, 4045–4063, doi:10.5194/acp-12-4045-2012.
4. Barnaba, F. and Gobbi, G. P. 2004: Aerosol seasonal variability over the Mediterranean region and relative impact of maritime, continental and Saharan dust particles over the basin from MODIS data in the year 2001, *Atmos. Chem. Phys.*, 4, 2367–2391, doi:10.5194/acp-4-2367-2004.
5. Cavazos C, Todd M. C. and K. Schepanski**,** 2009: Numerical model simulation of the Saharan dust event of 6–11 March 2006 using the Regional Climate Model version 3 (RegCM3), *Journal of Geophysical Research*, Vol. 114,pp.1-24, D12109, doi:10.1029/2008JD011078.
6. Chen, Y.S., Sheen, P.C., Chen, E.R., Liu, Y.K., Wu, T.N., Yang, C.Y., 2004. Effects of Asian dust storm events on daily mortality in Taipei⁄ Taiwan. Environ. Res. 95, 151–155, doi: 10.1016/j.envres.2003.08.008, 2004.
7. Davitashvili,T., Kutaladze, N., Kvatadze, Rand and G. Mikuchadze, 2018: Effect of dust aerosols in forming the regional climate of Georgia. *Scalable Computing: Practice and Experience*, 2018, Volume 19, Number 2, pp. 199-208. http://www.scpe.org.
8. Das S. et al. 2013: Examining mineral dust transport over the Indian subcontinent using the regional climate model*, RegCM4.1,* Atmospheric Research 134 (2013) 64-76.
9. Dee, D. P., Uppala, S. M., Simmons, A. J.,et al 2011: The ERA-Interim reanalysis: configuration and performance of the data assimilation system, *Q. J. Roy. Meteorol. Soc*., 137, 553–597, doi:10.1002/qj.828.
10. Denjean C. et al. 2016: Size distribution and optical properties of mineral dust aerosols transported in the western Mediterranean, *Atmos. Chem. Phys.,* 16, 1081-1104, https://doi.org/10.5194/acp-16-1081-2016.
11. Forster, P., et al. 2007: Changes in atmospheric constituents and in radiative forcing, in Climate Change 2007: The Physical Science Basis. Contribution of Working Group I to the Fourth Assessment Report of the Intergovernmental Panel on Climate Change, edited by S. Solomon et al., pp. 129– 234, Cambridge Univ. Press, Cambridge, U. K.
12. Giorgi F. et al.2012: RegCM4: Model description and preliminary tests over multiple CORDEX domains, *Climate Research*, 52, 7–29, doi: 10.3354/cr01018
13. Giorgi Y, et al. 2001: Regional simulation of anthropogenic sulfur over East Asia 30 and its sensitivity to model parameters, *Tellus* B, 53, 171–191, doi:10.1034/j.1600-0889.2001.d01-14.x.
14. Gkikas, A., Hatzianastassiou, N., Mihalopoulos, N., and O.Torres. 2016: Characterization of aerosols episodes in the greater Mediterranean Sea area from

satellite observations (2000–2007), *Atmos. Environ.*, 128, 286–304, doi:10.1016/j.atmosenv.2015.11.056.

15. Gkikas, A., Hatzianastassiou, N., Mihalopoulos, N., Katsoulis, V., Kazadzis, S., Pey, J., Querol, X., and Torres, O. 2013: The regime of intense desert dust episodes in the Mediterranean based on contemporary satellite observations and ground measurements, *Atmos. Chem. Phys.,* 13, 12135–12154, doi:10.5194/acp-13- 12135-2013.
16. Gkikas, A., Houssos, E. E., Lolis, C. J., Bartzokas, A., Mihalopoulos, N., and Hatzianastassiou, N. 2015: Atmospheric circulation evolution related to desert-dust episodes over the Mediterranean, *Q. J. Roy. Meteor. Soc.*, 141, 1634–1645, doi:10.1002/qj.2466.
17. Grell G. A. Dudhia J. and D. R. Stauffer, 1994: *A description of the fifth-generation Penn State/NCAR Mesoscale Model (MM5),* NCAR Tech. Note NCAR/TN- 398+STR, p. 121.
18. Harris, I., Jones, P. D., Osborn, T. J., and Lister, D. H. 2014: Updated high-resolution grids of monthly climatic observations– the CRU TS3.10 Dataset, Int. J. Climatol., 34, 623–642, doi:10.1002/joc.3711.
19. Huang J., Fu, Q., Zhang, W., Wang, X., Zhang, R., Ye, H., Warren, S., 2011: Dust and black carbon in seasonal snow Across Northern China. *Bull. Am. Meteorol. Soc*. 92, 175–181. http://dx.doi.org/10.1175/2010BAMS3064.1.
20. Kaskaoutis D. G. et al.2012: Desert Dust Properties, Modelling, and Monitoring, *Advances in Meteorology*, vol. 2012, Article ID 483632, 2, doi:10.1155/2012/483632.
21. Kim K.W., Kim, Y.J., Oh, S.J., 2001: Visibility impairment during Yellow Sand periods in the urban atmosphere of Kwangju, Korea. *Atmos. Environ.* 35 (30), 5157–5167.
22. Knippertz P. and M. C. Todd. 2012: Mineral dust aerosols over the sahara: meteorological controls on emission and transport and implications for modeling, *Reviews of Geophysics*, 50, 1-28, RG1007 / 2012.
23. Kokkalis P., Mamouri R. E., Todua M., Didebulidze G. G., Papayannis A., Amiridis V., Basart S., Pérez C. & J. M. Baldasano 2012: Ground-, satellite- and simulation-based analysis of a strong dust event over Abastumani, Georgia, during May 2009, *International Journal of Remote Sensing,* 33:16, 4886-4901, DOI: 10.1080/01431161.2011.644593.
24. Konare A. et al. 2014: A regional climate modeling study of the effect of desert dust on the West African monsoon, *Journal of Geophysical Research*, Vol. 113, d12206, pp.1-15, doi:10.1029/2007jd009322.
25. Li Z. et al. 2017: Aerosols and Their Impact on Radiation, Clouds, Precipitation, and Severe Weather Event*s,* Environments, *Environmental Processes and Systems*, Online Publication Date: Sep 2017, DOI:10.1093/acrefore/9780199389414.013.126.
26. Li Z. 1998: Influence of absorbing aerosols on the inference of solar surface radiation budget and cloud absorption. *Journal of Climate,* 11, 5–17.

27. Mahowald N, et al. 2002: Understanding the 30-year Barbados desert dust record, *J. Geophys. Res.,* 107(D21), doi:10.1029/2002JD002097.
28. Mahowald N. M. and Kiehl L. M. 2003: *Mineral aerosol and cloud interactions*. *Geophysical Research Letters*, 30, 1475–1478.
29. Miller, R.L., I. Tegen, and J.P. Perlwitz, 2004: Surface radiative forcing by soil dust aerosols and the hydrologic cycle. *J. Geophys. Res.*, **109**, D04203, doi:10.1029/2003JD004085.
30. Myhre G. et al. 2007: Aerosol-cloud interaction inferred from MODIS satellite data and global aerosol models. *Atmospheric Chemistry and Physics*, 7, 3081–3101.
31. Nabat P. et al. 2012: Dust emission size distribution impact on aerosol budget and radiative forcing over the Mediterranean region: a regional climate model approach, *Atmos. Chem. Phys.*, 12, 10545–10567, doi:10.5194/acp-12-10545-2012.
32. Ozturk T. et al. 2017: Projected changes in temperature and precipitation climatology of Central Asia CORDEX Region 8 by using RegCM4.3.5, Atmospheric Research, 183 296–307.
33. Qian Y. and F. Giorgi. 1999: Interactive coupling of regional climate and sulfate aerosol models over East Asia, *J. Geophys. Res.,* 104, 6477–6499, doi:10.1029/98JD02347.
34. Shahgedanova M. et al. 2013: Using the significant dust deposition event on the glaciers of Mt. Elbrus, Caucasus Mountains, Russia on 5 May 2009 to develop a method for dating and "provenancing" of desert dust events recorded in snow pack, *Atmos. Chem. Phys*., 13, 1797–1808.
35. Shahgedanova M., Hagg W., Hassell d., Stokes C.R. and V. Popovin, 2009: Climate Change, Glacier Retreat, and Water Availability in the Caucasus Region, *In Book Threats to Global Water Security*, Editors: J. Anthony A. Jones, Trahel G. Vardanian, Christina Hakopian,Publisher Springer Netherlands, 2009, pp. 131-140.
36. Shao Y. P. et al. 2003: Northeast Asian dust storms: real-time numerical prediction and validation, *Journal of Geophysical Research,* vol. 108, article 4691.
37. Shengelia L., Kordzakhia G., Tvauri G., Davitashvili T., Begalishvili N. 2012: Possibilities of the use of remote sensing technologies for the estimation of modern climate change impact on the Caucasus glaciers, Georgian National Academ y of Sciences, Monthly Scientific-Reviewed Magazine, *Science and Technologies*, Vol.4-6, pp. 25-30.
38. Stokes, C.R., Gurney, S.D., Shahgedanova, M., and V. Popovnin, 2006: Late-20th-century changes in glacier extent in the Caucasus Mountains, Russia/Georgia, *J. Glaciol.*, 52: 99–109.
39. Sun H. Pan Z. and X. Liu 2912: Numerical simulation of spatialtemporal distribution of dust aerosol and its direct radiative effects on East Asian climate, *Journal of Geophysical Research, Atmospheres*, vol. 117, no. 13, Article IDD13206.

40. Sun H. and X. Liu 2016: Numerical Modeling of Topography-Modulated Dust Aerosol Distribution and Its Influence on the Onset of East Asian Summer Monsoon, Hindawi Publishing Corporation. *Advances in Meteorology*, Vol. 2016, Article ID 6951942, 15 pages, http://dx.doi.org/10.1155/2016/6951942.
41. Tao W.-K. et al. 2012: Impact of aerosols on convective clouds and precipitation. *Reviews of Geophysics*, *50,* 2012.
42. Tsikerdekis A. et al. 2016: *Modeling the trans-Atlantic transportation of Saharan dust*, Bulletin of the Geological Society of Greece, vol. L, p. 1052-1061, *Proceedings of the 14th International Congress*, Thessaloniki, May 2016.
43. Twomey S. 1997: The influence of pollution on the shortwave albedo of clouds. *Journal of the Atmospheric Sciences*, 34, 1149–1152.
44. Zakey A.S. Solmon F. and F. Giorgi 2006: Implementation and testing of a desert dust module in a regional climate model, *Atmos. Chem. Phys.,* 6, 4687–4704.
45. Zhang D. F. et al. 2009: Simulation of dust aerosol and its regional feedbacks over East Asia using a regional climate model, *Atmospheric Chemistry and Physics*, vol. 9, no. 4, 1095–1110.
46. Zhao C., Liu, X., Leung, L.R., Hagos, S., 2011: Radiative impact of mineral dust on monsoon precipitation variability over West Africa. *Atmos. Chem. Phys*. 11, 1879–1893. http://dx.doi.org/10.5194/acp-11-1879-2011.
47. Zhao C., Liu, X., Leung, L.R., Johnson, B., McFarlane, S., Gustafson Jr., W., Fast, J., Easter, R., 2010: The spatial distribution of mineral dust and its shortwave radiative forcing over North Africa: modeling sensitivities to dust emissions and aerosol size treatments. *Atmos. Chem. Phys.* 10, 8821–8838. http://dx.doi.org/10.5194/acp-10-8821-2010.
48. Zhao S. et al. 2014: Simulating direct effects of dust aerosol on arid and semi-arid regions using an aerosol–climate coupled system, *International Journal of Climatology*, Published online in Wiley Online Library (wileyonlinelibrary.com) DOI: 10.1002/joc.4093.